

**CONSOLIDATION OF
GEOLOGIC STUDIES OF
GEOPRESSURED GEOTHERMAL
RESOURCES IN TEXAS**

1984 Annual Report

By T. E. Ewing, M. P. R. Light, N. Tyler, and R. A. Morton

Prepared for the U.S. Department of Energy
Division of Geothermal Energy
Contract No. DE-AC08-79ET27111

Bureau of Economic Geology
W. L. Fisher, Director
The University of Texas at Austin
Austin, Texas 78713

March 1986

DISCLAIMER

This report was prepared as an account of work sponsored by the United States Government. Neither the United States nor the United States Department of Energy, nor any of their employees, makes any warranty, express or implied, or assumes any legal liability or responsibility for the accuracy, completeness, or usefulness of any information, apparatus, product, or process disclosed, or represents that its use would not infringe privately owned rights. Reference herein to any specific commercial product, process, or service by trade name, trademark, manufacturer, or otherwise, does not necessarily constitute or imply its endorsement, recommendation, or favoring by the United States Government or any agency thereof. The views and opinions of authors expressed herein do not necessarily state or reflect those of the United States Government or any agency thereof.

This report has been produced directly from the best available copy.

Printed in the United States of America.

Available from the National Technical Information Service, U.S. Department of Commerce, 5285 Port Royal Road, Springfield, Virginia 22161.

Price: Printed Copy A06
Microfiche A01

Codes are used for pricing all publications. The code is determined by the number of pages in the publication. Information pertaining to the pricing codes can be found in the current issues of the following publications, which are generally available in most libraries: Energy Research Abstracts (ERA); Government Reports Announcements and Index (GRA and I); Scientific and Technical Abstract Reports (STAR); and publication NTIS-PR-360, available from NTIS at the above address.

FOREWORD

This is the final report to be submitted to the Department of Energy under the Consolidated Geothermal contract (DE-AC08-79ET27111) with the Bureau of Economic Geology. The report contains two sections. Section I presents the conclusion of work under the "Resource Assessment and Seismic Studies" project topic. It ties together the prospect and study areas described previously with a regional statistical survey of fault compartments. Section II reports the conclusion of the "Synthesis of Data" project topic. New vitrinite reflectance and hydrocarbon data are combined with previous information to yield a revised theory of fluid migration and temperature history in the vicinity of the Pleasant Bayou test-well site.

In addition, the project topic of "Environmental Monitoring" has been concluded, under separate subcontractors' reports. Seismic monitoring under subcontract to Teledyne Geotech was completed, and a final report submitted (Mauk and others, 1984). A variety of significant events was detected, but it is difficult to assign causes to them. At the request of the U.S. Department of Energy, the Bureau subcontracted with the Meyer Group to conduct a first-order releveling of the Pleasant Bayou site to update and replace the 1978 baseline study. The work was performed in the summer of 1984, and a final report prepared in October 1984 was transmitted to the Bureau of Economic Geology and then to the U.S. Department of Energy (Meyer Group, 1984). Interpretation of the results of this study is funded under the current geopressured geothermal research contract, along with new studies of environmental effects--modeling of subsidence and fault reactivation--and production of liquid hydrocarbons from the geothermal test wells.

All other topics of the expired contract, including Sandstone Consolidation, Salinity, and Reservoir Continuity, have been fully documented in previous annual reports (Morton and others, 1983; Ewing and others, 1984), as well as in Bureau and outside publications.

References

- Ewing, T. E., Tyler, N., Morton, R. A., and Light, M. P. R., 1984, Consolidation of geologic studies of geopressured geothermal resources in Texas: 1983 Annual Report: The University of Texas at Austin, Bureau of Economic Geology, report prepared for Department of Energy, Division of Geothermal Energy under contract no. DE-AC08-79ET27111, 142 p.
- Mauk, F. J., Kimball, B., and Davis, R. A., 1984, Microseismic monitoring of Chocolate Bayou, Texas: the Pleasant Bayou #2 geopressured/geothermal energy test well program: The University of Texas at Austin, Bureau of Economic Geology technical report submitted to Department of Energy, Division of Geothermal Energy under contract no. DE-AC08-79ET27111, 75 p.
- Meyer Group, 1984, Project report for first order class 1 levels near Pleasant Bayou geothermal test well, Brazoria County, Texas: report prepared for The University of Texas at Austin, Bureau of Economic Geology under Department of Energy, Division of Geothermal Energy contract no. DE-AC08-79ET27111, unpaginated.
- Morton, R. A., Ewing, T. E., Kaiser, W. R., and Finley, R. J., 1983, Consolidation of geologic studies of geopressured geothermal resources in Texas: 1982 Annual Report: The University of Texas at Austin, Bureau of Economic Geology, report prepared for Department of Energy, Division of Geothermal Energy under contract no. DE-AC08-79ET27111, 195 p.

CONTENTS

FOREWORD iii

SECTION I. REGIONAL FAULT COMPARTMENT GEOMETRIES OF THE WILCOX AND FRIO GROWTH-FAULT TRENDS, TEXAS GULF COAST 1

ABSTRACT 1

INTRODUCTION. 1

METHODS 2

DISCUSSION 7

 Distributions 7

 Idealized models 12

SIGNIFICANCE 17

ACKNOWLEDGMENTS 18

REFERENCES 18

Figures in Section I

I-1. Study area, showing numbers of closed compartments found per Tobin quadrangle (7.5-minute quadrangle). 3

I-2. Well density of the Texas Gulf Coast in wells per 1,000 km² 5

I-3. Measurements performed on a typical Gulf Coast fault compartment 6

I-4. Histograms of size and shape parameters for the Wilcox trend 8

I-5. Histograms of size and shape parameters for the Frio trend. 9

I-6. Cumulative percentage of areas accounted for by blocks of less than a given area, for Wilcox and Frio trends 13

I-7. Parallelogram and trapezoid models for fault compartments 14

Tables in Section I

I-1. Summary of mean, 10th, 50th, and 90th percentiles for size and shape parameters, the Texas Gulf Coast, by sector 10

I-2. Cross-fault angles and validity tests for the parallelogram and trapezoid models as applied to Wilcox and Frio fault compartments.	16
---	----

SECTION II. THERMAL HISTORY AND HYDROCARBON ANOMALIES IN THE FRIO FORMATION, BRAZORIA COUNTY, TEXAS—AN INDICATOR OF FLUID FLOW AND GEOPRESSURE HISTORY 21

ABSTRACT	21
INTRODUCTION.	22
THERMAL MATURITY	22
ORIGIN OF HYDROCARBONS.	36
Relative Age of Hydrocarbons and Thermal Maturity of Source Rocks	36
Isotope Ratios of Gases	44
Oil Mobilization	50
SOLUBILITY OF CEMENTS IN AQUIFER FLUIDS	68
ORIGIN OF PERMEABLE AQUIFERS	71
SALINITY.	80
CONCLUSIONS	84
ACKNOWLEDGMENTS	85
REFERENCES	87

Figures in Section II

II-1. Vitrinite reflectance and thermal alteration index versus depth for the Pleasant Bayou No. 1 well	23
II-2. Well-log temperature corrected to equilibrium values versus depth, Pleasant Bayou No. 1 and No. 2 wells	25
II-3. Temperature versus depth, Chocolate Bayou - Danbury dome area, Brazoria County, Texas	26
II-4. Vitrinite reflectance profiles from core plugs from wells in the Chocolate Bayou - Danbury dome area	28
II-5. Histograms showing the population distribution of vitrinite reflectance analyses of core samples in the Chocolate Bayou - Danbury dome area	30
II-6. Vitrinite reflectance versus depth for samples from the Palo Duro Basin	31

II-7.	The estimated discrepancy in the measurement of vitrinite reflectance versus depth	32
II-8.	Vitrinite reflectance histograms from two laboratories for one sample of well core in the Pleasant Bayou No. 1 well	33
II-9.	Corrected vitrinite reflectance values for core samples from the Chocolate Bayou - Danbury dome area, Brazoria County, Texas, compared to regional paleogeothermal gradient for Oligocene rocks in Louisiana	35
II-10.	Northwest-southeast regional section showing the pressure regime distribution in the Pleasant Bayou area. Possible directions of shale water flow during compaction and diagenesis are shown	37
II-11.	Natural logarithm of the naphthene fraction versus the natural logarithm of the time-temperature integral for the Pleasant Bayou No. 1 geothermal test well	42
II-12.	Naphthene fraction expressed as time-temperature indices versus depth for the Pleasant Bayou No. 1 well compared to the burial history maturity profile and the corrected vitrinite reflectance, both expressed as time-temperature indices	43
II-13.	Relation between carbon isotopic composition of methane from natural gas reservoirs and maturity of their source rocks	46
II-14.	Geochemical survey of the Gulf of Mexico	46
II-15.	Relationship between methane isotopic composition and the carbon isotope fractionation between CH ₄ and CO ₂ in non-associated natural gases	49
II-16.	Computer-processed log, compensated neutron log, and density log for the "C" sandstone, Pleasant Bayou No. 2 well	52
II-17.	Residual water saturation versus porosity and permeability	56
II-18.	Compactional model for hydrocarbon production in geopressured brines	57
II-19.	Geometry of unicellular flow in an inclined fluid layer	63
II-20.	Time depth curve for the Pleasant Bayou No. 2 well showing the initiation and peak of secondary porosity development	66
II-21.	Plot of the natural logarithm of permeability versus porosity for geopressured sandstones	67
II-22a.	Explanation of symbols and key to abundance of selected sandstone components plotted against depth	73
II-22b.	Detailed core description and petrography of distributary-mouth-bar sandstones, Andrau sandstone, Phillips Houston "GG" No. 1 well	74

II-23.	Detailed core description and petrography of distributary-mouth-bar sandstones, Andrau sandstone, Phillips Houston "JJ" No. 1 well	75
II-24.	Core porosity versus permeability for high- and low-maturity wells in Brazoria County, Texas, and Vermilion Parish, Louisiana	78
II-25.	Chlorine-bromine ratio versus total dissolved solids for wells from the Gulf Coast region of Texas	81
II-26.	Stylized stratigraphic dip section across the Texas Gulf Coast showing the relative position of the GCO/DOE Pleasant Bayou No. 2 geothermal test well	86

Tables in Section II

II-1.	Vitrinite reflectance data for the Pleasant Bayou - Chocolate Bayou area	29
II-2.	Disproportionation of naphthenes to paraffins and aromatics	38
II-3.	Normalized naphthene concentration for the Pleasant Bayou No. 1 well	40
II-4.	Water soluble organic compounds in brine from the DOW-DOE L. R. Sweezy No. 1 well, Louisiana	47
II-5.	Composition of aromatic condensates	51
II-6.	Fluid convection calculations for the Andrau sandstone, Pleasant Bayou test well	60
II-7.	Convective flow boundary conditions	62
II-8.	Mass transport of silica in the Andrau sandstone, Pleasant Bayou test well	64
II-9.	Hypothetical porosity variation in the Andrau sandstone	69
II-10.	Scale of approximate (± 0.3) saturation index values	70
II-11.	Pressure, temperature, and salinity data for the Andrau sandstone and core analysis data for the T3 and Andrau sandstone, Brazoria County, Texas	76
II-12.	Core analysis data for the Andrau sandstone in the Pleasant Bayou No. 1 and No. 2 and Houston "GG" No. 1 and "JJ" No. 1 wells, Brazoria County and DOW-DOE L. R. Sweezy No. 1 well, Vermilion Parish, Louisiana	79

SECTION I. REGIONAL FAULT COMPARTMENT GEOMETRIES OF THE WILCOX AND FRIO GROWTH-FAULT TRENDS, TEXAS GULF COAST

by Thomas E. Ewing

assisted by Olufemi Babalola

ABSTRACT

Data on the sizes and shapes of fault compartments in the Texas Gulf Coast growth-fault and geopressure trends show meaningful differences between the Wilcox and Frio fault systems. The Frio compartments show less elongation and higher absolute curvature than Wilcox compartments. These variations are consistent with the distinct structural styles of the two trends determined from local studies. The areas of compartments are distributed exponentially but with slightly more very large compartments. A bimodal distribution of curvature is observed, paired positive and negative peaks of the same absolute value being within each trend, suggesting a simple trapezoid model for fault compartment geometry. The narrower, more elongate fault compartments of the Wilcox trend, combined with the commonly dip-oriented Wilcox sand bodies, suggest that large reservoirs occur less frequently there than in the Frio trend.

INTRODUCTION

The distribution of the geopressured sandstone reservoirs beneath the Texas Gulf Coast is strongly controlled by the geometry and movement history of major fault systems that formed contemporaneously with shelf-margin elastic deposition (Winker and Edwards, 1983). Previous work on the structural setting of geopressured resources (Winker and others, 1983; Ewing, 1983a, 1984) focused on the structural evolution of several study areas within the Wilcox and Frio growth-fault trends of the Texas Gulf Coast. This work led to

the distinction of a variety of structural styles, as well as to documentation of the complex interaction of growth faulting and salt tectonics (Ewing, 1983b).

To extend results from the detailed study areas to the entire region, a statistical study of faults and fault compartments in both Wilcox and Frio growth-fault trends was undertaken. The emphasis was placed on fault compartments, defined as blocks of strata enclosed laterally by faults, for the following reasons:

--A major growth fault generally merges laterally into other faults; hence its ends are not easily defined. A fault compartment, given adequate subsurface mapping, is a distinct entity.

--Most geopressured reservoirs are bounded by faults on at least one side; many are entirely fault-bounded. Hence consideration of the fault compartment size and geometry is necessary to assess reservoir area and volume. This analysis is especially useful in the highly faulted areas common in the deep geopressured trends.

--Information on fault compartment sizes and fault spacings can be used together with original sand-body geometry information (when compiled) to predict the distribution of reservoir sizes within a major progradational package.

METHODS

To achieve regional coverage, commercial maps of Gulf Coast structure were used. In general, the deepest map horizon available was selected in each area; however, two horizons were examined in some areas. The fault pattern studied is usually near the top of geopressure. The areas examined, with numbers of fault compartments found per Tobin grid (7.5-minute quadrangle) are shown on figure I-1. In all, 568 closed compartments were identified and measured.

The accuracy of regional structure mapping is of some concern. In general, well density is sufficient to determine the structural configuration at the horizons mapped

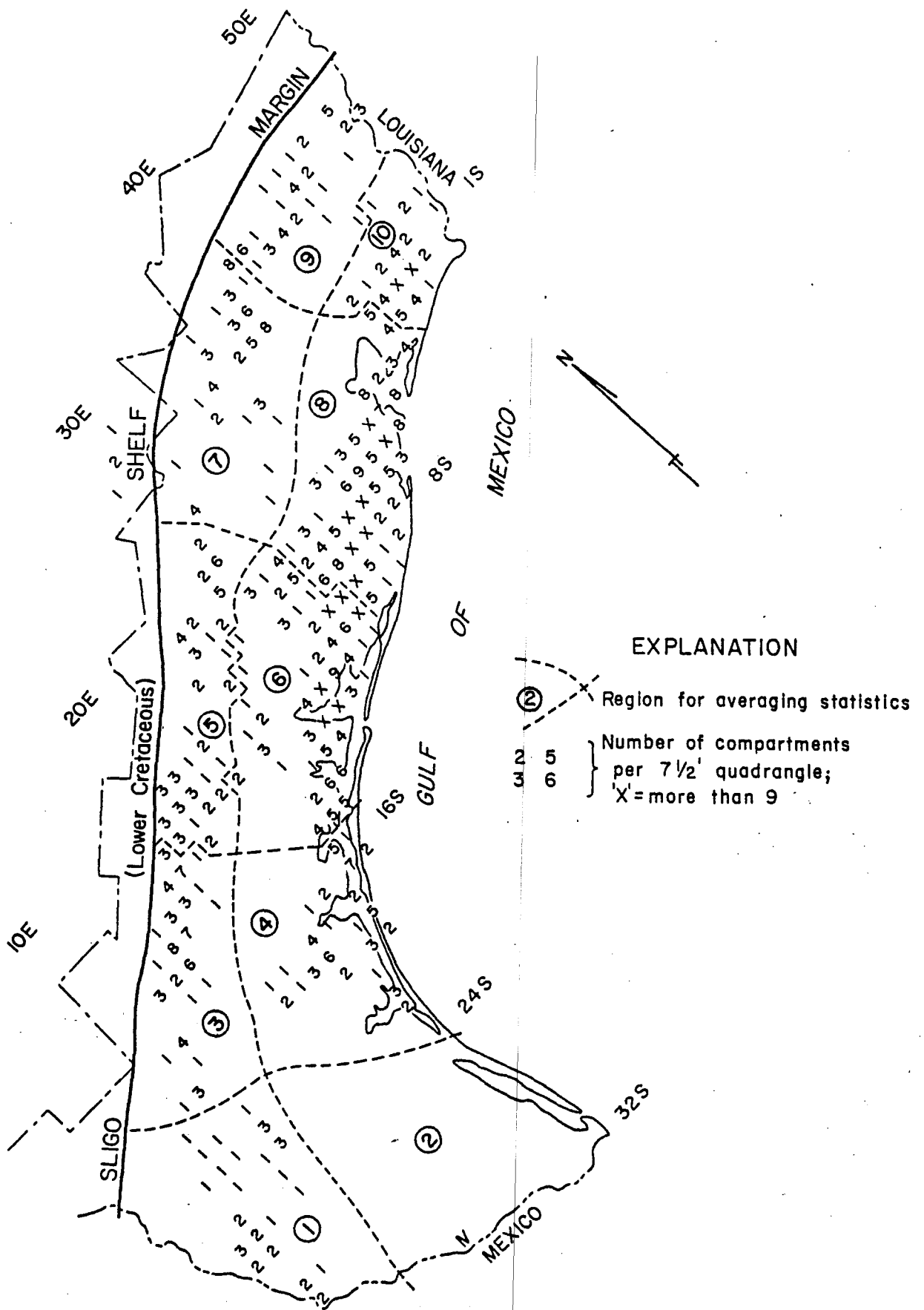


Figure I-1. Study area showing numbers of closed compartments found per Tobin quadrangle (7.5-minute quadrangle). Quadrangles with "X" have more than nine compartments; blank quadrangles have no sampled compartments.

QA-3418

(fig. I-2). The only significant area of sparse control is the South Texas Frio, which has not been included in this study. The mapping in the Houston Diapir Province is considered to be somewhat less reliable than that to the southwest because salt diapirism has modified or masked earlier growth-fault structures (Ewing, 1983b).

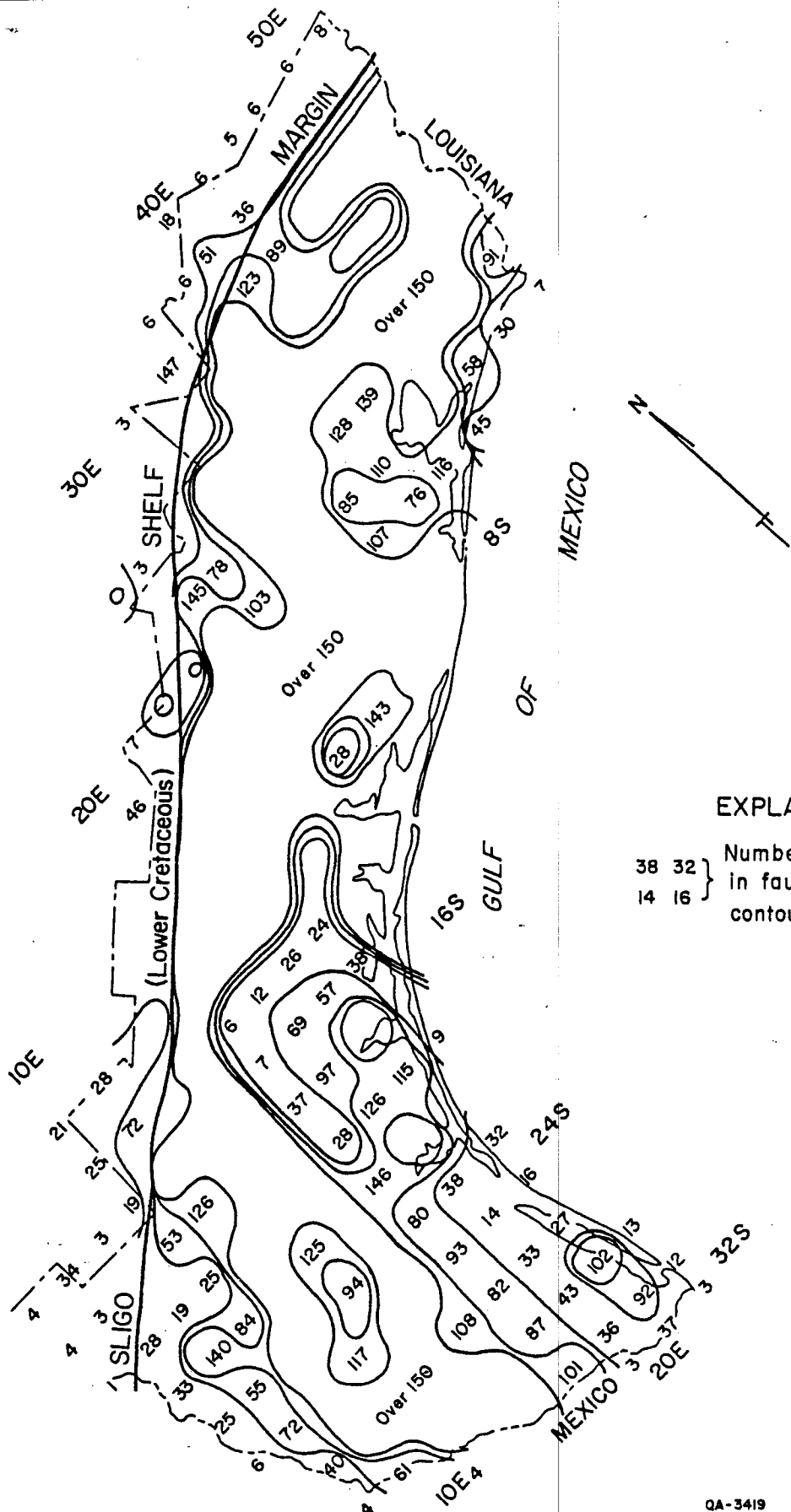
Each closed fault compartment was characterized (fig. I-3) by location (using the Tobin-Geomap location system), mapping horizon, average depth, area (A) (measured by planimeter, in mi^2), azimuth (α) of the long axis of the compartment, length of the long axis (a), and the distances to the sides of the compartment from the midpoint of the long axis (c_1 and c_2) (in feet; values are negative going toward the Gulf of Mexico). The long axis was chosen as the line joining the corners of the compartment that are farthest apart.

These raw data can be transformed into a set of shape factors, which describe the form of the compartment (fig. I-3). This transformation helps in visualizing the "typical" fault block and in comparing blocks of different size from different trends. The shape factors used are location, depth, datum, area (also plotted as log area), azimuth, oblateness, elongation, and curvature.

Oblateness (Ω) is measured by comparing the area of the compartment (A) to the area of an equivalent rectangle (A_r) formed by the long axis and the difference between the midpoint measurements (or the short axis). The factor $\Omega = A/A_r$ would equal 0.785 for a hypothetical elliptical compartment and 0.5 for a diamond-shaped (rhombic) compartment.

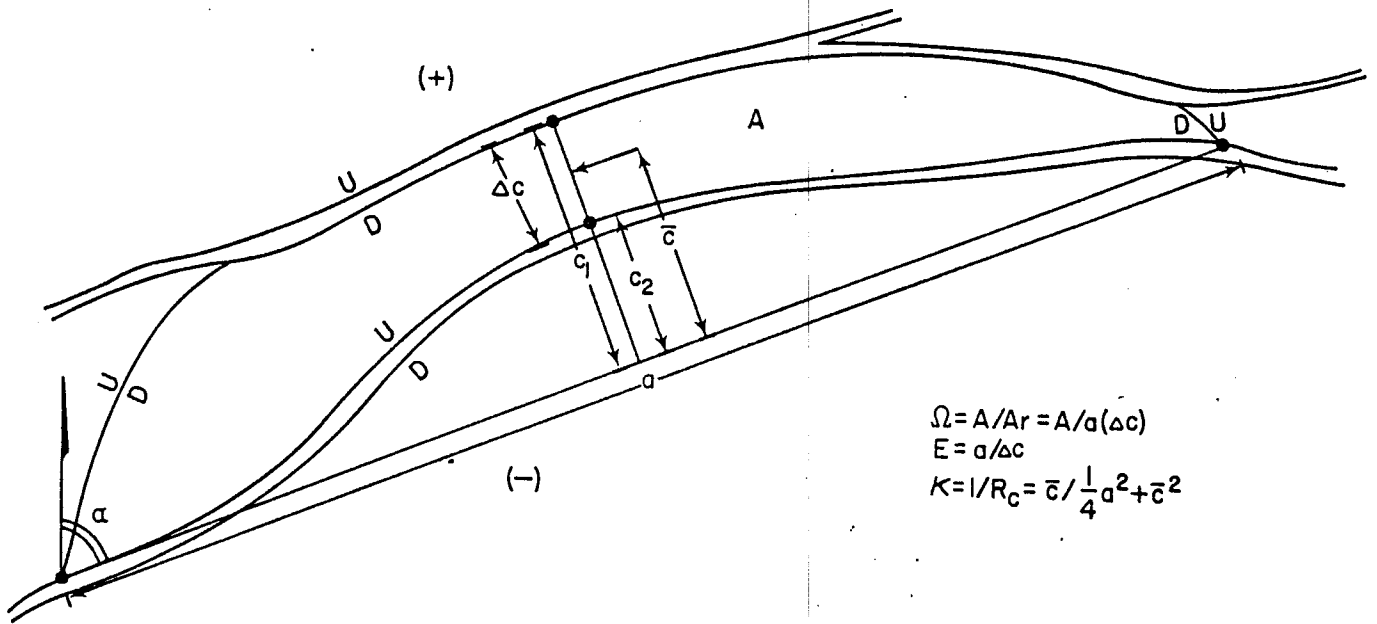
Elongation (E) is simply the ratio of the long axis (a) to the short axis (c). When this ratio is unity, the long and short axes are equal (as a square or circular compartment would be).

Curvature (k) of the compartment is determined by drawing a circle, using the long axis as a chord and the midpoint of the short axis (c) as a point on the circle (at a distance c from the midpoint of the long axis). This value is the reciprocal of the radius of curvature (Rc). The curvature is negative for compartments that are convex toward the



QA-3419

Figure I-2. Well density of the Texas Gulf Coast in wells per 1,000 km² (390 mi²). From the Tectonic Map of Texas (Ewing, in press). The low values in 28-29 N, 97-98 W do not reflect poor Geomap control but correspond to an area of deeper mapping for the Tectonic Map. L: more than 150 wells per 1,000 km² (390 mi²).



QA-4049

Figure I-3. Measurements performed on a typical Gulf Coast fault compartment. Symbols are defined in the text.

basin. A more enlightening graphical representation portrays the logarithm of the absolute value of curvature because curvature values vary by several orders of magnitude.

These transformed data were then separated into 11 sectors (fig. I-1), 5 each along the major Wilcox and Frio-Vicksburg structural trends and 1 in the Mesozoic structural trend. The calculated values were plotted on histograms for each sector, as well as aggregated for the Wilcox and Frio trends. Histograms for selected parameters in the two trends are shown in figures I-4 and I-5, and a summary of all values by sectors in table I-1.

DISCUSSION

Distributions

From table I-1, subtle but distinct differences between the Wilcox and Frio fault compartment geometries can be detected; there is comparatively little difference between sectors within a trend. Wilcox fault compartments tend to be somewhat more uniform in area, are more elongate (except in sector 7, which lies in the Houston Diapir Province), are less oblate, and show a lower absolute curvature. Frio compartments show a greater range in compartment areas (some being very large, though this may be an artifact of sample size); are less elongate, slightly more oblate, and commonly show higher curvatures. These variations are consistent with those observed in the fairway studies of Bebout and others (1978, 1982) and the area studies of Winker and others (1983) and Ewing (1983a, 1984).

The distribution of compartment areas within both trends shows a pronounced tail including some large values. Plotting values of log area gives an approximately normal (or log normal) distribution; however, this is probably an artifact of the measuring process. Small fault compartments are hard to locate and map because of limited well control, so that regional mapping underrepresents these small blocks. Therefore, fitting the observed distribution with exponential and hyperbolic models was attempted. Exponential models

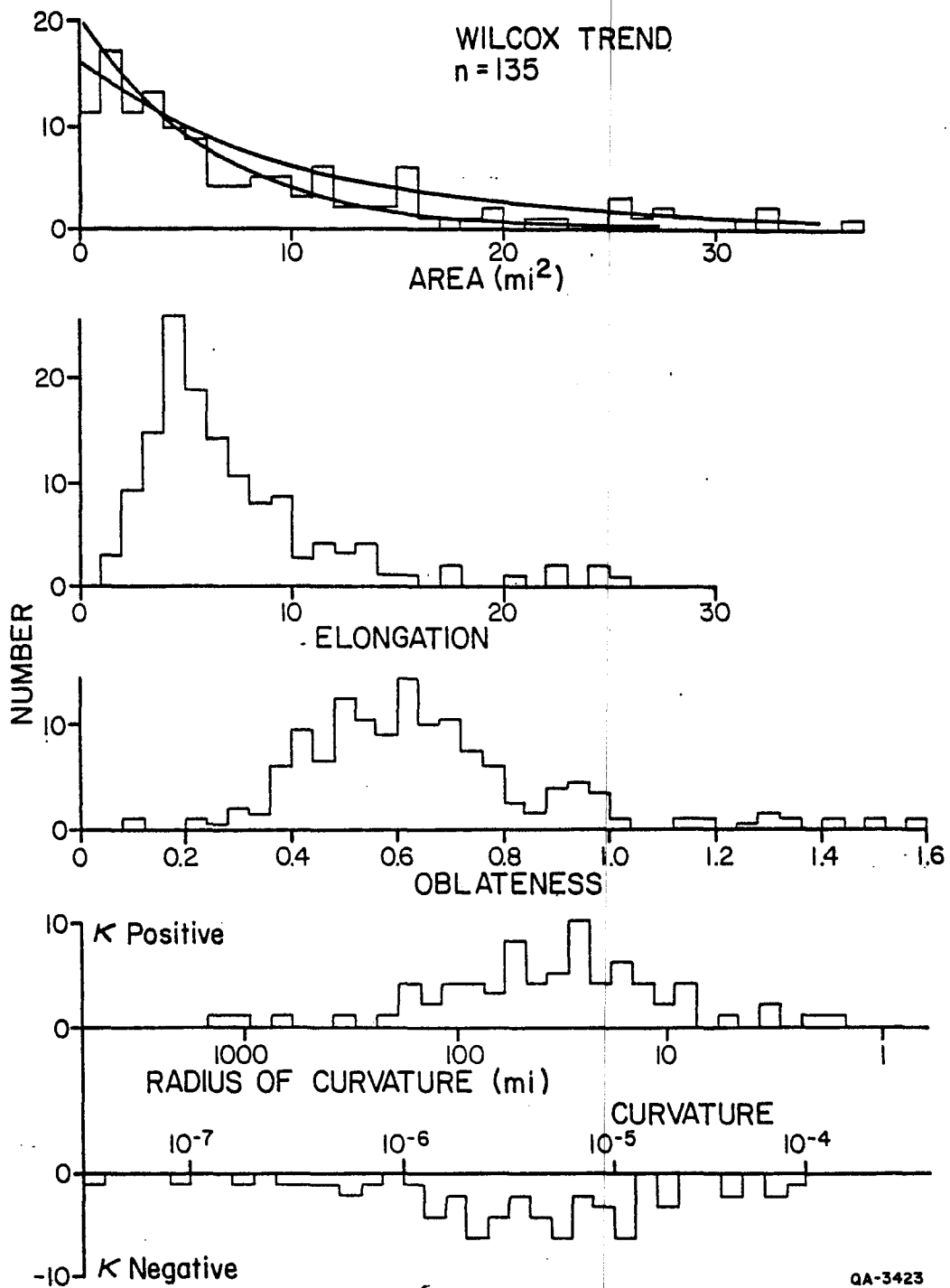


Figure I-4. Histograms of size and shape parameters for the Wilcox trend.

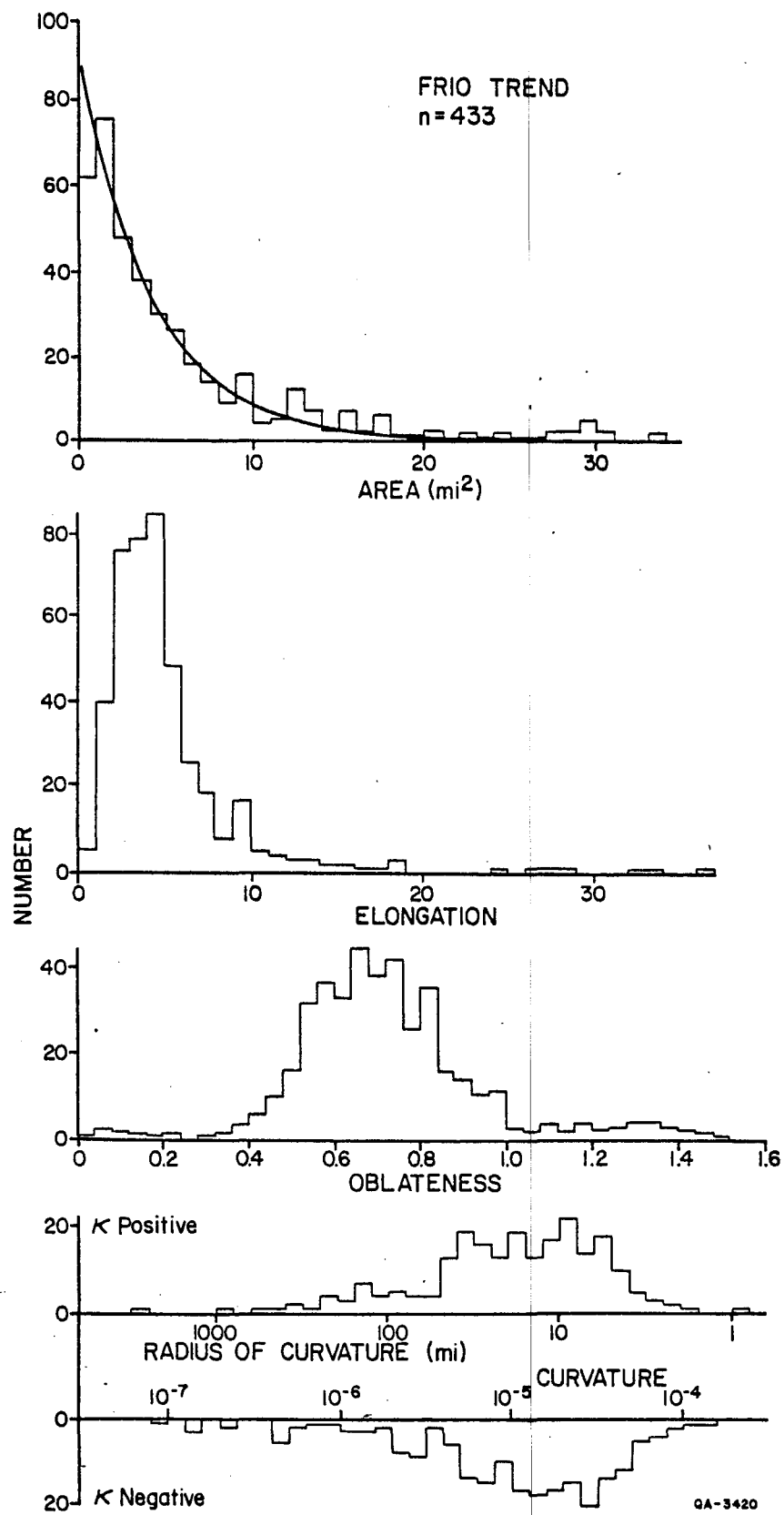


Figure I-5. Histograms of size and shape parameters for the Frio trend.

Table I-1. Summary of mean, 10th, 50th, and 90th percentiles for size and shape parameters, fault compartments of the Texas Gulf Coast, by sector.

Sector #	No. blocks	AREA				DEPTH				AZIMUTH				
		Ave.	Md ₁₀	Md ₅₀	Md ₉₀	Ave.	Md ₁₀	Md ₅₀	Md ₉₀	Ave.	Md ₁₀	Md ₅₀	Md ₉₀	
WILCOX TREND:														
1	17	9.75	0.85	8.25	30.3	5,600	3,270	5,550	8,330	19°	-1°	14°	67°	
3	51	7.79	1.23	4.13	14.9	7,810	6,410	7,613	9,595	50°	34°	51°	65°	
5	36	14.80	2.8	9.0	37.1	7,730	6,760	7,900	8,850	55°	39°	56°	69°	
7	22	8.50	1.07	5.0	16.8	8,670	5,770	9,300	9,980	67°	39°	63°	92°	
9	9	17.39	0.9	9.5	70.0	7,710	4,800	8,350	9,200	73°	58°	73°	91°	
All Wilcox:	135	10.66	1.39	6.0	29.6	8,120	5,750	7,880	9,590	not meaningful				
FRIO TREND:														
10	4	37	6.95	0.93	3.43	16.3	6,170	3,575	6,950	7,730	30°	-3°	28°	61°
	6	150	10.59	0.79	4.3	27.5	7,880	6,650	8,030	8,975	67°	30°	67°	105°
	8	204	8.94	0.67	3.55	22.6	9,030	7,330	8,920	10,740	62°	15°	61°	108°
	10	42	7.94	0.47	4.25	14.8	8,410	7,510	8,350	9,340	55°	18°	55°	107°
	All Frio:	433	9.24	0.83	4.13	22.5	8,328	6,800	8,480	10,260	not meaningful			
11	9	6.81	1.5	4.5	16.0	5,320	4,800	5,520	5,800	54°	39°	56°	63°	
ALL BLOCKS														
	577	9.54				8,233								

Table I-1. (cont.)

Sector #	ELONGATION				OBLATENESS				CURVATURE						
	Ave.	Md10	Md50	Md90	Ave.	Md10	Md50	Md90	(Positive . . .)			Negative)			
									Ave.	Md10	Md50	Md90	Md10	Md50	Md90
WILCOX TREND:															
1	9.00	2.85	7.25	24.3	0.47	0.28	0.40	0.83	+2.6	1.91	7.08	83.2	-0.19	-2.0	-75.9
3	6.35	2.78	5.23	10.9	0.59	0.42	0.53	0.80	-1.52	1.17	4.47	17.0	-0.54	-7.08	-70.8
5	7.99	4.05	5.67	15.4	0.74	0.52	0.67	0.98	+1.87	0.96	2.82	14.5	-0.29	-2.61	-5.82
7	7.12	2.40	6.50	11.8	0.87	0.56	0.69	1.30	+10.9	3.55	11.8	56.2	-1.48	-6.07	-17.0
9	6.67	4.45	6.33	12.1	0.72	0.60	0.71	0.92	+4.20	0.18	3.98	23.0	-0.09	-11.2	-12.0
All Wilcox:	7.27	2.1	5.84	13.1	0.67	0.41	0.62	0.95	+2.31	1.15	5.80	21.9	-0.47	-5.16	-18.9
FRIO TREND:															
4	4.90	2.06	3.73	8.3	0.80	0.56	0.72	1.00	+6.07	0.66	15.8	69.2	-1.12	-10.7	-42.2
6	5.02	2.29	4.26	9.3	0.70	0.48	0.66	0.95	+0.56	1.77	10.7	35.0	-0.63	-11.7	-39.8
8	5.54	1.86	4.45	10.3	0.80	0.53	0.72	1.20	+1.12	1.49	11.2	40.7	-2.22	-13.3	-29.0
10	3.75	1.35	3.6	6.3	0.72	0.52	0.66	0.92	-6.48	2.29	11.2	43.7	-1.12	-18.3	-44.7
All Frio:	5.13	1.96	4.66	9.2	0.76	0.51	0.71	0.97	+0.61	1.72	11.47	39.6	-1.66	-13.18	-39.7
11	5.06	3.2	4.3	9.3	0.66	0.50	0.65	0.82	-2.45	1.41	9.44	11.2	-5.25	-6.3	-36.0
ALL BLOCKS															
	5.63				0.74				+1.0						

11

give a good fit for the main body of blocks (figs. I-4 and I-5), with an overcount of blocks less than 1 mi² and an undercount of very large blocks. For the Wilcox,

$$n = (18 \pm 2)\text{Exp}(-0.12 \pm 0.03)A$$

and for the Frio,

$$n = (91)\text{Exp}(-0.22 \pm 0.01)A$$

give a reasonable fit. However, when cumulative functions with respect to area are plotted (fig. I-6), it is evident that these models predict only about half the total fault compartment area with any accuracy. The remaining area lies in a few very large blocks, which are not accounted for in the above model.

Elongation shows a skewed normal distribution (figs. I-4 and I-5). In part this is caused by the absence of elongations less than unity (noted above). However, a coarse tail is expected in the conceptual models presented below.

Oblateness has a roughly normal distribution in both fault compartment trends (figs. I-4 and I-5). The value of oblateness lies between the diamond and rectangle shapes.

Curvature yields an interesting histogram, which is significant in choosing a fault compartment model. Only the log of the absolute value of curvature can be conveniently plotted, with positive curvatures above the line and negative curvatures below the line (figs. I-4 and I-5). In this presentation, both trends show a peak of both positive and negative values at about 10E-5, curvatures of Frio compartments being somewhat larger than Wilcox compartments; the graph suggests a bell shape with fine tails.

Idealized Models

Using results of earlier area studies, we expect the compartments to lie between major growth faults within a growth-fault trend. The ends of the blocks are formed either by convergence of the two major faults or, more commonly, by smaller cross faults. Two models for this population can be tested: a parallelogram model and a trapezoid model (fig. I-7).

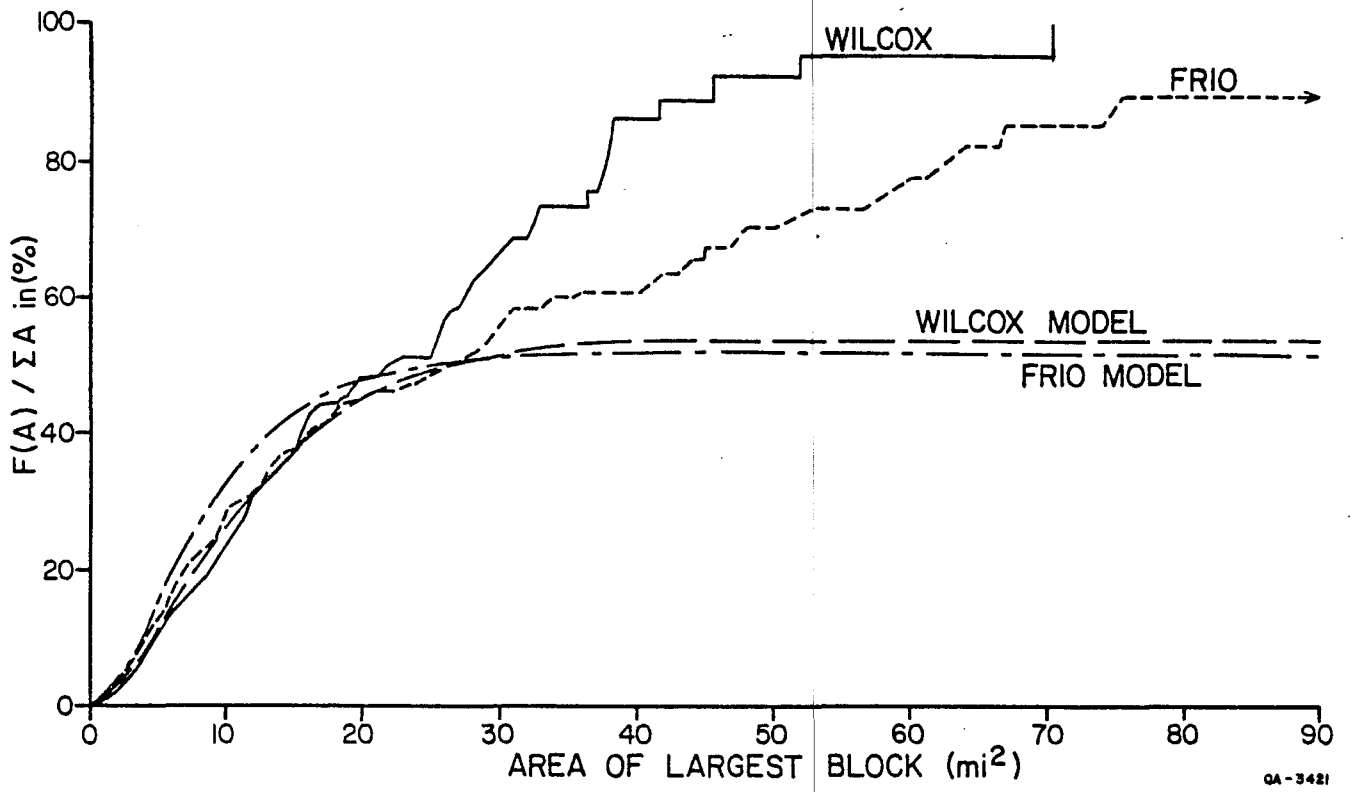
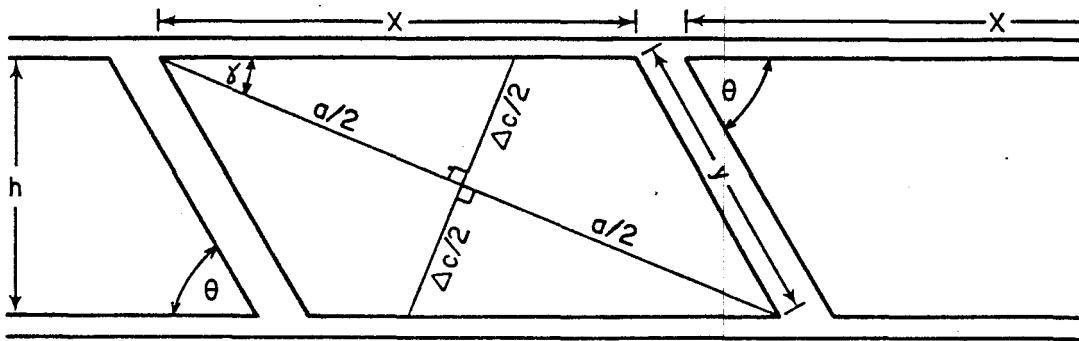
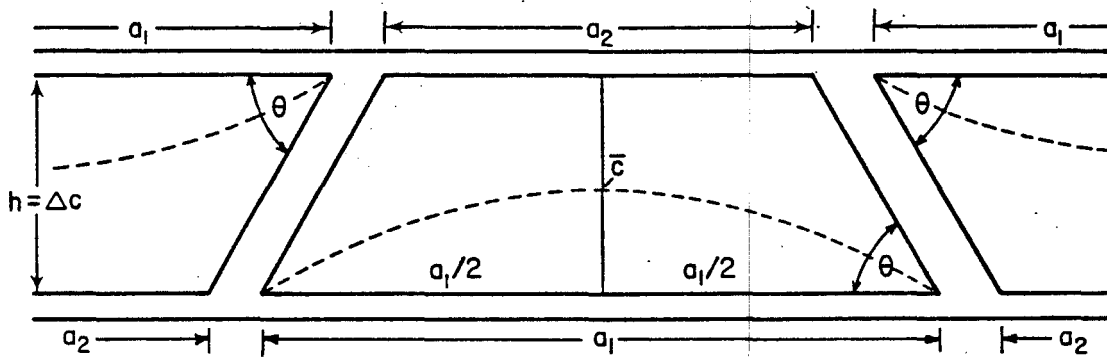


Figure I-6. Cumulative percentage of areas accounted for by blocks of less than a given area, for Wilcox and Frio trends. Exponential models are also shown.



a. PARALLELOGRAM: $E(\text{elongation}) = 1/\tan \gamma$
 $\Omega(\text{oblateness}) = E(\sin \gamma \cos \gamma - \sin^2 \gamma / \tan \theta)$
 $K(\text{curvature}) = 0$
 $\tan \theta = \sin \gamma \cos \gamma / (\cos^2 \gamma - \Omega)$



b. TRAPEZOID: $E = a_1 / \Delta c$
 $\Omega = 1 - 1/E \tan \theta$
 $K = 1 / [\Delta c (E^2 + 1)]$
 $\theta = \tan^{-1} [1 / \{E(1 - \Omega)\}]$

Valid only if $\cot \theta \leq 1/2E$

QA-3422

Figure I-7. Parallelogram and trapezoid models for fault compartments.

In the parallelogram model, the parallel cross faults connect major faults lying a distance (h) apart. They are oriented at an angle (theta) to the major fault. The measured long axis is inclined at an angle (gamma) to the major faults. For this model, zero curvature is predicted; the model is valid for all positive values.

The trapezoid model considers the cross faults to be nonparallel but still oriented at an angle (theta) to the major faults. Cross faults alternate in orientation, yielding a series of complementary trapezoids. The long axis of this model compartment lies along one of the major faults. For such a model, the absolute curvature is a finite value depending on (delta-c) and (a₁). This model can hold only when the short side of the trapezoid exists, that is, when the following criterion is met: $\text{Cot}\theta < \frac{1}{2}E$.

These models can be tested against the acquired data (table I-2). The trapezoid model is valid for most of the blocks in all sectors except no. 1 (South Texas Wilcox), where sample size is small. The angles of cross faults from the two methods are similar, both showing higher angles in the Frio than in the Wilcox. This is probably an artifact; the angle values are unlikely to be physically significant. The major difference between the models is the prediction of zero curvature from the parallelogram model versus the bimodal positive-negative curvature predicted from the trapezoid model. The latter is in fact observed, strongly favoring the trapezoid model for the main compartment populations. Indeed, it is hard to think of any other simple model that would yield evenly matched positive and negative curvature distributions.

The large blocks that skew the area distributions may be blocks located between groups of growth faults, such as the Pleasant Bayou compartment described by Winker and others (1983). This is a different population entirely and not covered by the models described above.

Table I-2. Cross-fault angles and validity tests for the parallelogram and trapezoid models as applied to Wilcox and Frio fault compartments.

Sector	n	TRAPEZOID MODEL		PARALLELOGRAM MODEL	
		Validity	Angle ave.	Validity	Angle ave.
WILCOX TREND:					
1	17	23.5%	18.7°	all	12°
3	51	58.8%	28.8°	all	22°
5	36	85.7%	35.4°	all	27°
7	22	81.8%	31.5°	all	51°
9	9	100%	32.6°	all	30°
FRIO TREND:					
4	37	91.9%	50.1°	all	51°
6	150	80.7%	41.7°	all	36°
8	204	79.9%	42.9°	all	46°
10	42	88.1%	50.1°	all	49°
Total Wilcox:					
	135	67%	32°		
Total Frio:					
	433	82%	44°		

SIGNIFICANCE

The statistical examination of regional fault compartment data has confirmed and extended the distinction of discrete Wilcox and Frio structural styles. The Wilcox style of growth faulting consists of a bundle of nearly straight, closely spaced faults showing little flattening with depth (reaching a décollement plane deep in the Mesozoic). The importance of shale mobilization ranges from slight (as in the De Witt area) to substantial (in the Zapata area). This fault style gives rise to fault compartments that are highly elongate, low in curvature, and of more uniform size. In contrast, the Frio style of growth faulting consists of several major sinuous faults having moderate flattening with depth, possibly flattening into a regional décollement at 20,000 to 25,000 ft; there is substantial mobilized shale in diapirs and ridges. This style gives rise to fault compartments that are more equidimensional, having substantial curvature and a wide range of sizes. The influence of salt tectonics was surprisingly small in the Frio trend but is strongly noted in the Wilcox trend, where sector 7 approaches the character of the Frio trend. However, this is suspected to be an artifact of mapping uncertainties (Ewing, 1983 a,b).

The distribution of fault compartment sizes and shapes has not been determined for areas of shallow décollement such as the South Texas Vicksburg fault zone or the offshore Brazos Ridge fault zone.

Eventually, information on the size and shape of fault compartments may be augmented by size and shape data for sand bodies and sand-body composites formed under various depositional settings. Then the two data sets could be statistically combined to yield a Monte-Carlo-type estimate by sector and trend of the number and size of reservoirs that might yield oil, gas, or geopressured water and the percentage of these reservoirs that have one, two, or more stratigraphic boundaries. Data on elongation, area, and azimuth will be especially important in this process because reservoir volumes will depend on the geometry of superposition of depositional sandstone, depositional azimuth and shape, and fault compartment azimuth and shape.

ACKNOWLEDGMENTS

This report is an outgrowth of an earlier study (reported in Morton and others, 1983). It has been word processed by Dorothy C. Johnson under the direction of Lucille Harrell. The figures were drafted under the supervision of R. L. Dillon, Chief Cartographer. This work was conducted under the Department of Energy Division of Geothermal Energy Contract No. DE-AC08-79ET27111.

REFERENCES

- Bebout, D. G., Loucks, R. G., and Gregory, A. R., 1978, Frio sandstone reservoirs in the deep subsurface along the Texas Gulf Coast, their potential for the production of geopressed geothermal energy: The University of Texas at Austin, Bureau of Economic Geology Report of Investigations No. 91, 100 p.
- Bebout, D. G., Weise, B. R., Gregory, A. R., and Edwards, M. B., 1982, Wilcox sandstone reservoirs in the deep subsurface along the Texas Gulf Coast, their potential for the production of geopressed geothermal energy: The University of Texas at Austin, Bureau of Economic Geology Report of Investigations No. 117, 125 p.
- Ewing, T. E., 1983a, Structural styles and structural evolution of the Frio growth-fault trend in Texas: constraints on geopressed reservoirs, in Morton, R. A., Ewing, T. E., Kaiser, W. R., and Finley, R. J., Consolidation of geologic studies of geopressed geothermal resources in Texas: The University of Texas at Austin, Bureau of Economic Geology, report prepared for the U.S. Department of Energy, Contract No. DE-AC08-79ET27111, p. 1-61.
- Ewing, T. E., 1983b, Growth faulting and salt tectonics in the Houston Diapir Province: timing and exploration significance: Gulf Coast Association of Geological Sciences Transactions, v. 33, p. 83-90.

Ewing, T. E., 1984, Structural styles of the Wilcox growth-fault trend in Texas: constraints on geopressed reservoirs, in Ewing, T. E., Tyler, N., Morton, R. A., and Light, M. P. R., Consolidation of geologic studies of geopressed geothermal resources in Texas: The University of Texas at Austin, Bureau of Economic Geology, report prepared for the U.S. Department of Energy, Contract No. DE-AC08-79ET27111, p. 1-32.

Ewing, T. E., in press, Tectonic Map of Texas: The University of Texas at Austin, Bureau of Economic Geology, scale 1:750,000.

Winker, C. D., and Edwards, M. B., 1983, Unstable progradational elastic shelf margins, in Stanly, D. J., and Moore, G. T., eds., The shelfbreak: critical interface on continental margins: Society of Economic Paleontologists and Mineralogists Special Publication 33, p. 139-157.

Winker, C. D., Morton, R. A., Ewing, T. E., and Garcia, D. D., 1983, Depositional setting, structural style, and sandstone distribution in three geopressed geothermal areas, Texas Gulf Coast: The University of Texas at Austin, Bureau of Economic Geology Report of Investigations No. 134, 60 p.

SECTION II. THERMAL HISTORY AND HYDROCARBON ANOMALIES IN THE
FRIO FORMATION, BRAZORIA COUNTY, TEXAS—AN INDICATOR OF
FLUID FLOW AND GEOPRESSURE HISTORY

by Malcolm P. R. Light, Thomas E. Ewing, and Noel Tyler

assisted by V. Lombeida

ABSTRACT

The Pleasant Bayou geopressured-geothermal test wells in Brazoria County, Texas, display a prominent thermal maturity anomaly in the Oligocene Anahuac and Frio Formations. Highly geopressured thermally mature shales are interbedded with hydropressured to moderately geopressured sandstones in the upper Frio and Anahuac. In contrast, shales and sandstones in the lower Frio, including the Andrau geopressured-geothermal production zone, are highly geopressured but exhibit lower thermal maturities.

Vitrinite reflectance measurements, hydrocarbon maturation data, and anomalous heavy hydrocarbon contents at Pleasant Bayou indicate that the upper Frio was subjected to an extended period of hot, extremely saline fluid flow from the basin, which caused the thermal anomaly. Regional salinity studies (Morton and others, 1983) suggest that growth faults were the conduits for vertical basinal brine movement. Anomalously mature hydrocarbons in the gasoline range (C5 to C7) were introduced into the upper Frio by this process. Early formation of high geopressure in the lower Frio limited fluid influx; consequently maturity in the deep Frio section, greater than 14,000 ft (4,270 m), remained consistent with the regional thermal gradient.

Late-stage porosity and the permeability destruction by carbonate cementation seen elsewhere in the Gulf Coast was inhibited in the deeper Frio by the low influx of Ca^{2+} ions contained in the brines. These Ca^{2+} ions were released during albitization of feldspars at more mature, deeper levels of the basin.

INTRODUCTION

Studies of geopressed geothermal resources of the Texas Gulf Coast conducted by the Bureau of Economic Geology have integrated information from the Pleasant Bayou test well area with relevant data from other geopressed test wells in Texas and Louisiana.

A large amount of regional and local information on depositional environments, sandstone petrology, diagenesis, fluid compositions, and salinities has been combined with estimated thermal and hydrocarbon maturities for the Pleasant Bayou test well (Ewing and others, 1984a, b). Questions of particular pertinence to this project are:

- What are the nature and cause of the thermal maturity anomaly at the Pleasant Bayou test wells and its relationship to geopressure, fluid flow, and hydrocarbon migration?
- Where do the liquid hydrocarbons in the highly geopressed saline brines originate?
- Why do reservoirs in the lower Frio show anomalously high porosities and permeabilities?

THERMAL MATURITY

The level of thermal maturity in a subsiding basin is a result of its age and temperature history. Various organic geochemical parameters including vitrinite reflectance (R_o) and thermal alteration indices (TAI) are used to estimate maturity (Bostick, 1973; Wright, 1980).

The Pleasant Bayou test wells display a maturity anomaly (fig. II-1) that cannot arise as a consequence of simple conduction (Ewing and others, 1984a). As will be discussed later, the uncorrected estimated maturity appears much lower than that indicated when the present (and apparent regional) geothermal gradient is applied to the burial history of those strata (Ewing and others, 1984a).

Though temperature and burial time are the most important parameters affecting rank, pressure is still thought to be influential at low levels of maturation (Bostick, 1979,

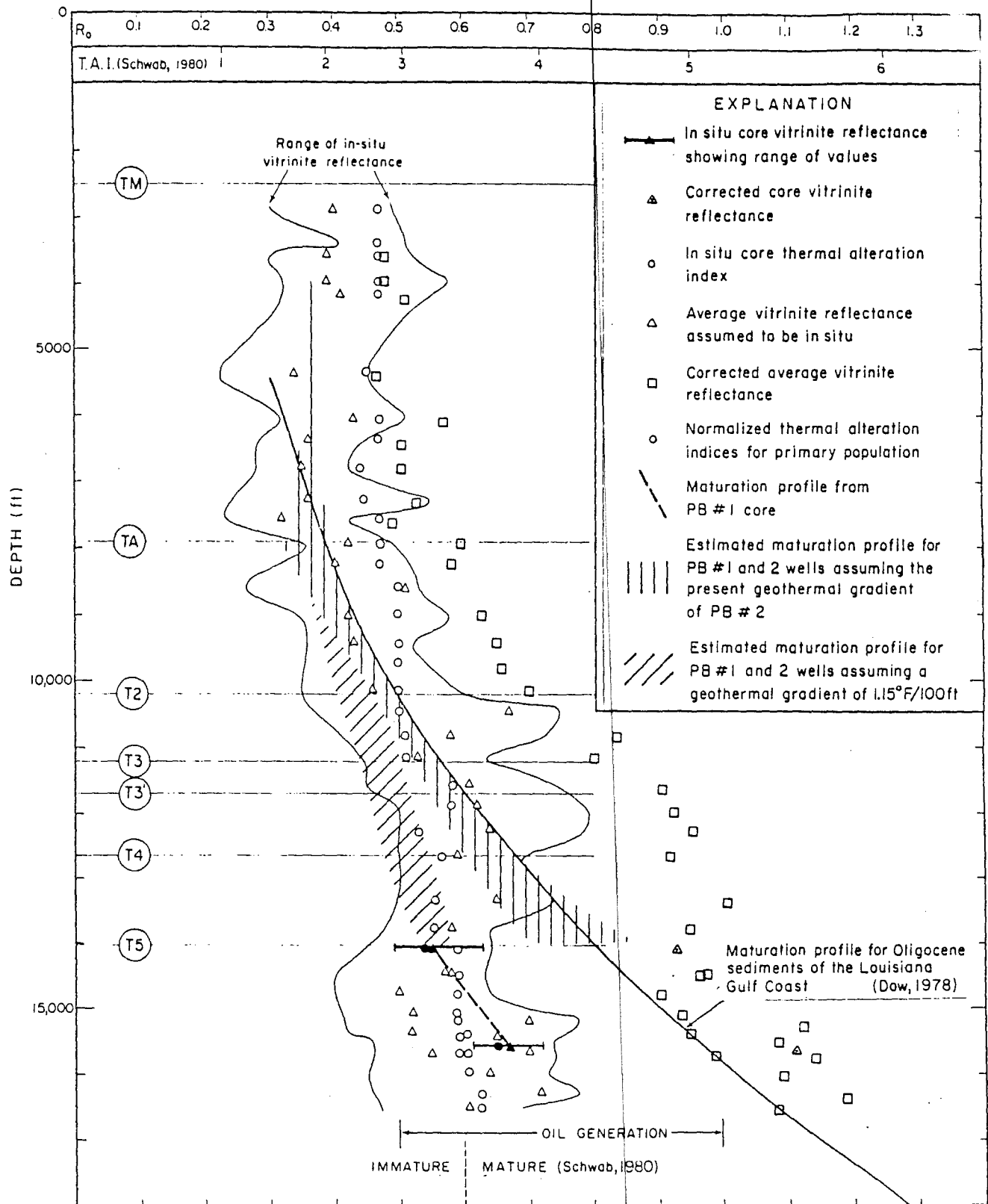


Figure II-1. Vitrinite reflectance and thermal alteration index versus depth for the Pleasant Bayou No. 1 well (Brown, 1980; Schwab, 1980). The reflectance profile is compared to the regional reflectance (Dow, 1978) and to calculated profiles using the present-day geothermal gradient at the test well and a low gradient of 1.15° F/100 ft (2.1° C/100 m) (modified from Ewing and others, 1984a).

Damberger, 1968). Vitrinite is known to be optically anisotropic in bituminous coals and may be a useful gauge for measuring burial pressures, as has been demonstrated for coals in the Appalachians (Teichmuller and Teichmuller, 1954; Wege, 1954; Hower and Davis, 1981).

Low maturation of the geopressured interval is not unique to the Pleasant Bayou area but has been documented elsewhere on the Gulf Coast. The geopressured interval at the L. R. Sweezy No. 1 well (Vermilion Parish, Louisiana), which contains very porous and permeable sandstones (28% porosity; 3,297 md permeability, respectively), is immature (Hamilton and Stanley, 1984). Higher maturities would normally be expected in the geopressured zones because of the increased geothermal gradient (Lewis and Rose, 1970). Such an increase is observed in the present geothermal gradient both in the Pleasant Bayou test wells and regionally in Brazoria County at the initiation of geopressure near the top of the Anahuac (figs. II-2 and II-3) (Ewing and others, 1984a; Loucks and others, 1981). The continuous increase in geothermal gradient at the Pleasant Bayou test wells (fig. II-2) does not match the anomalous vitrinite reflectance profile (Ewing and others, 1984a).

E. D. Pittman (personal communication, 1984) states that large concentrations of liptinitic macerals (Type 1 of Tissot and Welte, 1978) may retard vitrinite reflectance; as a result of heating, the vitrinite particles become coated in oil, reducing their reflectivity. Hence the organic matter may have been heated to a higher temperature than its vitrinite reflectance implies (E. D. Pittman, personal communication, 1984). However, the shales at Pleasant Bayou and L. R. Sweezy No. 1 are of poor source rock quality, and contain relatively small amounts of oil-prone amorphous organic matter (Brown, 1980; Hamilton and Stanley, 1984). In contrast to the low maturities present in many geopressured environments, the Sweet Lake test well (Terrebone Parish, Louisiana) shows an increased rate of indigenous vitrinite reflectance change compared to thermal alteration indices in the geopressured interval (Bayliss and Hart, 1981). Bayliss and Hart (1981) suggest that geopressing of the shales below 9,100 ft (2,700 m) at Sweet Lake may result in a higher induced surface maturation.

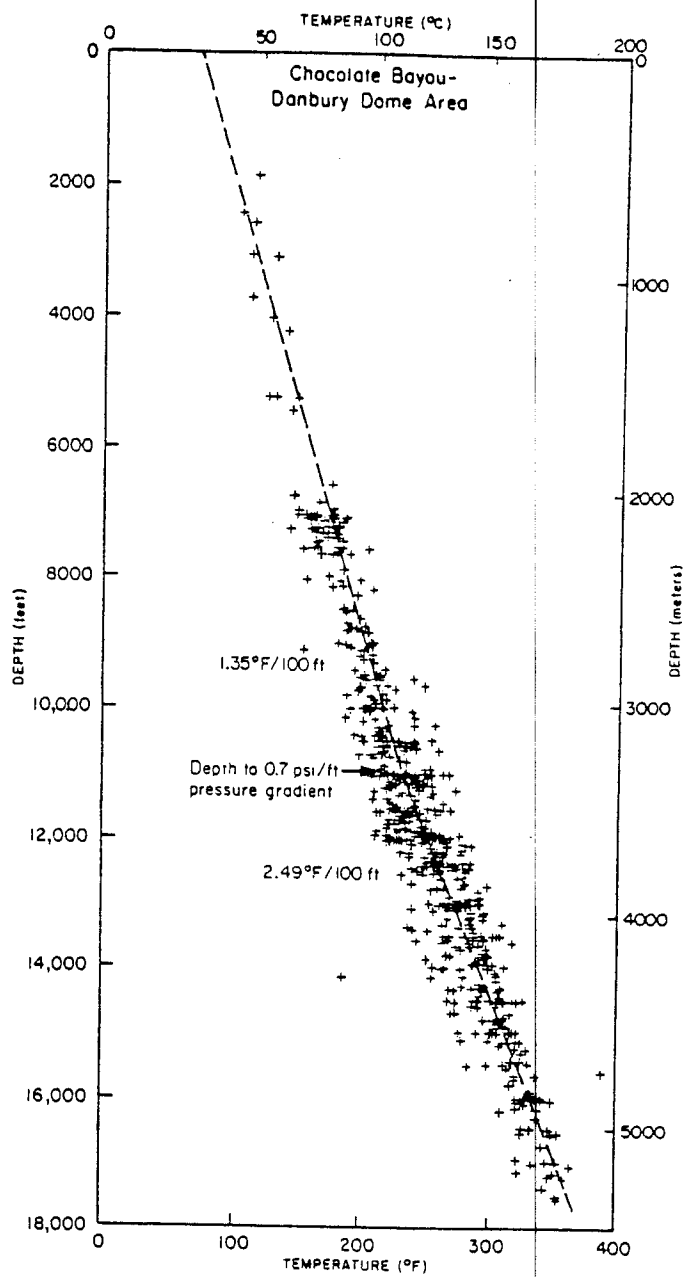


Figure II-3. Temperature versus depth, Chocolate Bayou - Danbury dome area, Brazoria County, Texas (Loucks and others, 1981).

To define more precisely the anomalous maturity profile at the Pleasant Bayou test wells and achieve a clearer understanding of its nature and origin, an estimate was made of the regional paleogeothermal gradient in the Chocolate Bayou - Danbury dome area. Vitrinite reflectance measurements were made for seven core samples from the Phillips Houston "GG" No. 1 and "JJ" No. 1 wells (Chocolate Bayou dome) and the Humble No. 1 Skrabanek and No. 1 Vieman wells on the south flank of the Danbury dome (fig. II-4, table II-1).

Histograms showing the population distribution for six of the samples are given in figure II-5. Though several populations are present, the lowest average vitrinite reflectance value in a core should represent the in situ organic maturity as caving contamination is eliminated (Schwab, 1980). Only two vitrinite reflectance measurements (0.46% Ro, 0.61% Ro) were possible for the Houston "GG" No. 1 core at 10,289 to 10,311 ft (3,136 to 3,143 m). The average maturity of 0.545 Ro is therefore highly suspect.

It is evident that the vitrinite reflectance values when plotted against depth do not form a clear linear trend (fig. II-4). Vitrinite reflectance profiles normally define linear maturation profiles when plotted on a logarithmic scale for basins that have experienced continuous sedimentation, such as the Gulf Coast (Galloway and others, 1982; Katz and others, 1984).

Vitrinite reflectance is a routine measurement made by estimating either maximum reflection in polarized reflected light or random ("average" or "mean") reflectance in non-polarized light (Hower and Davis, 1981). A large discrepancy exists between vitrinite reflectance measurements made by different laboratories on the same samples, or samples from the same depth, in both the Palo Duro Basin and the Pleasant Bayou test wells (S. Dutton, personal communication, 1984; unpub. data). The average range in vitrinite reflectance estimated by different laboratories on the same samples is about 0.14% Ro (fig. II-6), but the range increases with increasing depth, suggesting that it is related to vitrinite anisotropy due to burial pressure (figs. II-7 and II-8). GeoStrat, Inc., values tend

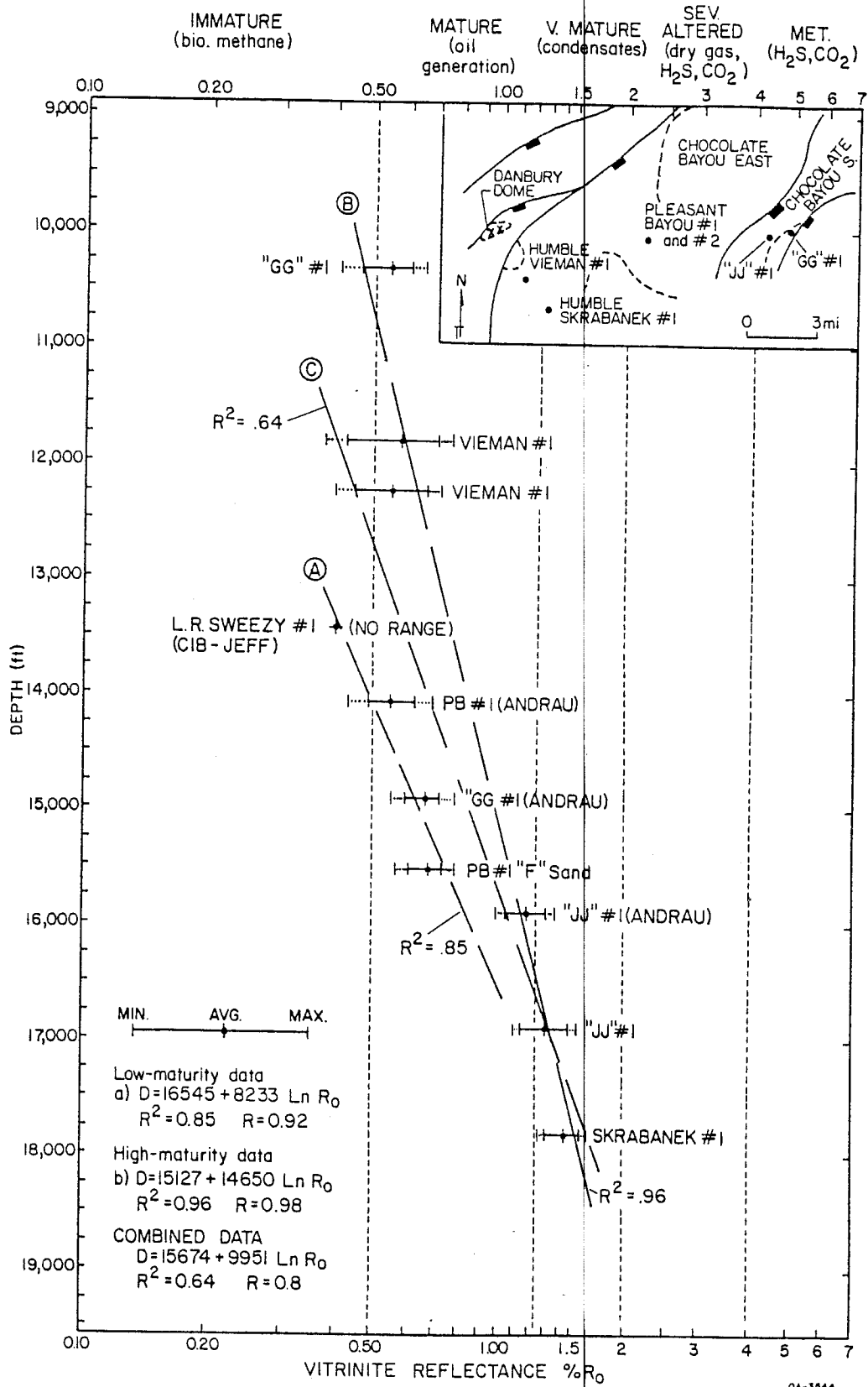


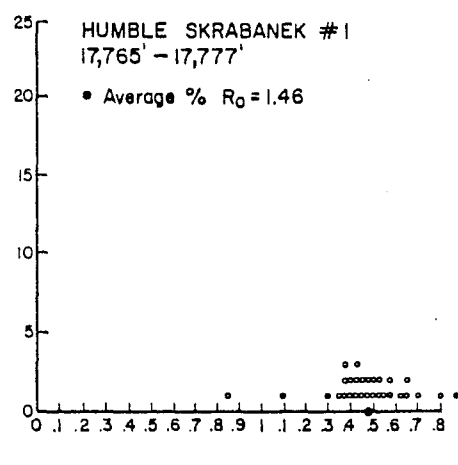
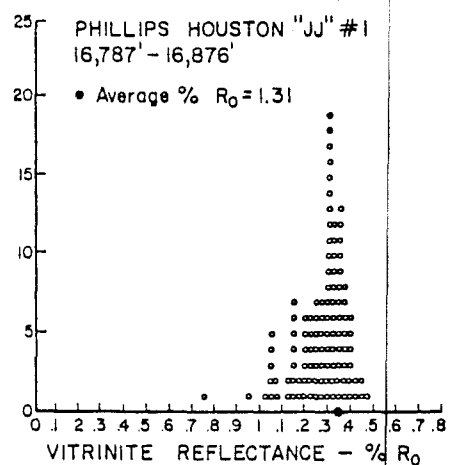
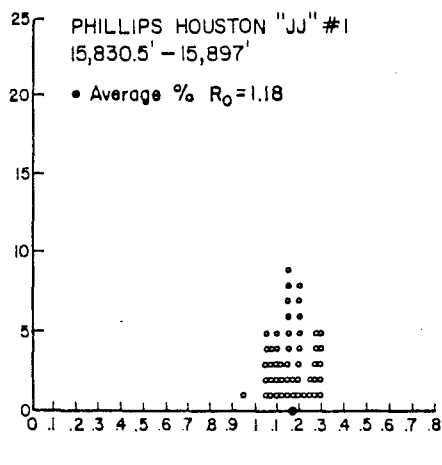
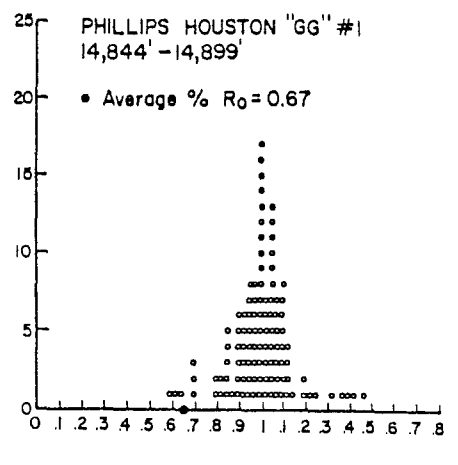
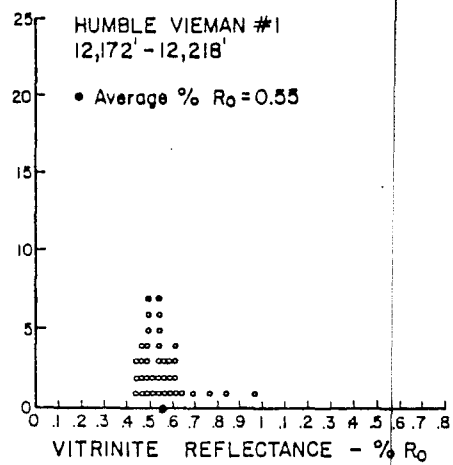
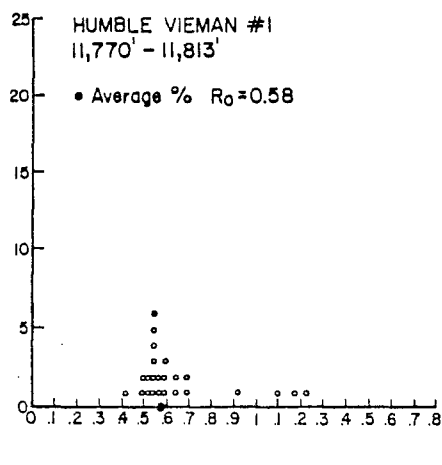
Figure II-4. Vitrinite reflectance profiles from core plugs from wells in the Chocolate Bayou-Danbury dome area (Schwab, 1984). DOW-DOE L. R. Sweezy No. 1 well. Data from Hamilton and Stanley (1984).

Table II-1. Vitrinite reflectance data for the Pleasant Bayou - Chocolate Bayou area.

29	Phillips Houston "GG"-1*			Phillips Houston "JJ"-1*			Humble Skrabanek #1*			Humble Vieman #1*			Pleasant Bayou #1**					
	Data points 14844'-14899'			Data points 15830.8'-15897'			Data points 16787'-16876'			Data points 17765'-17777'			Data points 11770'-11813'			Data points 12172'-12218'		
	1: 0.60	39: 0.98	77: 1.06	1: 0.96	39: 1.27	1: 0.75	39: 1.27	77: 1.34	1: 0.85	1: 0.43	1: 0.45	1: 0.77						
	2: 0.63	40: 0.98	78: 1.06	2: 1.05	40: 1.27	2: 0.97	40: 1.27	78: 1.34	2: 1.10	2: 0.51	2: 0.45	2: 0.80						
	3: 0.67	41: 0.98	79: 1.06	3: 1.05	41: 1.28	3: 1.03	41: 1.28	79: 1.35	3: 1.32	3: 0.52	3: 0.47	3: 0.82						
	4: 0.70	42: 0.98	80: 1.07	4: 1.05	42: 1.28	4: 1.05	42: 1.28	80: 1.35	4: 1.35	4: 0.53	4: 0.48	4: 0.84						
	5: 0.71	43: 0.99	81: 1.07	5: 1.06	43: 1.28	5: 1.06	43: 1.28	81: 1.35	5: 1.38	5: 0.54	5: 0.49	5: 0.85						
	6: 0.72	44: 0.99	82: 1.08	6: 1.07	44: 1.29	6: 1.06	44: 1.28	82: 1.35	6: 1.39	6: 0.55	6: 0.49	6: 0.86						
	7: 0.80	45: 1.00	83: 1.08	7: 1.08	45: 1.29	7: 1.07	45: 1.29	83: 1.35	7: 1.39	7: 0.56	7: 0.49	7: 0.87						
	8: 0.82	46: 1.00	84: 1.08	8: 1.08	46: 1.30	8: 1.07	46: 1.29	84: 1.35	8: 1.42	8: 0.56	8: 0.50	8: 0.91						
	9: 0.84	47: 1.00	85: 1.09	9: 1.09	47: 1.30	9: 1.08	47: 1.29	85: 1.36	9: 1.42	9: 0.57	9: 0.51	9: 0.92						
	10: 0.84	48: 1.00	86: 1.09	10: 1.09	48: 1.30	10: 1.08	48: 1.30	86: 1.36	10: 1.43	10: 0.57	10: 0.51	10: 0.92						
	11: 0.85	49: 1.00	87: 1.09	11: 1.11	49: 1.31	11: 1.14	49: 1.30	87: 1.36	11: 1.43	11: 0.57	11: 0.51	11: 0.94						
	12: 0.86	50: 1.00	88: 1.09	12: 1.11	50: 1.32	12: 1.14	50: 1.30	88: 1.37	12: 1.44	12: 0.58	12: 0.52	12: 0.96						
	13: 0.86	51: 1.00	89: 1.10	13: 1.12		13: 1.15	51: 1.30	89: 1.37	13: 1.46	13: 0.59	13: 0.52	13: 1.00						
	14: 0.87	52: 1.00	90: 1.11	14: 1.12		14: 1.15	52: 1.30	90: 1.37	14: 1.46	14: 0.61	14: 0.52	14: 1.05						
	15: 0.87	53: 1.00	91: 1.11	15: 1.12		15: 1.16	53: 1.30	91: 1.37	15: 1.48	15: 0.61	15: 0.53	15: 1.05						
	16: 0.89	54: 1.01	92: 1.12	16: 1.13		16: 1.17	54: 1.30	92: 1.38	16: 1.49	16: 0.61	16: 0.53	16: 1.05						
	17: 0.90	55: 1.01	93: 1.12	17: 1.13		17: 1.17	55: 1.31	93: 1.38	17: 1.50	17: 0.65	17: 0.55	17: 1.09						
	18: 0.90	56: 1.01	94: 1.12	18: 1.13		18: 1.17	56: 1.31	94: 1.38	18: 1.52	18: 0.66	18: 0.55	18: 1.15						
	19: 0.91	57: 1.01	95: 1.12	19: 1.15		19: 1.17	57: 1.32	95: 1.38	19: 1.53	19: 0.70	19: 0.55	19: 1.15						
	20: 0.91	58: 1.01	96: 1.12	20: 1.15		20: 1.18	58: 1.32	96: 1.38	20: 1.54	20: 0.71	20: 0.55	20: 1.17						
	21: 0.92	59: 1.02	97: 1.13	21: 1.16		21: 1.18	59: 1.32	97: 1.39	21: 1.55	21: 0.94	21: 0.56	21: 1.20						
	22: 0.92	60: 1.02	98: 1.13	22: 1.17		22: 1.20	60: 1.32	98: 1.39	22: 1.59	22: 1.09	22: 0.56	22: 1.23						
	23: 0.93	61: 1.02	99: 1.14	23: 1.17		23: 1.20	61: 1.32	99: 1.39	23: 1.59	23: 1.16	23: 0.57	23: 1.23						
	24: 0.93	62: 1.03	100: 1.14	24: 1.17		24: 1.21	62: 1.32	100: 1.40	24: 1.64	24: 1.24	24: 0.58	24: 1.34						
	25: 0.93	63: 1.03	101: 1.15	25: 1.17		25: 1.21	63: 1.32	101: 1.40	25: 1.65		25: 0.59	25: 1.35						
	26: 0.93	64: 1.03	102: 1.21	26: 1.17		26: 1.22	64: 1.32	102: 1.41	26: 1.67		26: 0.59	26: 1.36						
	27: 0.94	65: 1.03	103: 1.21	27: 1.17		27: 1.22	65: 1.32	103: 1.41	27: 1.72		27: 0.60	27: 1.48						
	28: 0.94	66: 1.04	104: 1.24	28: 1.18		28: 1.23	66: 1.32	104: 1.42	28: 1.82		28: 0.62	28: 1.50						
	29: 0.95	67: 1.04	105: 1.26	29: 1.18		29: 1.23	67: 1.33	105: 1.42	29: 1.89		29: 0.62	29: 1.51						
	30: 0.95	68: 1.04	106: 1.33	30: 1.21		30: 1.23	68: 1.33	106: 1.43			30: 0.63	30: 1.53						
	31: 0.96	69: 1.05	107: 1.39	31: 1.21		31: 1.23	69: 1.33	107: 1.44			31: 0.64	31: 1.53						
	32: 0.96	70: 1.05	108: 1.40	32: 1.21		32: 1.24	70: 1.33	108: 1.45			32: 0.64	32: 1.58						
	33: 0.96	71: 1.05	109: 1.44	33: 1.22		33: 1.24	71: 1.33	109: 1.46			33: 0.64							
	34: 0.96	72: 1.05	110: 1.48	34: 1.22		34: 1.25	72: 1.33	110: 1.48			34: 0.67							
	35: 0.97	73: 1.06		35: 1.22		35: 1.26	73: 1.33				35: 0.72							
	36: 0.97	74: 1.06		36: 1.22		36: 1.26	74: 1.33				36: 0.78							
	37: 0.98	75: 1.06		37: 1.22		37: 1.26	75: 1.34				37: 0.87							
	38: 0.98	76: 1.06		38: 1.24		38: 1.26	76: 1.34				38: 0.98							

*Geo-Strat Inc.

**Roberston Research Inc.



QA-3543

Figure II-5. Histograms showing the population distribution of vitrinite reflectance analyses of core samples in the Chocolate Bayou - Danbury dome area (Schwab, 1984).

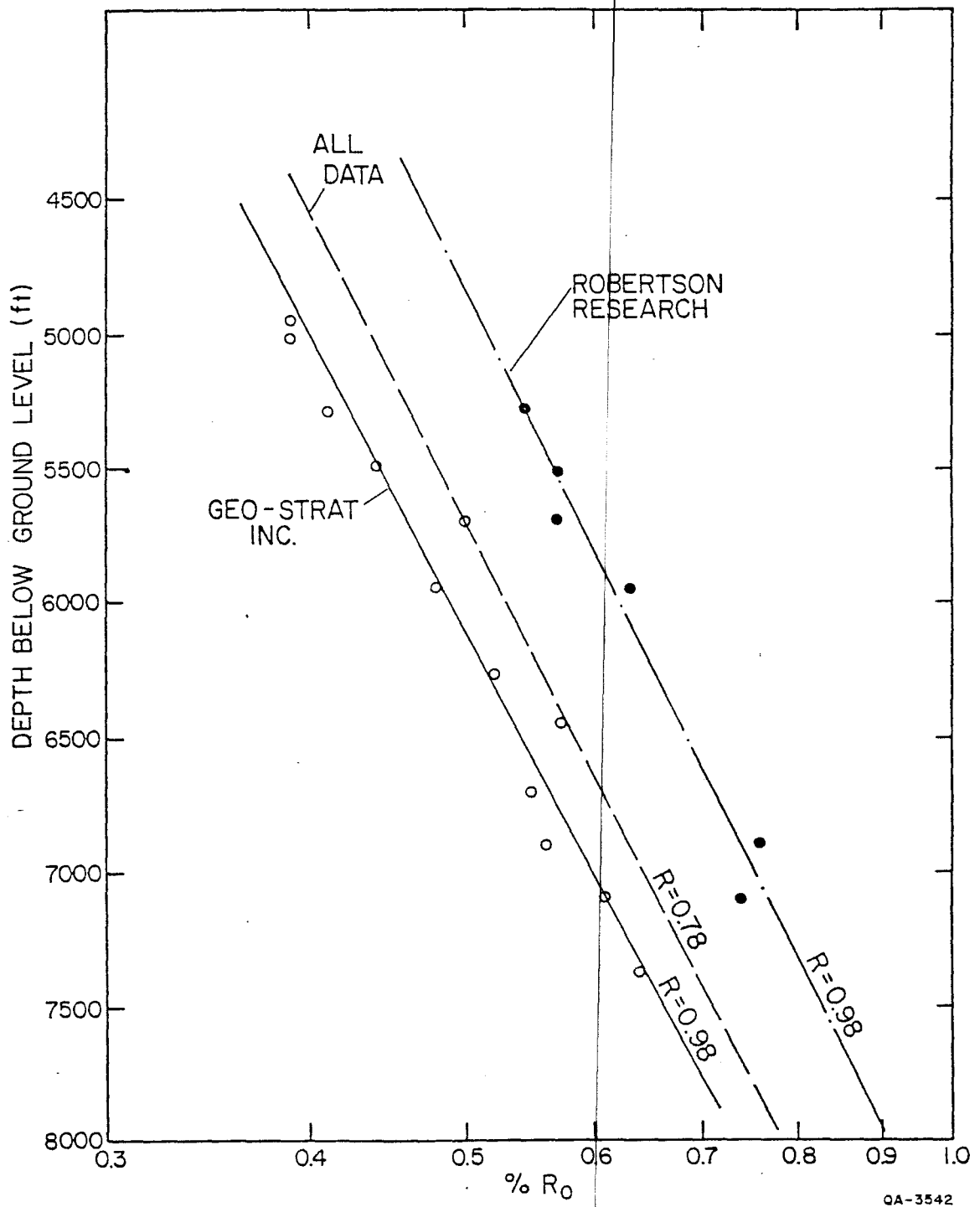
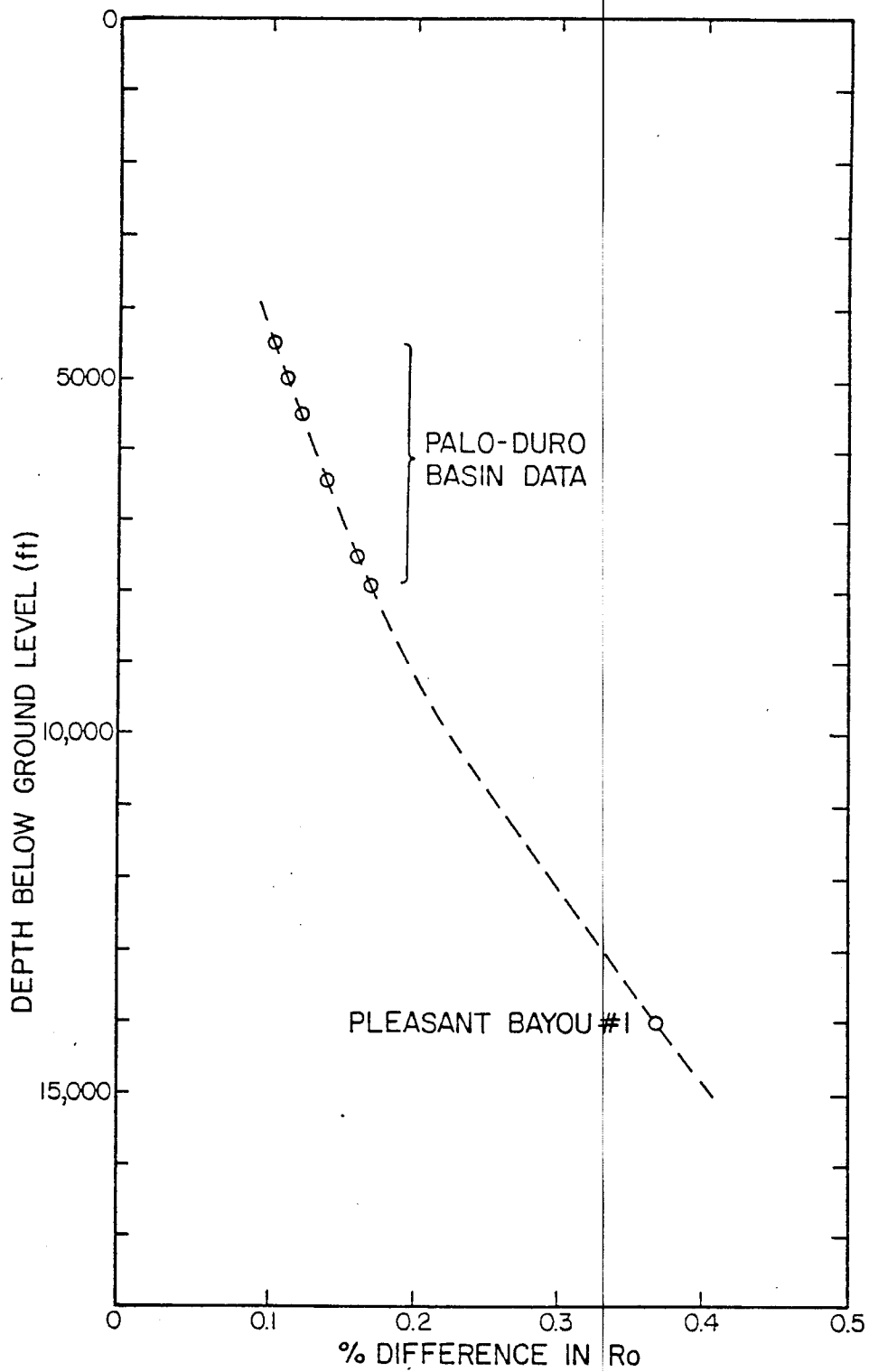
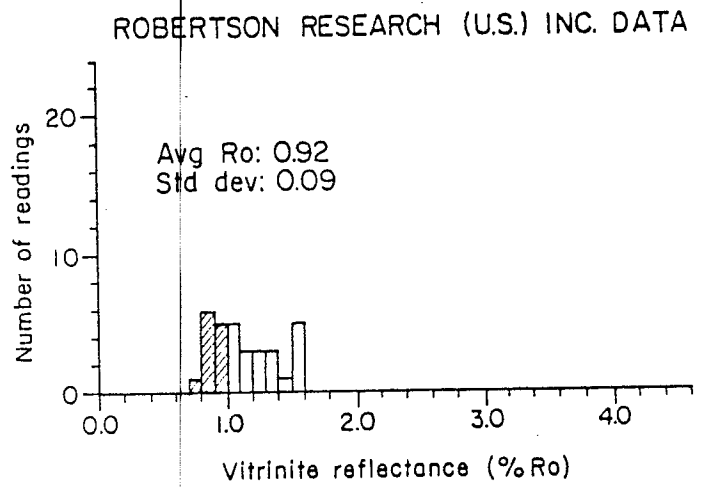
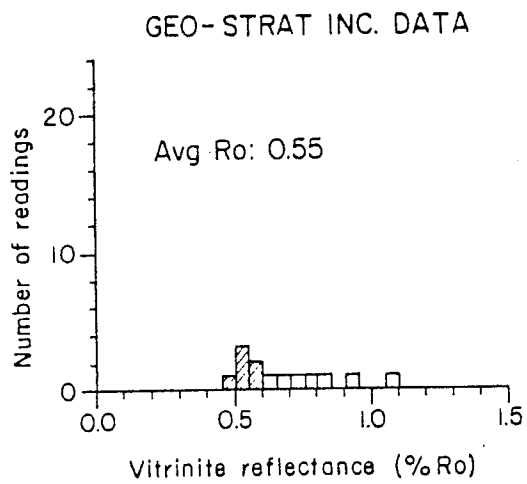


Figure II-6. Vitrinite reflectance versus depth for samples from the Palo Duro Basin (S. P. Dutton, personal communication, 1984).



QA-3541

Figure II-7. The estimated discrepancy in the measurement of vitrinite reflectance versus depth. Data from S. P. Dutton, personal communication, 1984; Schwab, 1980; and O'Connor, 1984.



Population used in Ro estimate

QA3540

Figure II-8. Vitrinite reflectance histograms from two laboratories for one sample of well core taken at 14,078 ft in the Pleasant Bayou No. 1 well (Schwab, 1980; O'Connor, 1984).

to be consistently lower than those of Robertson Research (S. Dutton, K. W. Schwab, and W. G. Dow, personal communications, 1984). Despite the differences in the absolute values of the estimates of the vitrinite reflectance made at these two laboratories, they show similar trends with depth (fig. II-6; S. Dutton, personal communication, 1984). GeoStrat's estimate of the vitrinite reflectance profile for Pleasant Bayou No. 1, therefore, requires the addition of an increasing correction with depth before it can be compared to Robertson Research's estimates of the average maturity profile for Oligocene rocks in Louisiana (fig. II-9). These errors place severe limitations on the interpretation of thermal maturities unless a correction is applied, but this problem could be resolved if a system of standards were introduced. Corrected low maturity data for the Pleasant Bayou No. 1 and Phillips Houston "GG" No. 1 wells (figs. II-1 and II-9) plot near the normal maturity profile and give results consistent with models using the extant geothermal gradient superimposed over the Pleasant Bayou subsidence curve (Ewing and others, 1984a). Moreover the "normal maturity group" in figures II-1 and II-9 now show an anomalously high thermal maturity.

There are several possible explanations for the range in vitrinite reflectance values in the Chocolate Bayou - Danbury dome area. One explanation is that there is a large inherent error in their estimation. In this instance the average paleogeothermal gradient will be a least squares linear estimate of the natural logarithms of the vitrinite reflectance data. K. W. Schwab (personal communication, 1984) states that the accuracy of measuring vitrinite reflectance is on the order of 0.05% R_o ; for vitrinite reflectance values lower than 0.45% R_o , the error is so large that values are unreliable. Addition of this error to the standard deviations of the vitrinite measurements in figure II-9 essentially eliminates the low maturity anomaly in the Andrau sandstone at Pleasant Bayou (fig. II-4, line C). However, the modified data still defines a low maturity anomaly at the "F" sandstone level in Pleasant Bayou, the Andrau sandstone in the Houston "GG" No. 1 well, and the L. R. Sweezy No. 1 well (fig. II-4).

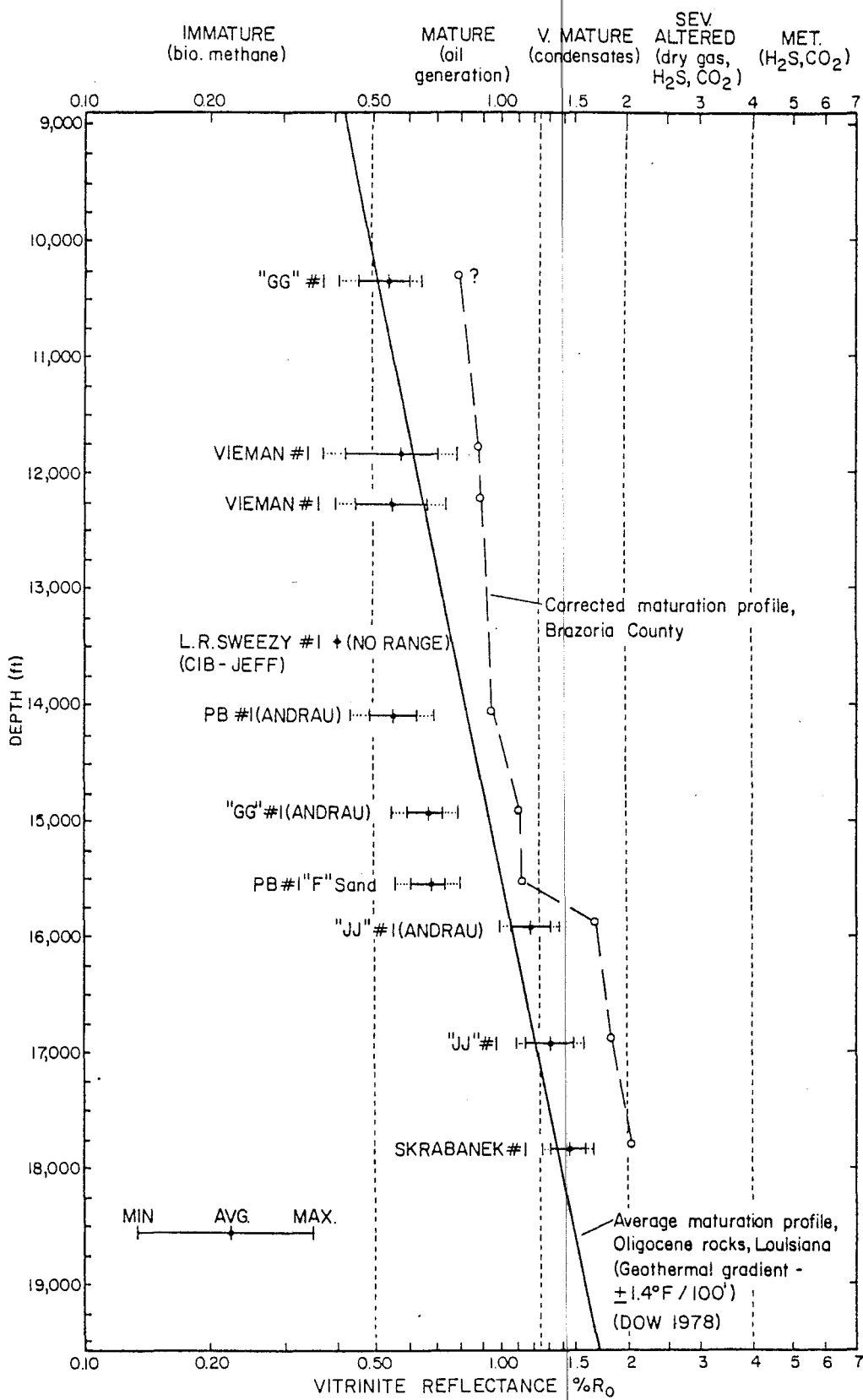


Figure II-9. Corrected vitrinite reflectance values for core samples from the Chocolate Bayou-Danbury dome area, Brazoria County, Texas, compared to Dow's (1978) regional paleogeothermal gradient for Oligocene rocks in Louisiana.

The alternative explanation requires subdivision of the maturity data into two groups. A least squares linear estimate has been made for the "normal" and "high" maturity groups and for the combined data. The linear correlation coefficient for the "normal" and "high" maturity groups is 0.92 and 0.98, respectively. The correlation coefficient for the combined data is 0.8, which suggests that they form two distinct populations. Evidently as seen at present, the highly geopressured lower Frio (pre-T5) succession (figs. II-1 and II-9) has been subjected to an average geothermal gradient between 1.4 and 1.6° F/100 ft (2.5 to 2.9° C/100 m) (figs. II-2 and II-3). The higher thermal maturity of the upper Frio (T2 to T5 succession) is thought to be a consequence of heating by the updip migration of hot basinal fluids formed during compaction and diagenesis of slope shales (fig. II-10, Model 2, Ewing and others, 1984a, b; Burst, 1969). A reduction to almost normal pressure in the upper Frio may have allowed fluid migration to occur, while fluid movement would have been slower or static in the highly geopressured lower Frio (pre-T5 succession) (fig. II-10; Flanagan, 1980). Hence the lower Frio will show a thermal maturity consistent with the existing geothermal gradient. The anomaly in the extant geothermal gradient at Pleasant Bayou in the T2 to T5 interval is evidence that this fluid flow has not yet terminated (fig. II-2).

ORIGIN OF HYDROCARBONS

Relative Age of Hydrocarbons and Thermal Maturity of Source Rocks

Because hydrocarbons in oils change as they mature, compositional variations may be used to estimate an oil's age (Young and others, 1977). These computations require a knowledge of the burial history and geothermal gradient and require a detailed chemical analysis of oils for the section with which the oil samples are associated.

The calculation of ages for gasoline-range hydrocarbons is based on the apparent disproportionation of naphthenes to give paraffins and aromatics (table II-2). Ten naphthenes (cyclopentane to ethylcyclopentane), 17 paraffins (isopentane to N. heptane), and 2 aromatics (benzene and toluene) are used in the hydrocarbon age calculation (Young

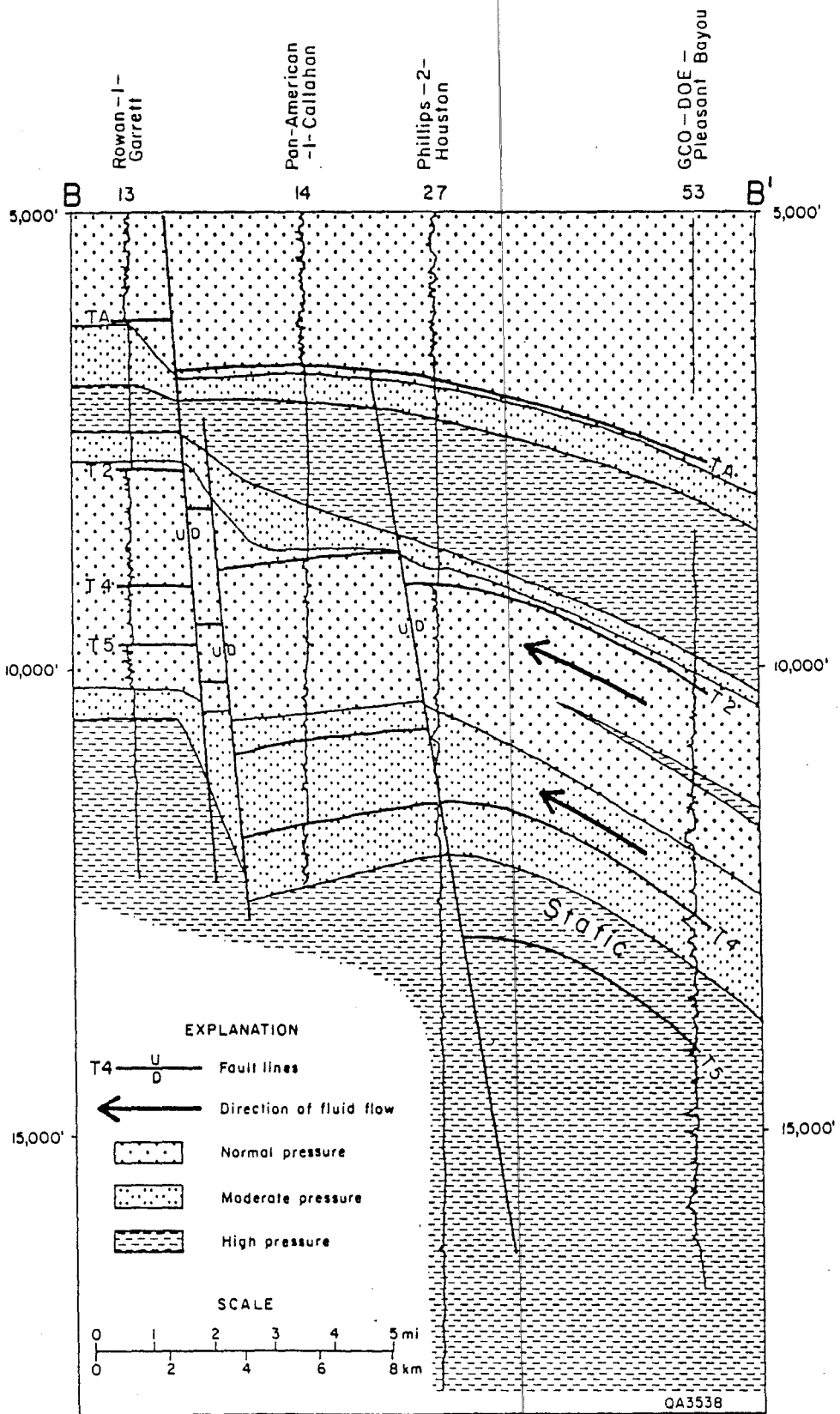


Figure II-10. Northwest-southeast regional section showing the pressure regime distribution in the Pleasant Bayou area. Possible directions of shale water flow during compaction and diagenesis are shown. Modified from Flanagan (1980).

Table II-2. Disproportionation of naphthenes to paraffins and aromatics.

Disproportionation reaction for naphthenes



Normalized naphthene concentration

$$[N] = \frac{N}{N+P+A} \quad \text{-----} \quad \text{---2}$$

Time rate change of concentration

$$\frac{d[N]}{dt} = -K[N] \quad \text{-----} \quad \text{---3}$$

Reaction rate "constant"

$$K = be^{-\frac{E}{RT}} \quad \text{-----} \quad \text{---4}$$

Natural logarithm of normalized naphthene concentration

$$\ln [N] = -b \cdot TTI + a \quad \text{-----} \quad \text{---5}$$

Time temperature index

$$TTI = \int_{t=0}^{t=t} e^{-\frac{E}{RT}} dt \quad \text{-----} \quad \text{---6 (equations 2 through 6 from Young and others, 1977)}$$

N = naphthenes

R = universal gas constant

P = paraffins

T = absolute temperature °K

A = aromatics

b = constant

[N] = normalized naphthene concentration

t = time at which reaction concentration is C

K = reaction rate constant at temperature t

e = base of natural logarithmic system

E = activation energy of the reaction

a = constant (equal to LnC at t=0)

and others, 1977). It was not possible to improve the accuracy of the method by deleting certain of the individual compounds or groups of compounds. Detailed chromatographic analyses of only the C5 to C7 (light gasoline-range) hydrocarbons were available for the Pleasant Bayou test wells over the interval of 2,072 to 16,500 ft (630 to 5,030 m) (table II-3; Brown, 1980). These analyses of cuttings and core samples include 9 naphthenes, 16 paraffins, and 2 aromatics. Though the relative ages are therefore not directly compatible with ages reported by Young and others (1977), the error is probably small because almost the complete suite of light gasoline-range hydrocarbons is considered.

The time and temperature integrals for various marker horizons have been estimated for the Pleasant Bayou wells using a burial history plot (Ewing and others, 1984a, b) and equation 6 of table II-2. The theoretical normalized naphthene concentration (N) calculated with equation 5 of table II-2 is given for the different marker horizons on figure II-11. The marker horizons within the Oligocene Frio (T2 to Andrau sandstone interval) plot within the zone of Oligocene unmigrated hydrocarbons defined by Young and others (1977) (fig. II-11). However, the analyzed light hydrocarbon (naphthene) concentrations for the entire succession at Pleasant Bayou suggest that they are derived from much older rocks (fig. II-11). This is consistent with Young and others' (1977) findings that hydrocarbons in the upper Tertiary reservoirs of offshore Louisiana were derived from Oligocene or older sediments buried from 12,000 to 24,000 ft (3,600 to 7,300 m). There has been a general upward migration of hydrocarbons in sediments both in this area and the Gulf Coast region (Young and others, 1977; Burst, 1969).

It is clear that the hydrocarbons have a deep source if the naphthene fraction of the Pleasant Bayou data is expressed as TTI (using equation 5, table II-2) and is plotted against depth (fig. II-12). The high thermal maturities (TTI) shown by hydrocarbons above the T5 marker horizon (Miocene, upper and lower Frio) compared to the estimated thermal maturity of the sediments derived from burial history indicate that they have migrated up from more deeply buried, more mature source rocks. High geopressure below T5 probably

Table II-3. Normalized naphthene concentration for the Pleasant Bayou No. 1 well.

Avg. Depth	Paraffins SISOP.*Wi	Naphthenes SCyclo.Wi	Aromatics SBenz.*Wi	Ratio =		ln Ratio
				$\frac{\text{Naphthenes}}{\text{P} + \text{N} + \text{A}}$	$\frac{\text{P} + \text{N} + \text{A}}{\text{P} + \text{N} + \text{A}}$	
2,088	4,082.2	2,141.25	861.01	7,084.46	0.30	-1.20
2,894	4,200.53	2,552.83	723.62	7,476.98	0.34	-1.07
3,386	5,344.52	1,884.55	639.70	7,868.77	0.24	-1.43
3,693	3,184.88	1,211.89	344.09	4,740.86	0.26	-1.36
3,974	4,137.46	1,020.63	139.80	5,297.89	0.19	-1.65
4,160	4,401.69	500.64	141.20	5,043.53	0.10	-2.31
5,330	4,528.44	894.79	172.44	5,595.67	0.16	-1.83
5,690	4,308.66	838.38	216.31	5,363.35	0.16	-1.86
6,050	4,006.43	1,485.66	194.27	5,686.36	0.26	-1.34
6,350	4,209.62	885.37	158.82	5,253.61	0.17	-1.78
6,770	4,383.54	999.89	174.45	5,557.88	0.18	-1.72
6,950	2,740.31	609.25	161.03	3,510.59	0.17	-1.75
7,250	3,453.44	1,704.73	297.83	5,456.0	0.31	-1.16
7,550	3,861.64	1,203.17	390.75	5,455.56	0.22	-1.51
7,860	3,416.84	1,119.31	312.04	4,848.19	0.23	-1.47
8,160	3,516.42	899.20	256.76	4,672.38	0.19	-1.65
8,570	4,353.91	969.43	248.95	5,572.29	0.17	-1.75
8,990	4,598.41	735.68	195.08	5,529.17	0.13	-2.02
9,410	6,264.71	987.36	348.29	7,600.36	0.13	-2.04
9,710	4,155.03	503.25	221.31	4,879.59	0.10	-2.27
10,130	4,634.10	709.83	306.43	5,650.36	0.13	-2.07
10,430	4,140.62	741.09	353.30	5,235.01	0.14	-1.96
10,790	3,898.26	677.57	325.66	4,901.49	0.14	-1.98
11,150	3,997.33	469.28	198.68	4,665.29	0.10	-2.30
11,570	4,493.86	481.71	262.57	5,237.36	0.09	-2.39
11,870	4,991.96	1,194.64	295.22	6,481.82	0.18	-1.69
12,230	4,241.89	1,019.32	287.41	5,548.62	0.18	-1.69
12,650	3,979.70	917.82	419.99	5,317.51	0.17	-1.76
12,950	5,669.12	908.70	262.57	6,840.39	0.13	-2.02
13,310	4,499.18	582.49	205.09	5,286.76	0.11	-2.21
13,730	3,635.02	806.41	353.30	4,794.73	0.17	-1.78
14,030	6,253.12	859.11	166.03	7,278.26	0.12	-2.14

Table II-3. (cont.)

Avg. Depth	Paraffins SISOP.*Wi	Naphthenes SCyclo.Wi	Aromatics SBenz.*Wi	P + N + A	Ratio =	ln Ratio
					$\frac{\text{Naphthenes}}{\text{P} + \text{N} + \text{A}}$	
14,460	5,448.60	686.29	90.13	6,225.02	0.11	-2.21
14,470	4,982.99	2,771.79	199.88	7,954.66	0.35	-1.05
14,770	4,790.28	2,118.57	156.62	7,065.47	0.30	-1.20
15,070	4,684.18	1,990.44	92.13	6,766.75	0.29	-1.22
15,110	4,325.34	1,494.00	163.83	5,983.17	0.25	-1.39
15,370	4,664.75	1,741.67	92.13	6,498.55	0.27	-1.32
15,410	4,738.92	1,711.79	154.62	6,605.28	0.26	-1.35
15,650	4,658.02	2,126.18	171.64	6,955.84	0.31	-1.19
15,670	4,612.51	1,781.24	55.28	6,449.03	0.28	-1.29
15,970	3,819.75	1,531.18	186.46	5,537.39	0.28	-1.29
16,270	4,570.85	1,631.16	147.41	6,349.42	0.26	-1.36
16,490	4,421.54	1,667.63	143.20	6,232.26	0.27	-1.32

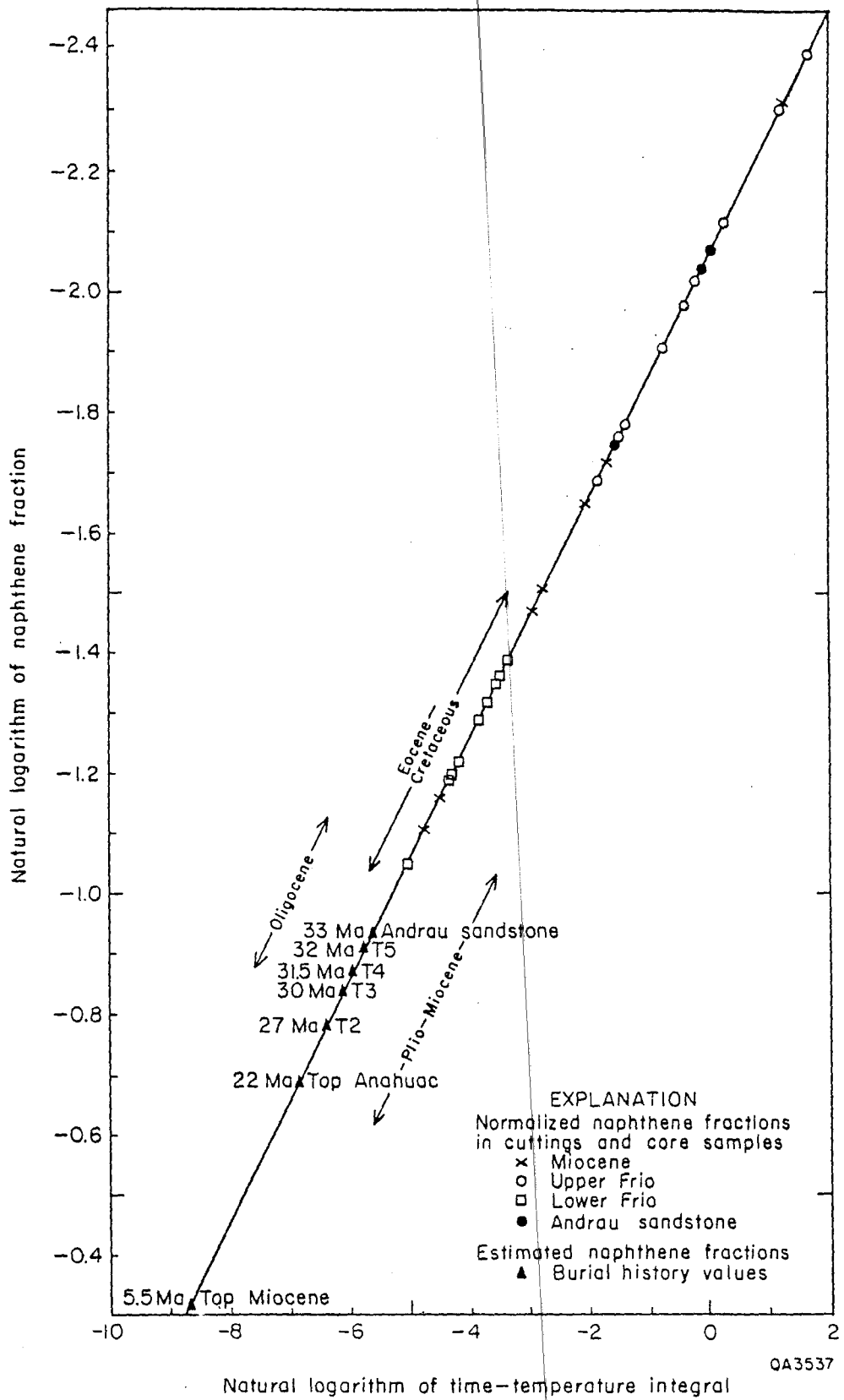


Figure II-11. Natural logarithm of the naphthene fraction versus the natural logarithm of the time-temperature integral for the Pleasant Bayou No. 1 geothermal test well. Age ranges of naphthene fractions are from Young and others (1977).

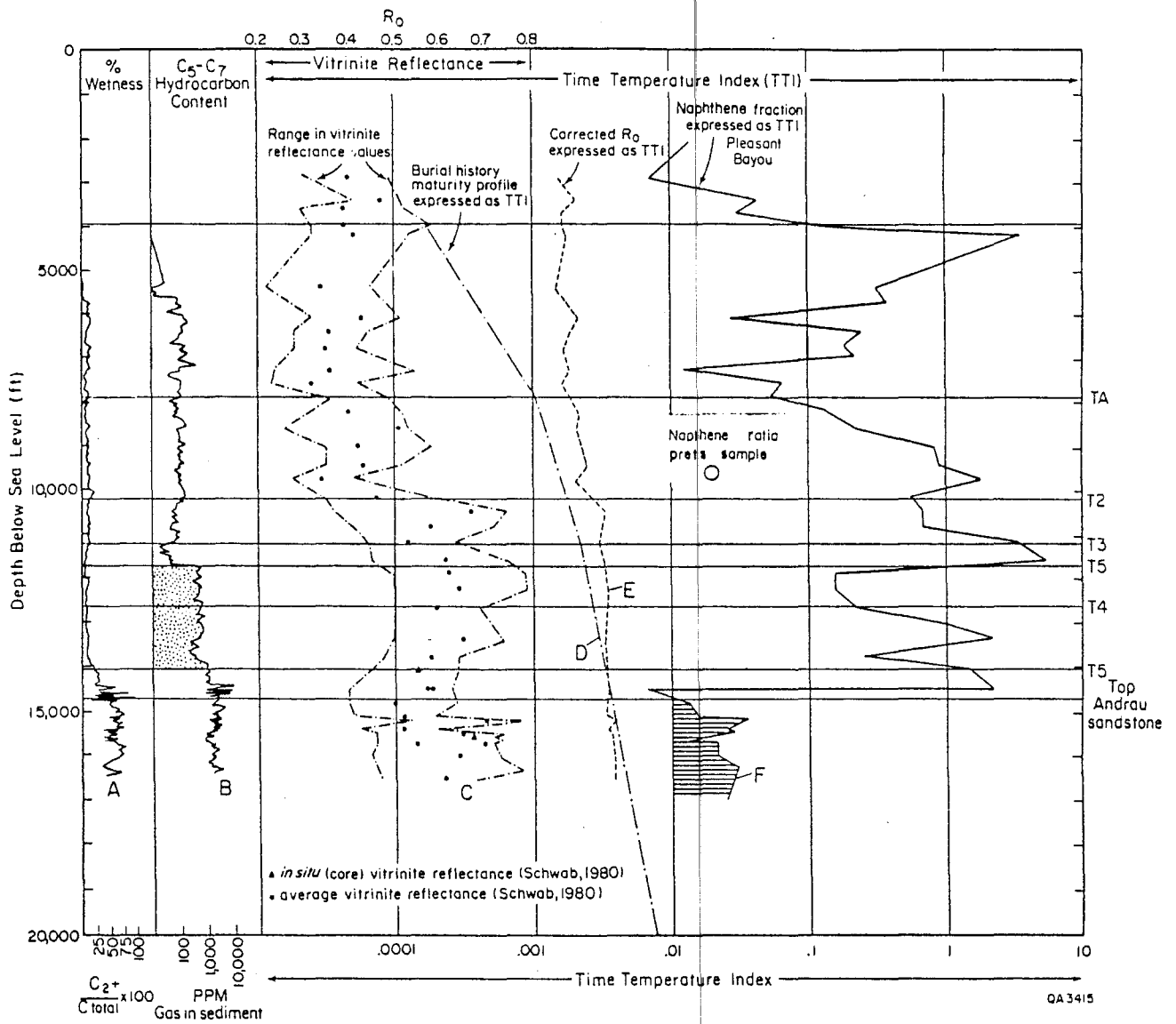


Figure II-12. Naphthene fraction expressed as time-temperature indices (TTI) versus depth for the Pleasant Bayou No. 1 well compared to the burial history maturity profile and the corrected vitrinite reflectance, both expressed as time-temperature indices (TTI). The uncorrected vitrinite reflectance, percent wetness, and C5-C7 hydrocarbon content in 1 million volumes of sediment versus depth is shown for comparison (Schwab, 1980).

arrested fluid flow, and the hydrocarbons present are more locally derived. The discrepancy between the hydrocarbon maturity data and the burial history thermal maturity profile (expressed as TTI) of the lower Frio Formation (below T5) may represent a slight systematic error in the calculation of the thermal maturity (TTI) from the naphthene concentration.

The overmature hydrocarbon anomaly in the upper Frio (T2 to T5 interval) is matched by an equivalent vitrinite reflectance anomaly over the same section as described above. This vitrinite reflectance when corrected and expressed as TTI is consistent with the burial history thermal maturity profile for the lower Frio (pre-T5) (fig. II-12). The vitrinite reflectance shows higher thermal maturities in the upper Frio (T2 to T5 interval) than the estimated (burial history) maturities (fig. II-12). This is similar to the behavior of the hydrocarbon maturation data suggesting that the upper Frio has been heated by hot, hydrocarbon-bearing fluids. The presence of an anomalous concentration of C5 to C7 hydrocarbons in the upper Frio (T3 to T5 succession) in a zone of relatively low wetness is consistent with the idea that they have been introduced (fig. II-12, Brown, 1980). The thermal maturity (vitrinite reflectance) above T5 (upper Frio) is far lower than the maturity of the contained hydrocarbons (fig. II-12). This indicates that the fluids had lost much of their heat to their surroundings by the time they had reached these shallower levels. However, the hydrocarbon composition still records the high maturity of the source rocks in which it was generated. High thermal maturities above T2 (Miocene and Anahuac) are highly suspect because they are based on vitrinite reflectance values of less than 0.45% Ro.

Isotope Ratios of Gases

The isotopic composition of carbon (ΔC^{13} expressed as o/oo) in hydrocarbons depends on the thermal history and type of source material (Galimov, 1968; Stahl, 1977; Chung and Sackett, 1979). Bacterially derived methane has a carbon isotope composition more

negative than -55 o/oo; oil associated methane ranges from -30 to -55 o/oo; coal and magmatic methane from -20 to -30 o/oo (Stahl and others, 1981; Schoell, 1983).

The carbon isotopic ratio of methane from natural gas reservoirs increases in response to the increasing maturity of its source (fig. II-13; Galimov, 1968; Stahl, 1977). Indigenous gas (still trapped in its source rock) has the same carbon isotopic maturity as the thermal maturity of the rock in which it formed (Schoell, 1983). However, the isotopic compositions of gases do not alter appreciably if they migrate (Stahl and Carey, 1975; Fuex, 1980; Schoel, 1983; James, 1983). Hence hydrocarbons within the surface sediments from the Gulf of Mexico have carbon isotopic values which record the isotopic composition of their source (Stahl and others, 1981). Methane sampled directly from offshore Brazoria County has a carbon isotopic composition close to -37 o/oo. This converts to an isotopic maturity of about 2% Ro (figs. II-13 and II-14) (Stahl, 1977, 1978). This methane probably originated in Oligocene or older sediments at depths below 20,000 ft (6,100 m) (Dow, 1978).

Carbon dioxide and methane are believed to undergo isotopic exchange during their formation, and the carbon isotope fractionation between them changes as a function of temperature (Craig, 1953; Bottinga, 1969). Humic acid and carboxylic acids on high molecular weight will decompose in high-temperature water and oil shale to produce abundant acetate and similar anions (Weres and others, 1984). This appears to be the major decomposition mechanism for aliphatic carboxylic acid groups, and fully accounts for the presence of acetate in gas field waters. Once formed, the acetate decomposes more slowly to methane (Weres and others, 1984). Carothers and Kharaka (1978) have reported the presence of acetate and other organic acid anions in many oil and gas field brines from reservoirs between 176° and 356° F (80° and 180°C). At the L. R. Sweezy No. 1 well, acetic acid is the most abundant carboxylic acid present in the geopressured brine (table II-4). Carothers and Kharaka (1978) proposed that these anions are precursors of methane and other light hydrocarbons. Acetic acid will decarboxylate to form methane

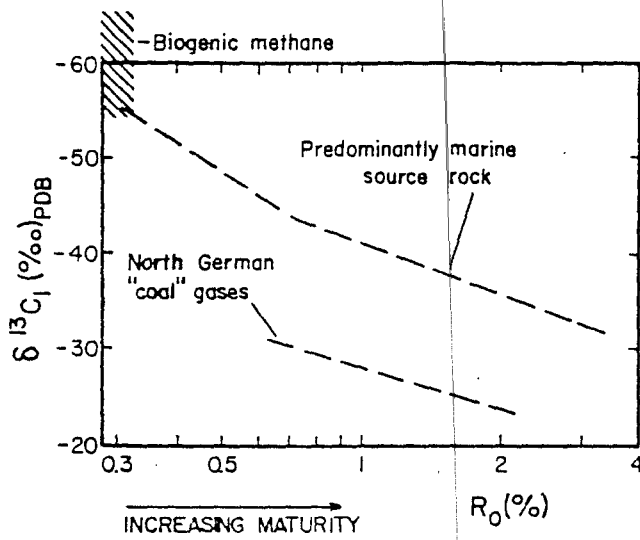


Figure II-13. Relation between carbon isotopic composition of methane from natural gas reservoirs and maturity (vitrinite reflectance R_0) of their source rocks (modified from Stahl, 1977, 1978; and Faber, 1979).

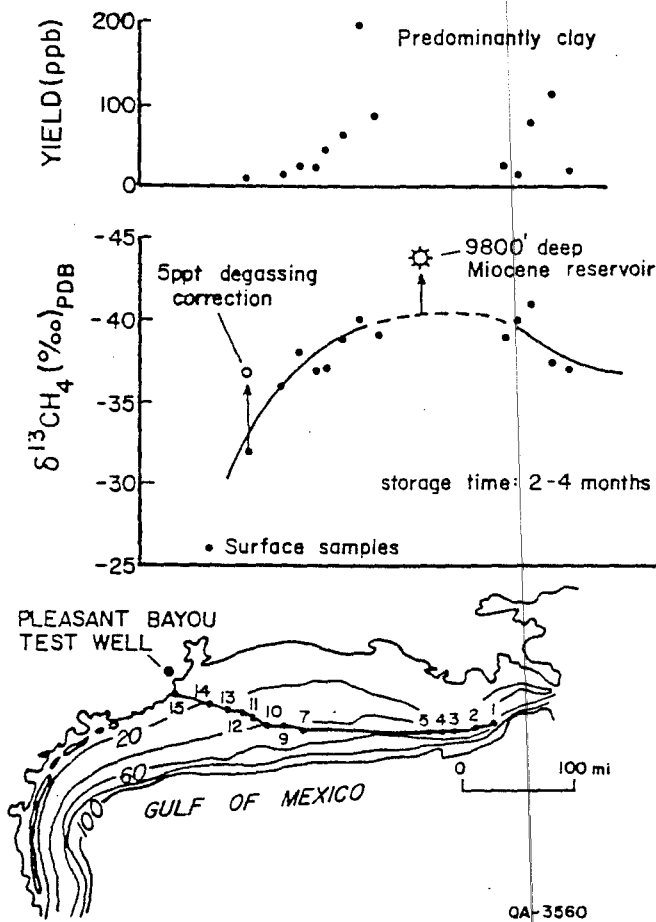


Figure II-14. Geochemical survey of the Gulf of Mexico (bathymetry in fathoms). Carbon isotopic composition for a surface sample from offshore Brazoria County is corrected by 5 ppt for degassing (Stahl and others, 1981).

Table II-4. Water soluble organic compounds in brine from
the DOW-DOE L. R. Sweezy #1 well, Louisiana
(Weres and others, 1984).

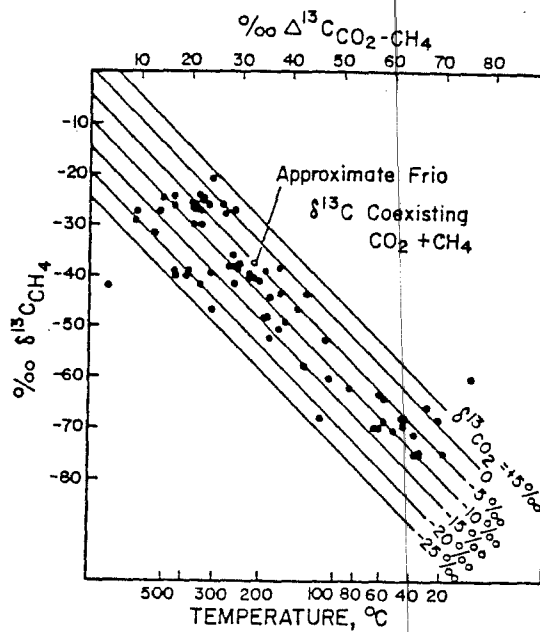
acetic acid
propionic acid
butyric acid
isobutyric acid
butanedioic (succinic) acid
pentanedioic (glutaric) acid
benzoic acid
isovaleric acid
valeric acid
methylsuccinic acid
p-toluic acid

and carbon dioxide at high temperatures; this is probably the source of coexisting carbon dioxide and methane in oil field brines (Kharaka and others, 1983).

For some coexisting methane and carbon dioxide there is an approximate correspondence between the temperature at which they form and the temperature deduced from carbon isotopic composition (Bottinga, 1969). The average carbon isotope composition for methane for the coastal zone of Brazoria County has been shown to be about -37 o/oo (Stahl and others, 1981). The average carbon isotopic composition of carbon dioxide gas produced from Frio reservoirs is 5.3 o/oo (Lundegard and others, 1984). The temperature of formation of these gases is estimated from figure II-15 to be 428°F (220°C). This converts to a depth of about 20,000 ft (6,100 m) using the present geothermal gradient of the Pleasant Bayou wells (Ewing and others, 1984a). These gases appear to have formed in the slope facies of the Vicksburg or lower Frio in Brazoria County.

Lundegard and others (1984) stated that material balance considerations, timing of decarboxylation, and carbon isotope data all indicate that simple decarboxylation of kerogen was not the cause of the secondary porosity in the Frio. There is only one-tenth of the required amount of carbon dioxide, insufficient acid and water to account for secondary porosity and sandstone diagenesis (Land and Dutton, 1978; Bjorlykke and Malm, 1979). Carbon dioxide produced by complete decarboxylation of organic matter has an approximate carbon isotope composition of -20 o/oo (Stahl and Tang, 1971; Claypool and Kaplan, 1974). The Frio and Wilcox isotope data, though indicating an influence of organically derived carbon dioxide by simple decarboxylation, do not support input of carbon dioxide with carbon isotope compositions as light as -20 o/oo (Lundegard and others, 1984).

Franks and Forester (1984) have demonstrated that the carbon dioxide content of gases in the Eocene Wilcox varies systematically with both reservoir age and temperature, which suggests a kinetic control of generation. The stable isotope analyses of carbonate cements also seem to indicate a strong component of organically derived carbon. Similar



QA-3559

Figure II-15. Relationship between methane isotopic composition and the carbon isotope fractionation between CH_4 and CO_2 in non-associated natural gases. The relationship between carbon isotope fractionation and temperature was derived from the work of Bottinga (1969).

relationships have been found for wells in the Department of Energy test well program including the Pleasant Bayou test wells (Morton and others, 1981). Morton and others (1981) stated that the generation of carbon dioxide in conjunction with thermal maturation of organic material would partly explain the differences in carbon dioxide concentrations for waters of different ages. Land (1984) has shown that the strontium isotope ratios of fluids in the Plio-Pleistocene rocks in the Gulf Coast have chemical signatures that could have been derived only from Mesozoic sediments, probably Jurassic-age carbonates. Hence the carbon dioxide in the Frio Formation may have both a local organic and a basinal source, implying vertical fluid transport over several kilometers.

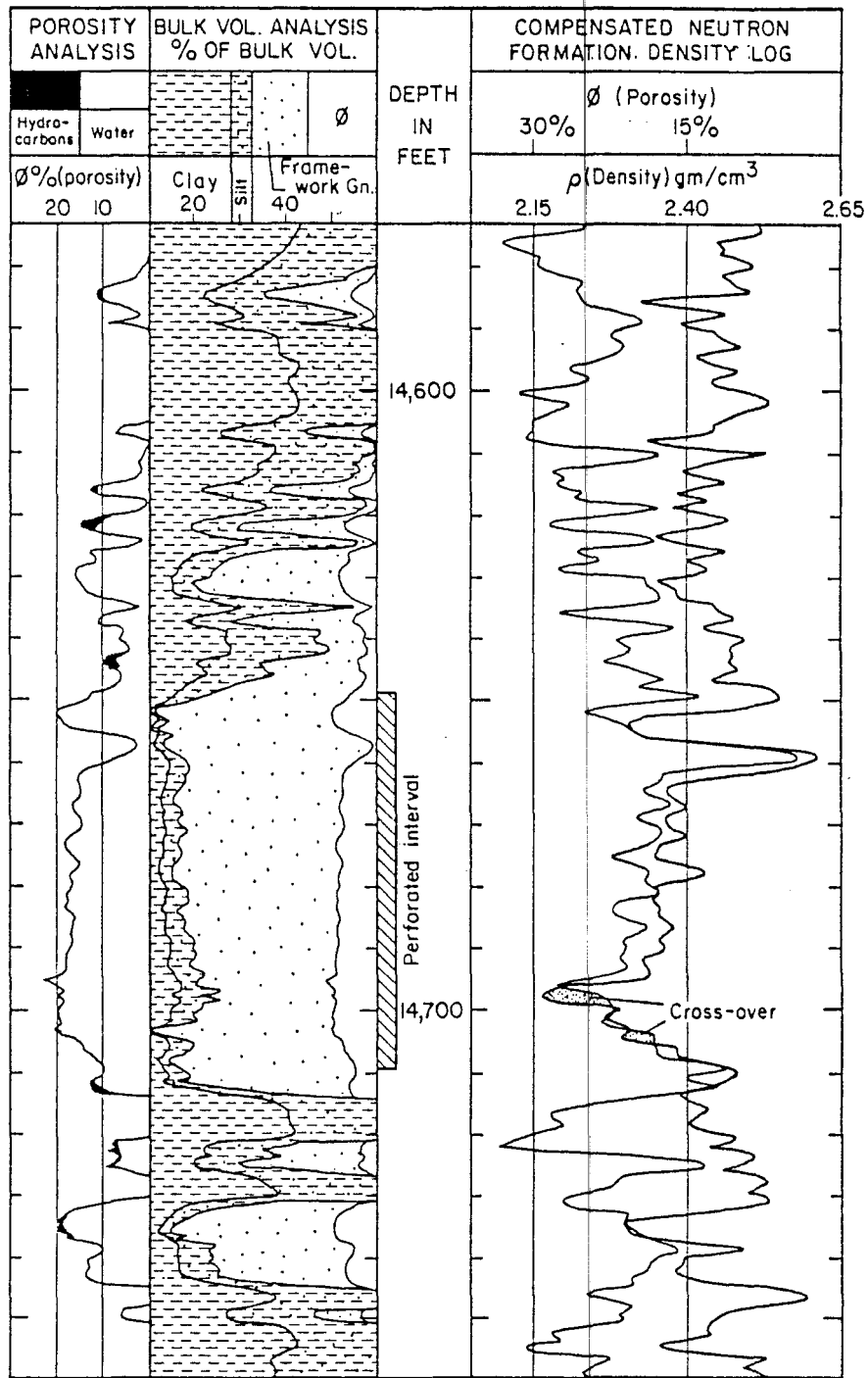
Oil Mobilization

Aromatic constituents of liquid hydrocarbons condensed from solution gas in geopressured brines have relatively high solubility at formation temperatures and pressures (table II-5; Price, 1976). They entered the brine during past or present contact with a free hydrocarbon phase (Finley and Saucier, 1983). Water in contact with petroleum accumulations may contain 1 to 10 ppm benzene, whereas brines in aquifers without hydrocarbon accumulations have no detectable benzene (0.01 ppm) (Zarrella and others, 1967). The quantity of dissolved benzene has even been used as a hydrocarbon proximity indicator (Dickey and Hunt, 1972, quoted in Coustau, 1977). The relatively high concentration of aromatics in the Pleasant Bayou and L. R. Sweezy No. 1 test well brines (2.8 ppm) suggests past or present proximity of hydrocarbon reservoirs (± 0.5 mi, 1 km) (Zarrella and others, 1967).

Log data for the Andrau sandstone indicates that small amounts of stratigraphically trapped free hydrocarbons are probably present (fig. II-16; Ewing and others, 1984a). Either these local hydrocarbons or the adjacent Chocolate Bayou and Danbury oil and gas fields could form the source of the aromatics in the brine. Alternatively, the hydrocarbons in the Andrau could reflect secondary migration as a dispersed phase derived from deeper

Table II-5. Composition of Aromatic Condensates (Price, 1976).

	Pleasant Bayou	Gladys McCall	Sweet Lake	L. R. Sweezy
Benzene	49.3	56.5	46.6	26.0
Toluene	19.8	18.7	28.5	12.4
C-2 benzenes	14.3	12.4	15.3	19.2
C-3 benzenes	5.3	3.6	4.0	10.4
Naphthalenes	2.7	trace	1.3	3.4
Total aromatics	91.4	91.2	95.7	71.4
Cycloalkanes	6.0	6.9	2.7	5.7
n-alkanes	0.6	0.5	0.4	10.8
Branched alkanes	1.9	1.5	1.2	11.8
Total alkanes	8.5	8.9	4.3	28.3



QA1600

Figure II-16. Computer-processed log, compensated neutron log, and density log for the "C" sandstone, Pleasant Bayou No. 2 well. Cross-over zones may be due to stratigraphically trapped free gas (Ewing and others, 1984a).

units. These fluids would move up along growth faults and out along permeable units into petroleum traps such as the Chocolate Bayou dome (Morton, 1983).

Shale dewatering has been investigated as a possible source of aromatic hydrocarbons in the brines in the Pleasant Bayou and L. R. Sweezy No. 1 well. Finley and Saucier (1983) indicated that the influx of any hydrocarbon components from shales in contact with the brine reservoir would probably require that a significant percentage of the total reservoir volume be withdrawn by production. Only then would any remaining compaction waters or waters resulting from clay diagenesis bearing a different suite of hydrocarbons enter the brine reservoir in quantity. They suggested that actual fluid transfer would be required to result in any change observable at a well because diffusion processes during the time of a pumping test are not likely to be sufficiently rapid. No geopressured geothermal well testing to date has removed a significant proportion of the calculated reservoir volume; the Sweezy No. 1 well produced less than 2 percent of the estimated reservoir fluid volume (Keeley and Meriwether, in press).

Shales in the Sweezy No. 1 well are almost devoid of external movable water, which is present as only a two-molecule-thick unit on shale in the geopressured zone (Kraemer, 1982). This monolayer can be removed at fairly low pressures when the temperature exceeds 300°F (149°C). The calculated contribution to water influx at the L. R. Sweezy No. 1 well from shale dewatering (22 bbls/psi) is minimal compared with the depletion performance of 3,800 bbls/day (Hamilton and Stanley, 1984). Keeley and Meriwether (in press) noted that no change in the trace element chemistry of produced waters occurred during production of the Sweezy No. 1 well, as might occur if shale compaction waters had been produced.

Radium concentration in the brine at Pleasant Bayou directly correlates with salinity because the radium is controlled by the ionic efficiency of the brine in removing sorbed multivalent ions from the clay minerals (Kraemer, 1981). A decrease in the radium 226 during production at Pleasant Bayou may result either from the uranium content declining

away from the aquifer or from progressive dewatering of shale, which has matrix particles of a lower uranium concentration than that of the aquifer (Kraemer, 1981). Both Brown (1980) and Schwab (1980) stated that the lower Frio section in the Pleasant Bayou test wells is organically lean and, though mature, has no potential for generating producible quantities of liquid or gaseous hydrocarbons. In addition, Schaefer and others (1983) have found that polarity-related absorption effects on clay minerals cause retention of aromatic hydrocarbons at or near a shale interface rather than their release to non-shale strata. It is therefore unlikely that the aromatic hydrocarbons present in the geopressured brines were introduced by shale dewatering (Finley and Saucier, 1983).

Retrograde condensation of local gas pockets within the producing sandstones has been considered as a possible mechanism for causing the increase in liquid hydrocarbons during brine production at the geopressured test wells (Morton, 1983). In retrograde reservoirs, liquid begins to condense when the fluid pressure drops below the dew point (Craft and Hawkins, 1959). This condensed liquid is immobile and adheres to the walls of the pore spaces, whereas the produced gas has a declining liquid content. Condensation continues until a maximum liquid volume is reached after which revaporization of the retrograde liquid results in a decreasing gas-oil ratio at the surface (Craft and Hawkins, 1959). The continuous decrease in the gas-oil ratios during production at the Sweezy No. 1 well (Hamilton and Stanley, 1984) is evidence that the aromatic and paraffinic hydrocarbons are not derived from retrograde condensation of a gas cap. Retrograde condensation also seems unlikely at Pleasant Bayou because major pressure decreases were not achieved during brine production. The static bottom-hole pressure decreased by only 37 psi (11,117 to 11,080 psi) during production of 537,000 bbls of brine between September 1980 and March 1981 (Finley and Saucier, 1983).

The amount of aromatic material condensed out of the gas stream at the L. R. Sweezy No. 1 geopressured geothermal well increased during production until finally a dark, heavy, highly paraffinic oil accumulated in the separator. Hamilton and Stanley

(1984) suggested that this oil may have been dead or residual oil, which became producible because of pore volume relaxation near the well bore. An oil front may have built up as production progressed, broken through, and collected in the separator on the surface (Hamilton and Stanley, 1984). This is similar to oil banks that form between displaced gas and advancing water in producing oil and gas fields (Slider, 1976).

Pressure drawdown leads to rock compaction during production from geopressured reservoirs (Knutson, 1982). Compaction tests on cores from the Pleasant Bayou wells indicate a greater rate of decrease in permeability than in porosity, which is thought to be a consequence of the preferential closure of flow channels or cracks due to compaction (Jogi and others, 1981). The porosity of the Cib-Jeff production interval in the L. R. Sweezy No. 1 well was reduced from 29.45 to 29.40% by compaction during production (Hamilton and Stanley, 1984). However, the calculated permeability decreased by almost ten fold (1,037 to 117.3 md) in the vicinity of the wellbore during the intermediate stages of testing (Hamilton and Stanley, 1984). The reduction of the effective permeability to water at the L. R. Sweezy No. 1 well is probably not a result of the damming up of fines or exsolved gas near the wellbore as the effective permeability showed a partial recovery when the pore pressure returned to the normal reservoir pressure at the end of the test (Hamilton and Stanley, 1984).

For ideal granular systems, a relationship exists between irreducible water saturation, porosity, and permeability (fig. II-17) (Morris and Biggs, 1967; Timur, 1968). The irreducible water saturation of the L. R. Sweezy No. 1 geopressured reservoir is seen to increase by some 40% (19% to 59%) as a result of the reduction in permeability of about an order of magnitude at almost constant porosity (fig. II-17). Water in a water-wet medium tends to coat the pores (Slider, 1976). Residual oil, being the more mobile and pore-centered phase, may be forced by the compaction to move into larger pores as the irreducible water saturation of the rock is increased (fig. II-18). This process could continue until the oil-water ratio in the mobile pore center approaches 1 to 2, after which

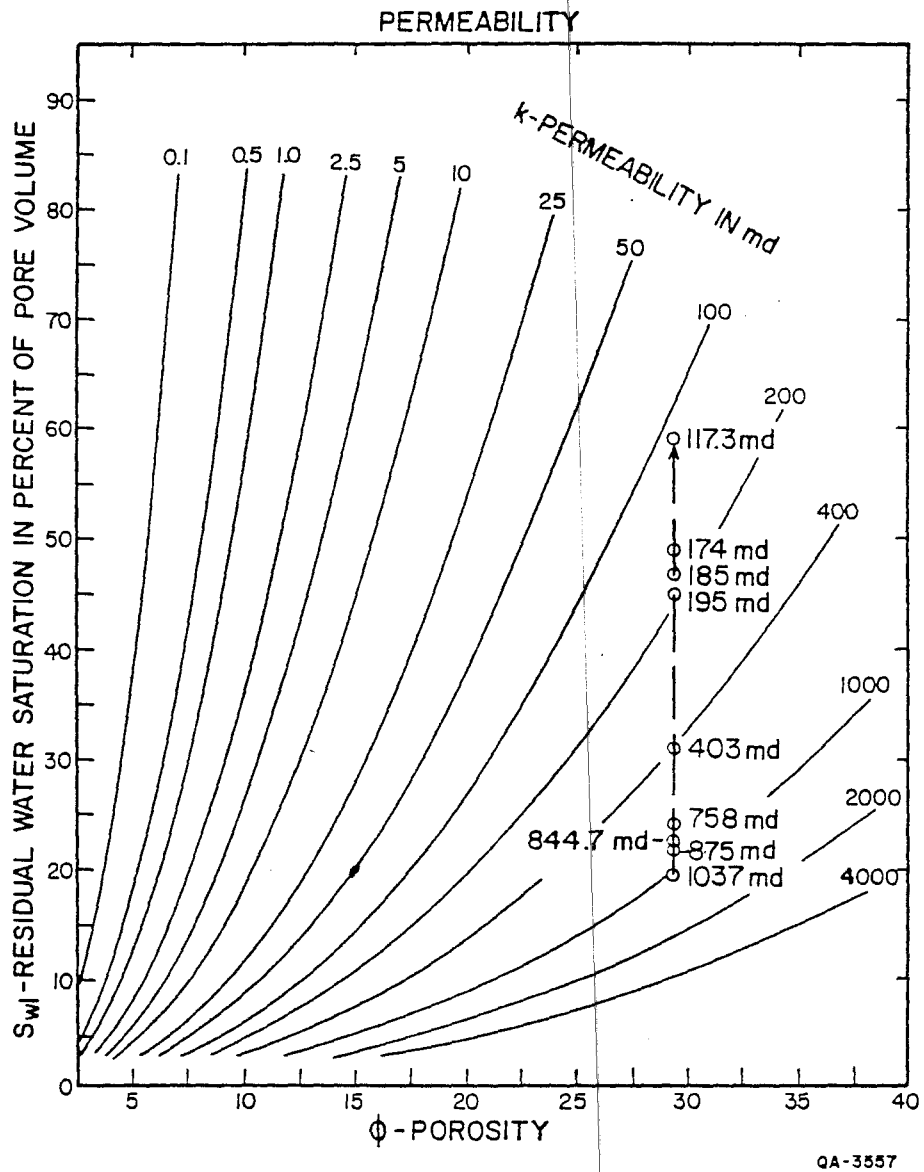
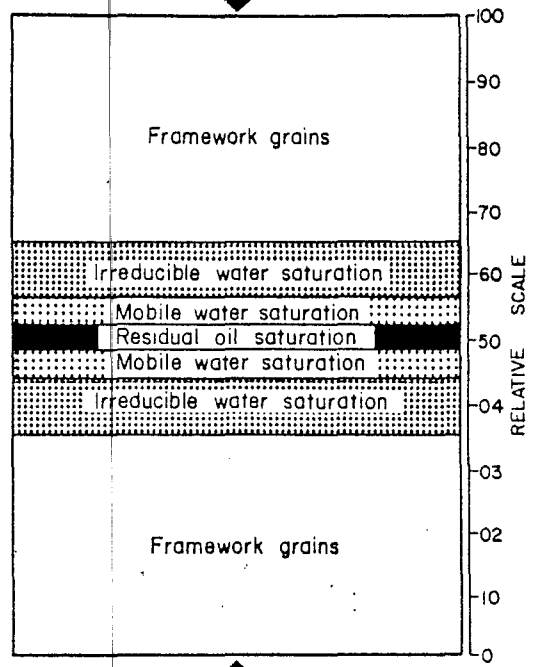
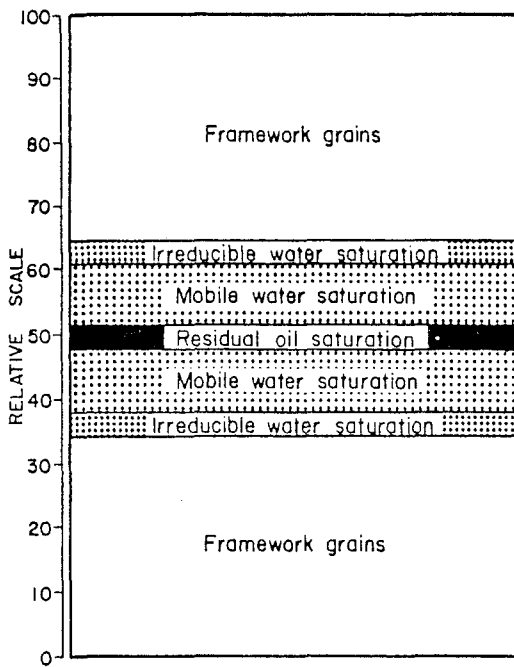


Figure II-17. Residual water saturation versus porosity and permeability (modified from Timur, 1968). Permeability decline trend for Sweezy No. 1 well (Hamilton and Stanley, 1984).

1) GEOPRESSURED SANDSTONE
BEFORE PRODUCTION WITH
WATER AS WETTING PHASE

SANDSTONE AFTER PRODUCTION
WITH 40% INCREASE IN
RESIDUAL WATER SATURATION



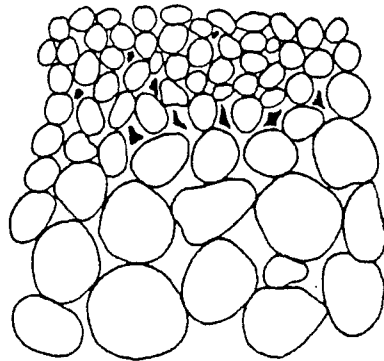
Porosity = 29.45 %
Mobile water saturation = 70.7 %
Irreducible water saturation = 19.3 %
Oil saturation = 10 %
Permeability = 1,037 md

Porosity = 29.40 %
Mobile water saturation = 31.1 %
Irreducible water saturation = 58.9 %
Oil saturation = 10 %
Permeability = 117.3 md

SILTSTONE
(Irreducible water saturation)

Residual oil in
larger pore centers

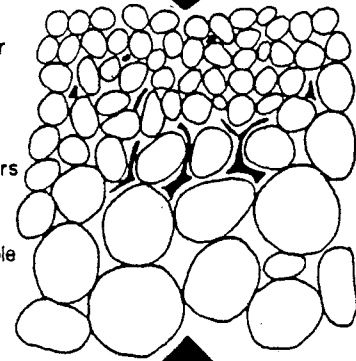
SANDSTONE
(19.31 % irreducible
water saturation)



SILTSTONE
(Irreducible water saturation)

Migration of
residual oil into
larger pore centers

SANDSTONE
(58.9 % irreducible
water saturation)



COMPACTION

QA-3556

Figure II-18. Compactional model for hydrocarbon production in geopressured brines.

the oil can be produced (Slider, 1976). The movement of this oil into the larger pore center network could be assisted by the expansion of the irreducible water, resulting in a further reduction in the pore volume of the reservoir (Slider, 1976). Such a mechanism may be adequate for the production of the heavy paraffinic oil at the L. R. Sweezy No. 1 well as it represents only 0.00005% of the total volume of fluids produced (Hamilton and Stanley, 1984). However, pressures and densities of the L. R. Sweezy No. 1 gas cap approach those of gas condensate. These are favorable conditions for tertiary oil recovery by gas flooding utilizing carbon dioxide (Weres and others, 1984). Under these conditions, oil hydrocarbons are soluble in natural gas (Zhuze and others, 1962; Price and others, 1983). Either of these mechanisms may explain the presence of heavy hydrocarbons at the Sweezy No. 1 well.

Natural convection (Wood and Hewitt, 1982) is a possible mechanism for introducing aromatic hydrocarbons into the geopressured Andrau ("C" sandstone) brines at the Pleasant Bayou test wells. These hydrocarbons could be derived from the base of a gas-condensate cap farther updip. A convective system may also explain the thermal anomalies and porosity development in the Pleasant Bayou test wells. Diagenetic data indicate that about 10,000 pore volumes of water are required to carry the quartz needed to cement a sandstone (Land and Dutton, 1979; Wood and Hewett, 1982). Similar quantities of fluid may be necessary for calcite cementation or the generation of secondary porosity (Blanchard, in press). Shale-sand ratios on the order of 10,000 are required for locally derived compaction waters to be sufficient (Land and Dutton, 1979), but sandstones vary from 11% to 48% of the Frio Formation (Galloway and others, 1982). Secondary porosity is not likely to have been caused by meteoric waters deeply penetrating a compacting basin (Blanchard, in press). Material-transport calculations indicate that the volumes of fluid involved far exceed the volume of connate water deposited in the Gulf Coast basin, strongly suggesting some mechanism of thermally driven convective flow (Land, 1984).

Blanchard (in press) has modeled convection in the entire Frio Formation, considering it as a large, flat (800 m thick and 15 km wide) sandstone body of indeterminate lateral

dimension isolated by bounding shales and growth faults. He also presented evidence suggesting that free convection could occur in the Frio Formation as a whole, its existence controlled by the degree of layering (McKibben and O'Sullivan, 1980; McKibben and Tyvand, 1983).

Natural convection occurs when buoyant forces due to density differences exceed viscous forces resisting motion (Wood and Hewett, 1984). The buoyancy force that causes convection in a porous medium is given in dimensionless form by the filtration Rayleigh number "Ra*" (table II-6; Bories and Combarous, 1973). For the Andrau sandstone at Pleasant Bayou the Rayleigh number is 0.03. The Andrau reservoir is isolated from sandstones above and below and is more highly geopressed than shallower units. Convection is therefore unlikely between the Andrau and the rest of the Frio.

Though the stability of natural convection in horizontal porous layers has been modeled by numerous researchers, there are no published works reporting on inclined porous layers with temperature gradients oblique to the trend of the layer (Bories and Combarous, 1973). Weber (1973) has demonstrated that for moderate values of the Rayleigh number and tilt angle, the non-linear system of equations governing stationary convection in an inclined porous layer is identical to that in a horizontal porous layer with varying horizontal and vertical temperature gradients. However, the acceleration due to gravity must be diminished by the angle of inclination ϕ (B. Dahlberg, personal communication, 1984). The southwest dip of the Andrau sandstone at Pleasant Bayou No. 2 is small (6°); the vertical temperature gradient ($2.04^\circ\text{F}/100\text{ ft}$, $3.72^\circ\text{C}/100\text{ m}$) is about 15 times the horizontal gradient ($0.14^\circ\text{F}/100\text{ ft}$, $0.25^\circ\text{C}/100\text{ m}$), which exists between this well and the Chocolate Bayou dome. This small lateral gradient will have a negligible effect on a convective system.

Natural convection occurs in a horizontal layer when the Rayleigh number exceeds 40 (Lapwood, 1948). However, Aziz and others (1973) have speculated that convection could occur in a horizontal aquifer with critical Rayleigh numbers between 12 and 40, depending

Table II-6. Fluid convection calculations for the Andrau sandstone, Pleasant Bayou test well.

1) FILTRATION RAYLEIGH NUMBER

$$Ra = Kg \frac{\alpha (pc)fH \Delta T}{\nu \lambda^*} \quad (1)$$

2) FILTRATION RAYLEIGH NUMBER CORRECTED FOR SLOPE INCLINATION

$$Ra^* = Ra \cos \theta \quad (1)$$

3) CHARACTERISTIC FLUID VELOCITY SCALE

$$U = Kg \frac{\alpha \sin \theta \Delta T}{\nu} \text{ m/sec} \quad (1)$$

Andrau sandstone
= 2.19 mm/yr

4) FLUID PARTICLE VELOCITY = $\frac{U}{\phi}$ (2)

5) MASS TRANSFER PECLET NUMBER

$$Pe = \frac{UH}{De} \quad (2)$$

mean value Andrau
sandstone

K	= permeability of medium	= 0.2 Darcy = $2 \times 10^{-13} \text{m}^2$	(3)
α	= volumetric thermal expansion coefficient of the fluid	= $2 \times 10^{-4} \text{K}^{-1}$	(4)
(pc)f	= volumetric heat capacity of fluid	= $4 \times 10^6 \text{w sec/m}^3 \text{K}$	(4)
H	= thickness of porous layer	= 60' = 18.29 m	(3)
ΔT	= temperature difference across layer	= 1.2° F = 0.68° K	(5)
ν	= Kinematic viscosity of fluid	= $4 \times 10^{-7} \text{m}^2/\text{sec}$	(4)
λ^*	= effective thermal conductivity of the fluid-filled medium	= 1.5 w/mK	(5)
g	= acceleration due to gravity		
ϕ	= porosity	= 19% = 0.19	(3)
θ	= angle of inclination of porous medium	= 6°	(5)
De	= typical value for solute diffusivity in aqueous solutions	= $10^{-9} \text{m}^2/\text{sec}$	(4)

- (1) Bories and Combarous (1973)
- (2) Wood and Hewett (1982)
- (3) Morton (1981)
- (4) Pryor (1971)
- (5) Author's estimate

on the thermal conductivity of the bounding layers (table II-7). Most analyses consider the aquifer boundaries to be isothermal and impermeable as is assumed in the case of the Andrau sandstone. For fluids in inclined porous layers of this sort, there is no stability criterion. The temperature and gravity vectors are not coincident, so the fluid will always be in motion when a temperature gradient exists across the layer (Wood and Hewitt, 1982). The flow will be slow and unicellular in the Andrau sandstone because of its low angle of inclination and small filtration Rayleigh number (fig. II-19; Combarous and Bories, 1975).

Hart (1971) has empirically determined the temperature distribution from free convection in fluid in a differentially heated inclined box for various tilt angles. This empirical data suggests that the temperature in the Andrau sandstone at the Pleasant Bayou test wells will be depressed only $4.5 \times 10^{-8}^{\circ}\text{F}$ ($2.5 \times 10^{-8}^{\circ}\text{C}$) below the temperature of the stationary fluid by convective flow. Convection would have a negligible effect on the maturity of the sediments.

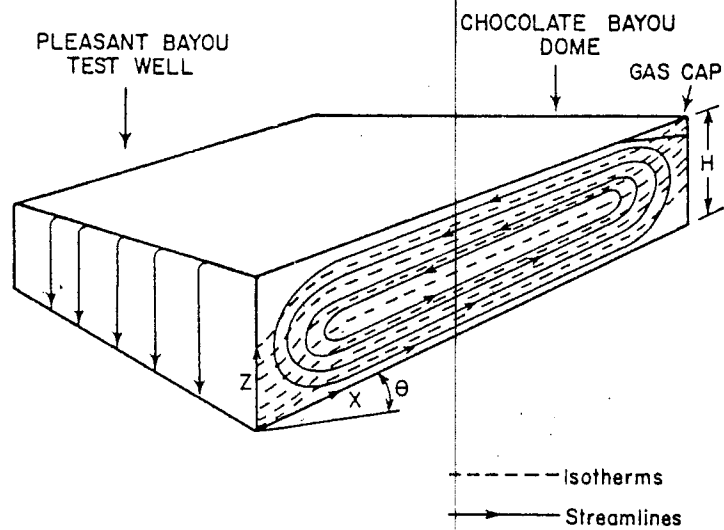
The Peclet number (Pe) (table II-6) relates the effectiveness of mass transfer by fluid flow to that by diffusion. Convection ceases to be important where Pe is less than or equal to 1 (Wood and Hewett, 1982). The Andrau sandstone has a Pe of 1.27. The change in porosity per unit time due to the mass transport and diffusion of silica depends on several factors including the porosity and the Peclet number (equation 1, table II-8; Wood and Hewett, 1982). The ratio of porosity to Peclet number in the Andrau sandstone is 0.15. Hence most of the transport will be due to mass flow (table II-8; Wood and Hewett, 1982), so the diffusion term can be neglected.

The convective fluid velocity (U) in the parallel region of a unicellular flow field is 0.08 inch (2.19 mm)/year in the Andrau sandstone using present-day permeabilities and temperatures (table II-6). The fluid particles have a mean velocity of 7.1 mi (11.5 km)/Ma and could have completed several circuits between the Pleasant Bayou No. 2 well and the Chocolate Bayou dome in a 5 to 10 Ma period.

Table II-7. Convective flow boundary conditions (Nield, 1968).

Lower Boundary	Upper Boundary	Critical Ra
ISO,IMP	ISO,IMP	$4\pi^2 \approx 40$
ISO,IMP	INS,IMP	27.1
INS,IMP	INS,IMP	12
ISO,IMP	ISO,FRE	27.1
INS,IMP	ISO,FRE	17.65
ISO,IMP	INS,FRE	$\pi^2 \approx 10$
INS,IMP	INS,FRE	3
ISO	ISO	
or	or	0
INS	INS	

INS = INSULATED
 IMP = IMPERMEABLE
 ISO = ISOTHERMAL
 FRE = FREE SURFACE



QA-3555

Figure II-19. Geometry of unicellular flow in an inclined fluid layer (modified from Wood and Hewitt, 1982).

Table II-8. Mass transport of silica in the Andrau sandstone, Pleasant Bayou test well.

Accumulation rate of silica in pore space

$$\frac{\delta\phi}{\delta t^*} = \frac{\rho_w}{\rho_s} \frac{\delta C_s}{\delta s^*} - \frac{\phi}{\rho_e} \frac{\partial^2 C_s}{\partial s^{*2}} \quad (1)$$

$$\frac{\phi}{\phi_0} = 1 - \frac{t}{T} \quad (2)$$

$$T = - \frac{U_0}{\phi_0} \frac{\rho_w}{\rho_s} \frac{\delta C_s}{\delta T} \frac{dT}{dS}^{-1} \quad (3)$$

$$\frac{dT}{dS} = \text{geothermal gradient} = 3.72 \times 10^{-2} \text{ }^\circ\text{K/m} \quad (2)$$

$$\phi = \text{final porosity} = 30\% \quad (4)$$

$$\phi_0 = \text{original porosity} = 19\% \quad (3)$$

$$T = \text{characteristic time in m.y.}$$

$$U = U_0 = \text{free convective velocity} = 2.19 \times 10^{-3} \text{ m.y.} \quad (1)$$

$$\rho_w = \text{density of water} = 1,000 \text{ Kg/m}^3 \quad (2)$$

$$\rho_s = \text{density of precipitated silica} = 2,600 \text{ Kg/m}^3 \quad (2)$$

$$C_s = \text{mass fraction of silica in water}$$

$$De = \text{effective diffusion coefficient through a porous medium of silica in water}$$

$$S = \text{distance measured along streamline}$$

$$\frac{dC_s}{dt} = 5 \times 10^{-6} \text{ K}^{-13} \quad (1)$$

$$\text{Dimensionless } t = \frac{tU}{H}$$

(H = length of porous layer)

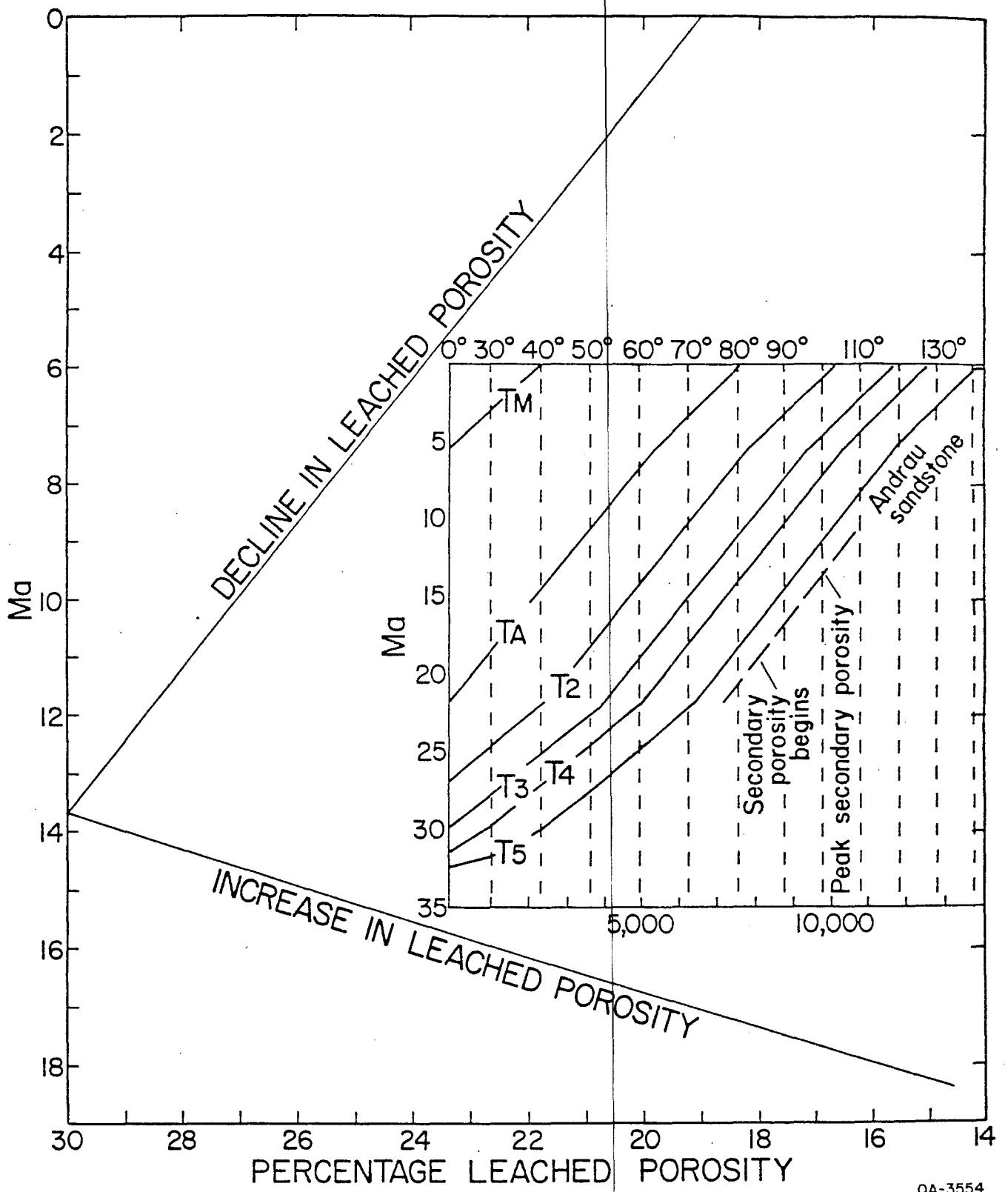
$$\text{Dimensionless } s = \frac{s}{H}$$

- (1) Author's estimate
- (2) Wood and Hewett (1982)
- (3) Morton (1981)
- (4) Bebout and others (1978)

However, the Andrau sandstone is less porous now than it was at the peak of secondary leaching of framework grains and cements (fig. II-20). Fourteen Ma ago the porosity was about 30% (Bebout and others, 1978). Secondary leaching began at approximately 185°F (85°C) because it postdates quartz overgrowths, while kaolinite, which formed at about 212°F (100°C), fills secondary pores (Loucks and others, 1981). However, the temperature of major secondary leaching occurred at about 100°C (212°F) (Kaiser and Richmann, 1981). The porosity variation versus time due to leaching and cementation in the Andrau sandstone has been modeled using a burial history diagram for the Pleasant Bayou wells (Ewing and others, 1984a) assuming a constant (present-day) geothermal gradient (fig. II-20). The variation in permeability with time was estimated with core porosity-permeability plots for geopressed sandstones (fig. II-21).

The mean characteristic convective fluid velocity derived from the modified permeability data is 0.7 inch (1.8 cm)/year. The calculated fluid particle velocity is estimated at 51 mi (83 km)/Ma. Hence these fluids could complete almost three 9-mi (15-km) long convective circuits every Ma. Thus, aromatic hydrocarbons in the saline brines at Pleasant Bayou could have been derived from the base of a gas cap in the Chocolate Bayou or Danbury dome gas fields. The silica geothermometer temperatures for the Andrau fluids is greater than the formation temperature (Kharaka and others, 1980), implying that the brines have migrated updip to their present location and indicating a deep source for the hydrocarbons (fig. II-2). The high aromatic content of the brines indicates either that they were isolated during migration by the high geopressure or that migration is still taking place. Present evidence supports the former for the lower Frio, while the extant geothermal gradient at Pleasant Bayou suggests that fluid flow continues in the upper Frio.

Wood and Hewitt (1982) have calculated the amount of porosity change related to the introduction of silica into a rock by convective flow mechanisms (table II-8). The estimated increase in Andrau sandstone porosity from 14.5% to 30% by leaching and decrease to 19% by cementation has been modeled using their methods. Although the



QA-3554

Figure II-20. Time depth curve for the Pleasant Bayou No. 2 well showing the initiation and peak of secondary porosity development. Variation of porosity versus time for the Andrau sandstone is also shown.

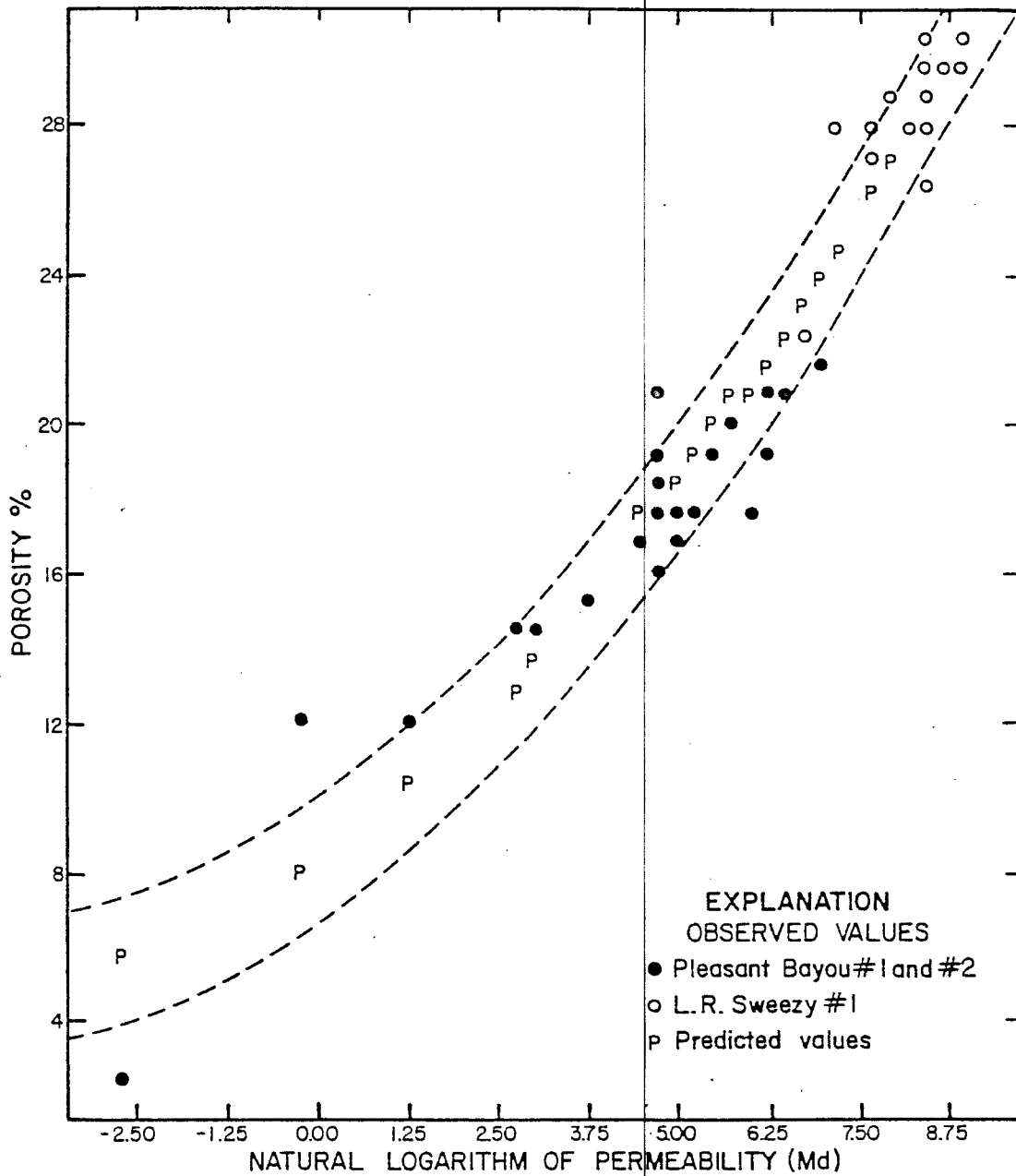


Figure II-21. Plot of the natural logarithm of permeability versus porosity for geopressed sandstones. Andrau sandstone, Pleasant Bayou No. 1 and No. 2 wells, "Cib-Jeff" sandstone, L. R. Sweezy No. 1 well, Vermilion Parish, Louisiana (Hamilton and Stanley, 1984).

minerals undergoing solution and precipitation in the Andrau sandstone are more variable than the pure silica used in this model, this calculation should still give an idea of the order of time involved. It requires about 8 Ma for the porosity to increase from 14.5% to 30% in the Andrau sandstone and a further 5.8 Ma for it to be reduced to 19% (table II-9). The total fluid flow period of 13.8 Ma is less than the time (18.4 Ma) allotted from burial history data (fig. II-20). These rough estimates of the period of secondary porosity formation and destruction suggest that the leaching and cementation of the Andrau sandstone can be adequately explained by convective flow. This convective flow can be superimposed on a migrating fluid system (Wood and Hewitt, 1982).

SOLUBILITY OF CEMENTS IN AQUIFER FLUIDS

The addition of sodium chloride and carbon dioxide to a brine increases the solubility of calcite in hydrothermal solutions (table II-10) (Barnes, 1979). The high salinity (131,320 mg/L) and carbon dioxide content of fluids (9.1 to 10.5 mole %) in the Andrau sandstone at Pleasant Bayou prevent calcite from precipitating (Morton, 1981; Kaiser and Richmann, 1981; Thomson, 1984). Morton and others (1981) have shown that the concentration of carbon dioxide in formation water in the U.S. Department of Energy geopressured test wells increases with temperature and in older formations.

The amount of carbon dioxide in natural gases in the Eocene Wilcox increases rapidly at about 212°F (100°C), which coincides with a rapid increase in the ratio of secondary to primary porosity in associated sandstones (Franks and Forester, 1984). Wells in Brazoria County including Pleasant Bayou show abundant secondary porosity below 10,000 ft (3,050 m), which corresponds to a temperature of about 212°F (100°C) (fig. II-2). This is the temperature of maximum carbon dioxide generation from humic material (Hunt, 1979) and kaolinite crystallization at Pleasant Bayou (Loucks and others, 1981). Surdam and others (1984) have shown that the oxidative degradation of type III kerogen results in

Table II-9. Hypothetical porosity variation in the Andrau sandstone.

POROSITY INCREASE: 14.5% to 30%

$$\bar{U} = 0.15 \text{ m/yr}$$

$$\phi_0 = 30$$

$$U_0 = .08 \text{ m/yr}$$

$$T = 52.2 \text{ Ma}$$

$$\text{period of porosity increase} = .155 T = \underline{8 \text{ Ma}}$$

POROSITY DECREASE: 30% to 19%

$$\bar{U} = .025 \text{ m/yr}$$

$$\phi_0 = 30$$

$$U_0 = .08 \text{ m/yr}$$

$$T = 52.2 \text{ Ma}$$

$$\text{period of porosity decrease} = .11 T = \underline{5.7 \text{ Ma}}$$

Table II-10. Scale of approximate (± 0.3) saturation index values.

SI Values		Comment
Supersaturated (+)	2.5	Instantaneous uncontrollable scale, probably
	2.0	Controllable with inhibitors
	1.5	CaCO ₃ precipitation will probably begin in a few minutes
		Metastable
Subsaturated (-)	0.0	Equilibrium gas-brine-solid
		Subsaturated
	2.0	Probably not a CaCO ₃ brine (From Thomson, 1983)

extremely high concentrations of difunctional carboxylic acids (up to 40% oxalic acid). Type III source rocks that contain only 0.5% total organic carbon can produce sufficient carboxylic acid to leach an additional 3 to 5% secondary pore volume in adjacent sandstones (Surdam and others, 1984). This period of acid formation, which coincides in time, temperature, and space with the transformation of smectite, immediately precedes hydrocarbon generation and could dissolve carbonates and/or alumino silicates (Surdam and others, 1984). Such a mechanism may partly explain the abundant secondary porosity in the Frio Formation but requires the updip movement of hot brines. These acidic waters have their origin in deeper organic-carbon-rich slope shales.

ORIGIN OF PERMEABLE AQUIFERS

Modeling of maturity data at the Pleasant Bayou test wells indicates that the regional paleogeothermal gradient was modified by the heating effects of waters flowing through the upper Frio sandstones while fluid movement was slow or static in the lower Frio. Water movement should produce diagenetic alteration or leaching of the sandstones. To test this hypothesis, the porosity, permeability, abundance of diagenetic cements and framework grains have been plotted against logged core descriptions for the Andrau sandstone in the Pleasant Bayou No. 1 and No. 2 and Phillips Houston "GG" No. 1 and "JJ" No. 1 wells (Tyler, 1982; Ewing and others, 1984a). The Andrau sandstone in the Houston "GG" No. 1 well shows a normal maturity similar to the Andrau in the Pleasant Bayou wells, whereas the Houston "JJ" No. 1 well only a few thousand feet away has an anomalously high maturity (Ewing and others, 1984a). The Houston "GG" No. 1 well is gas saturated and shallower and closer to a major normal fault than the Houston "JJ" No. 1 well.

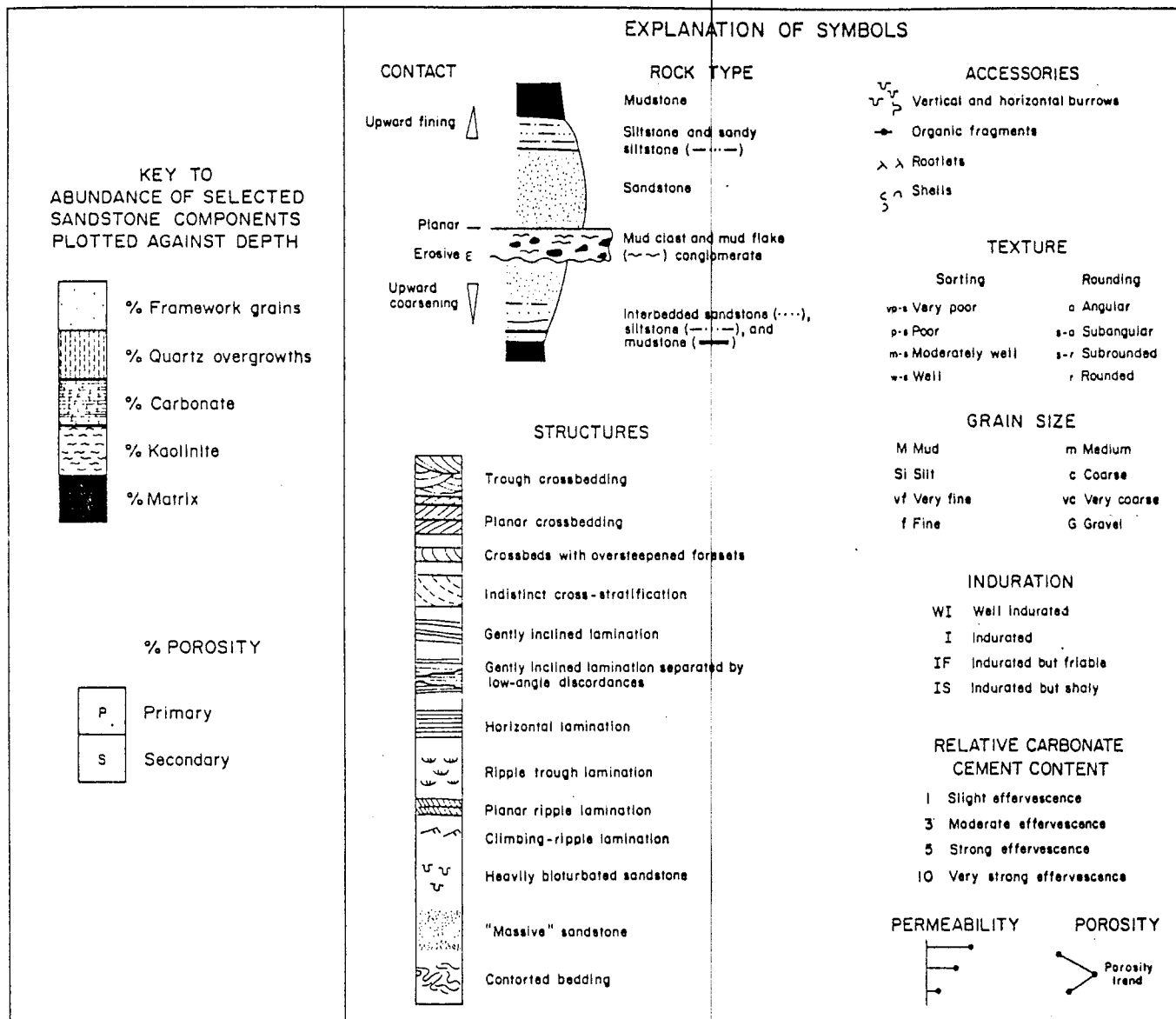
At the Pleasant Bayou test wells, the Andrau sandstone is a distributary-mouth-bar (delta-front) sandstone. It contains both quartz overgrowths and kaolinite filling leached pore spaces (Loucks and others, 1980). Quartz overgrowths and kaolinite show similar

relationships in the Andrau sandstone at the Phillips Houston "JJ" No. 1 and "GG" No. 1 wells (figs. II-22 and II-23). The Andrau sandstone at these wells is interpreted to have been deposited in a coalesced distributary-mouth bar. The geopressed "Cib-Jeff" sandstone in the DOW-DOE L. R. Sweezy No. 1 well (Vermilion Parish, Louisiana) is interpreted to have been an offshore barrier bar and appears to have normal thermal maturity (Hamilton and Stanley, 1984). It should be possible to see variations in the diagenetic and other characteristic parameters, which are not facies dependent at these four well sites because the sandstones were all deposited in similar environments.

A direct comparison is not possible between the Andrau sandstone in the Houston "GG" No. 1 and "JJ" No. 1 wells and the sandstone in Pleasant Bayou wells, which are water saturated. The Houston "GG" No. 1 well produced 19.5 million ft³ (0.55 million m³) of gas/day from this reservoir. The presence of higher but more erratic porosities in the Houston "GG" No. 1 well is probably related to the early entrapment of gas, which tends to inhibit diagenetic cementation and porosity occlusion (Selley, 1979). The presence of a gas cap at the Houston "GG" No. 1 well would isolate the Andrau sandstone from the heating effects of migrating fluids so that its maturity would remain consistent with the regional geothermal gradient.

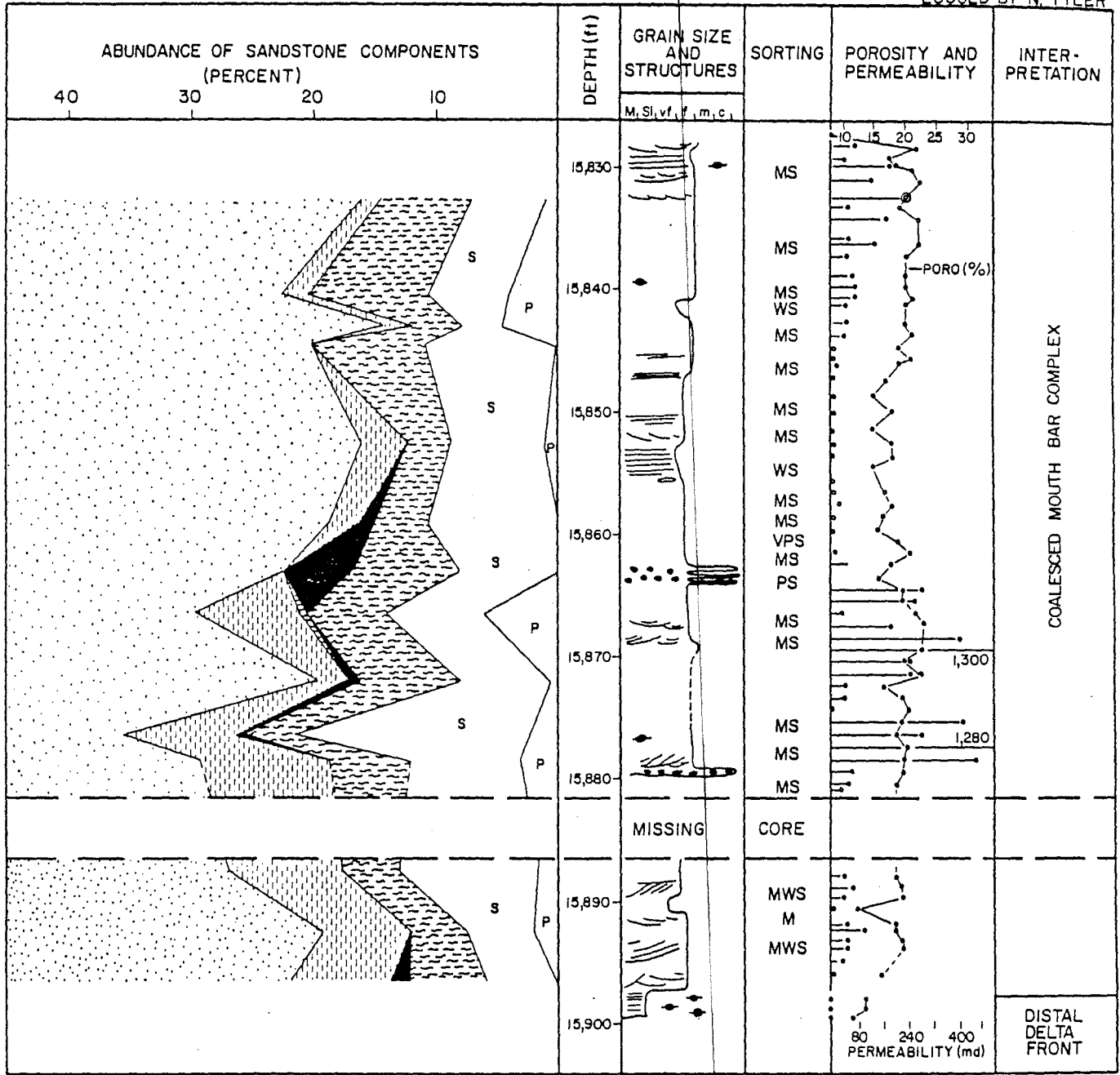
The Pleasant Bayou No. 1, Houston "JJ" No. 1, and Houston "GG" No. 1 wells have similar temperature gradients (1.55 to 1.65°F/100 ft, 2.83 to 3°C/100 m) and pressure gradients (0.75 to 0.84 psi/ft, 1.7 to 1.9 kPa/m) and high salinities (135,000 to 217,000 ppm NaCl) (table II-11). No trend is evident in the variation of these parameters although the calculated salinity of brines associated with trapped hydrocarbons (Houston "GG" No. 1 well) is almost twice that of the water-saturated wells (Pleasant Bayou and Houston "JJ" No. 1 wells).

Carbonate cement is very abundant in the Andrau sandstone in the Houston "GG" No. 1 well, is less abundant in the Pleasant Bayou test wells, and is almost absent in the Houston "JJ" No. 1 well (figs. II-22 and II-23). The T3 sandstones show similar porosities



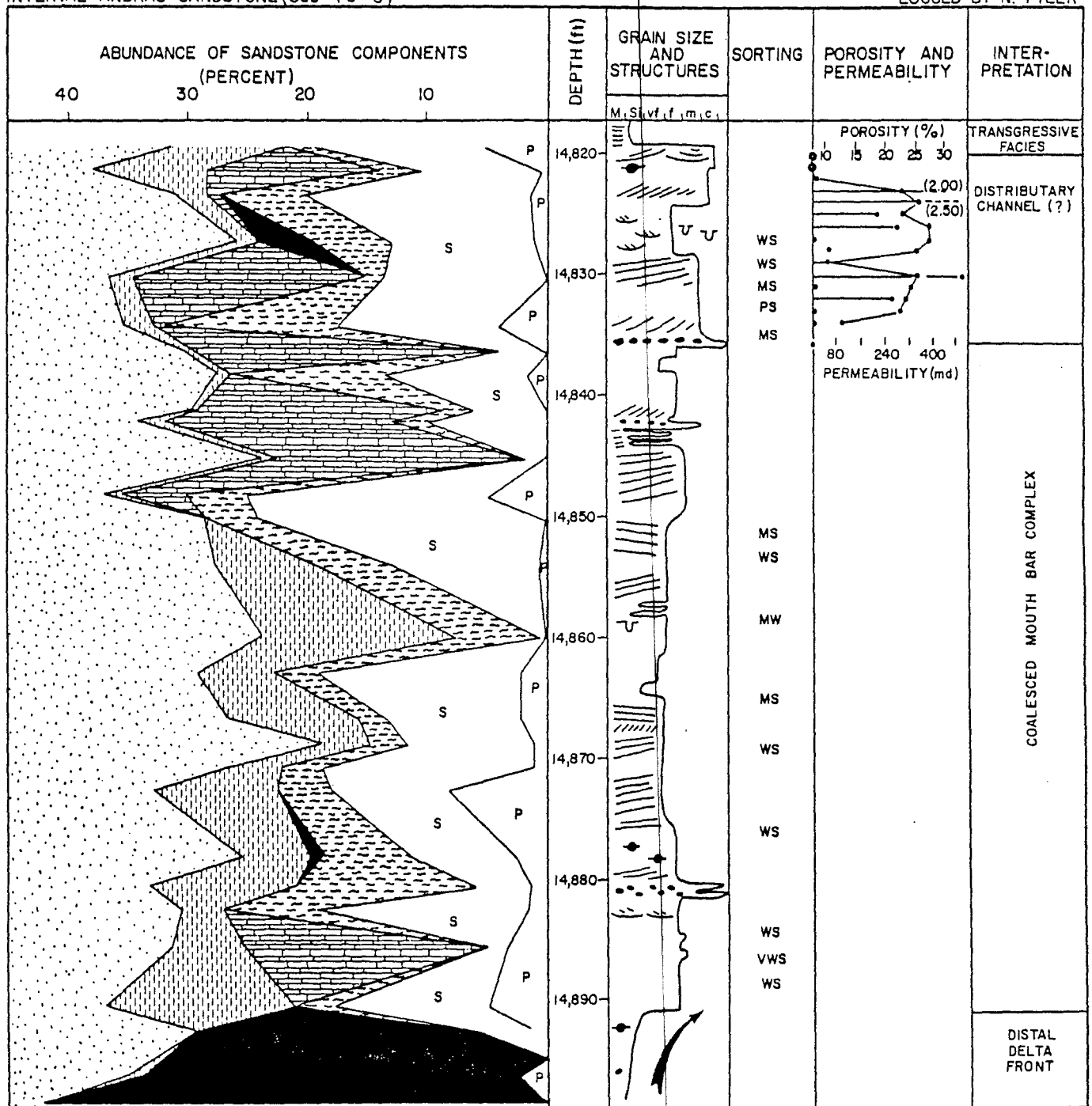
QA1781

Figure II-22a. Explanation of symbols and key to abundance of selected sandstone components plotted against depth (Ewing and others, 1984a).



QA-3550

Figure II-22b. Detailed core description and petrography of distributary-mouth-bar sandstones, Andrau sandstone, Phillips Houston "GG" No. 1 well (modified from Tyler, 1982).



QA-3551

Figure II-23. Detailed core description and petrography of distributary-mouth-bar sandstones, Andrau sandstone, Phillips Houston "JJ" No. 1 well (modified from Tyler, 1982).

Table II-11. Pressure, temperature, and salinity data for the Andrau sandstone at the Pleasant Bayou No. 2, Houston "GG" No. 1 and "JJ" No. 1 wells, Brazoria County.

	Average Depth Below M.S.L.	Measured Pressure (PSIG)	Pressure Gradient (PSI/ft)	Measured Temperature (° F)	Temperature Gradient (° F/100')	Salinity PPM
PB #2	14,674	11,250	0.753	301 m	1.55	135,000 _m
GG #1	14,851	11,227	0.756	315 e	1.65	217,000 _e
JJ #1	15,850	13,481	0.840 c	331 c	1.65	147,000 _c

Core analysis data from the more highly mature T₃ sandstone and less mature Andrau sandstone, Brazoria County, Texas

Porosity (%)

	Andrau PB #1 and 2	T ₃ sand PB #1
No. of readings	27	27
Mean	17.29	17.49
Standard deviation	3.82	4.35
Range	2.5 - 21.6	7.3 - 23.9

Permeability (md)

	Andrau PB #1 and 2	T ₃ sand PB #1
No. of readings	27	27
Mean	223.57	27.24
Standard deviation	240.8	40.09
Range	0.07 - 1041	<0.1 - 179

but lower permeabilities than the Andrau sandstone in the Pleasant Bayou wells (table II-11). The reservoirs in the four wells have a relatively low matrix content except for the T3 sandstone at Pleasant Bayou and the Andrau sandstone at the Houston "GG" No. 1 well (fig. II-22). Though the permeability appears to be good in the Pleasant Bayou wells except where matrix is present (Loucks and others, 1980), high permeabilities lie within the carbonate-cemented section in the Houston "GG" No. 1 well. An anomalous positive correlation between cement content and porosity was also recognized in the Pleasant Bayou test wells (Loucks and others, 1980). The correlation of high permeability and porosity with ample carbonate cement suggests preservation of high initial porosity and permeability by abundant carbonate cementation, which was variably leached by later fluid flow. The Humble No. 1 Skrabanek well, which lies on the southeast flank of the Danbury dome, shows a relatively high maturity (fig. II-9). The sandstones here are tightly cemented with quartz and calcite and have less leached porosity than those in the Chocolate Bayou field (Bebout and others, 1978).

The high-maturity and water-saturated reservoirs, such as the T3 sandstone in Pleasant Bayou No. 1 and the Andrau sandstone in Houston "JJ" No. 1, show similar trends on a porosity versus permeability plot as the normal-maturity and water-saturated reservoirs such as the Andrau sandstone, Pleasant Bayou No. 1, No. 2 and "Cib-Jeff" sandstone, L. R. Sweezy No. 1 (fig. II-24). However, the high-maturity samples are displaced by almost an order of magnitude toward lower permeabilities. The porosity and permeability data for the Andrau sandstone in the Pleasant Bayou, Houston "GG" No. 1 and "JJ" No. 1 wells have been subjected to a "t" test to determine whether all the samples come from the same normal population with the same standard deviation. The "t" test at 95% confidence shows that there is no significant difference between the porosity populations at the three wells. However, the Houston "GG" No. 1 and "JJ" No. 1 and Sweezy No. 1 wells revealed distinctly different permeability populations compatible with the reservoir sandstones being gas and water saturated, respectively (table II-12).

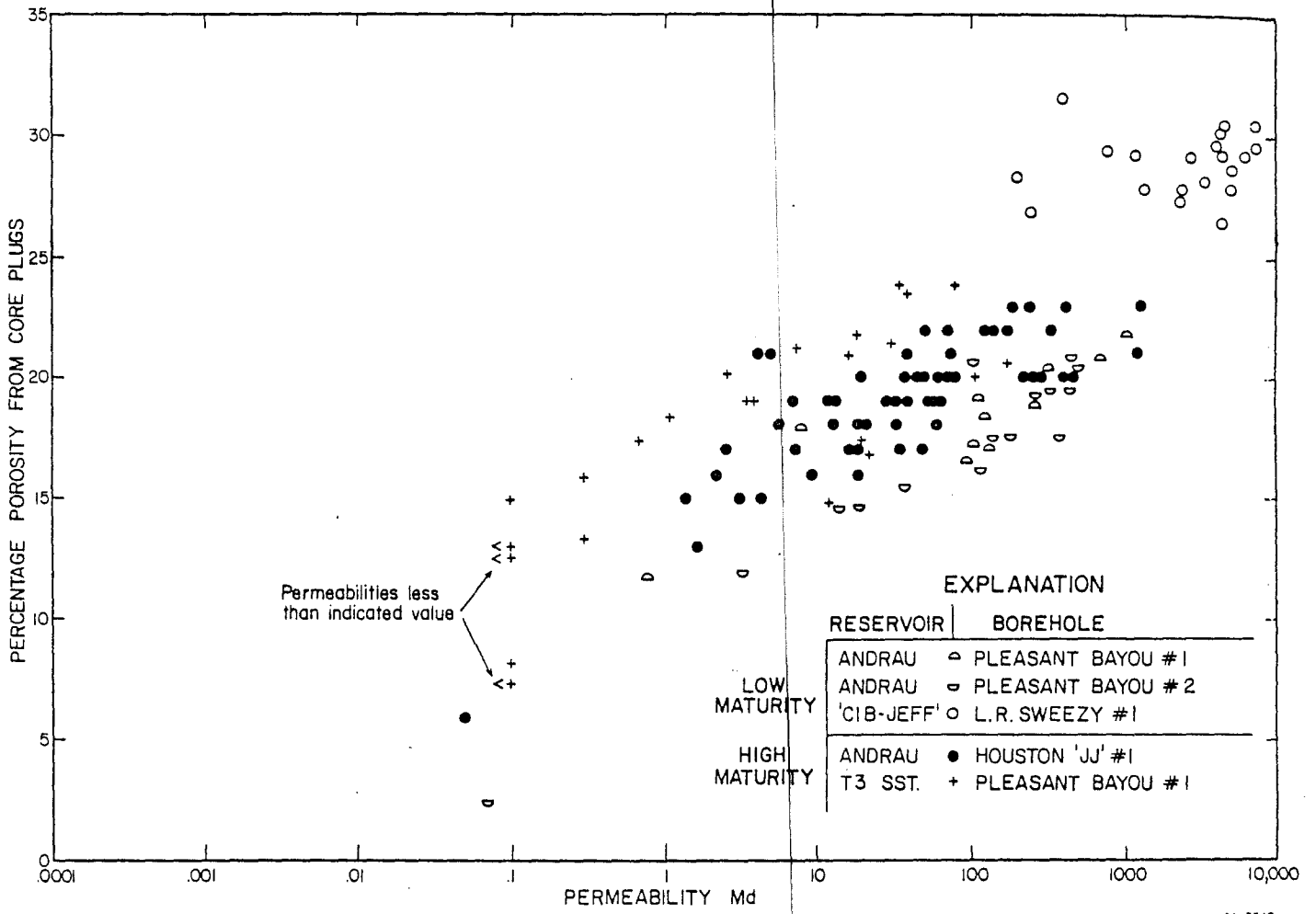


Figure II-24. Core porosity versus permeability for high- and low-maturity wells in Brazoria County, Texas, and Vermilion Parish, Louisiana (Hamilton and Stanley, 1984).

Table II-12. Core analysis data for the Andrau sandstone in the Pleasant Bayou No. 1 and No. 2, Phillips Houston "GG" No. 1 and "JJ" No. 1 wells, Brazoria County. Student's t distribution is used to test the hypothesis that the samples come from the same population with 95% confidence.

	Porosity (%)			Permeability (md)		
	PB #1 & 2	GG #1	JJ #1	PB #1 & 2	GG #1	JJ #1
No. of readings	27	15	68	27	15	74
Mean	17.29	19.15	18.88	223.57	443.57	119.46
Standard deviation	3.82	8.34	2.84	240.8	759.7	225.46
Range	2.5 - 21.6	2.6 - 27.3	6 - 23	0.07 - 1041	0.05 - 2180	.05 - 1300

	Porosity (%)		Permeability (md)		
	PB #1 & 2	JJ #1	PB #1 & 2	JJ #1	
GG #1	t	0.9637	0.2089	1.35	3.03
	95%	2.02	2.65	2.02	1.99
JJ #1	t	0.6918		0.29	
	95%	1.99		1.99	

Core analysis data for the DOW-DOE L. R. Sweezy No. 1 well in Vermilion Parish, Louisiana, and the Phillips Houston "GG" No. 1 well in Brazoria County, Texas. Student's t distribution is used to test with 95% confidence the hypothesis that the samples come from the same population.

<u>L. R. Sweezy #1</u>		
	<u>Porosity (%)</u>	<u>Permeability (md)</u>
No. of readings	22	22
Mean	28.23	3297.14
Standard deviation	2.24	2397.15
Range	22.2 - 31.5	27 - 7780

<u>L. R. Sweezy #1</u>			
	<u>Porosity (%)</u>	<u>Permeability (md)</u>	
GG #1	t	4.72	4.34
	95%	2.01	2.01

Though secondary porosity is predominant in all geopressed sandstones at Pleasant Bayou and is a result of the salinity and acidity of the brines (Kaiser and Richmann, 1981), permeability is better developed in the normal-maturity rather than high-maturity reservoirs (fig. II-24). Ewing and others (1984a) proposed that the release of Ca^{2+} ions from the albitization of feldspar and carbon dioxide from maturation of humic organic matter are chiefly responsible for the later occlusion of primary and secondary porosity at depth. They argued that preservation of high porosity and permeability of the lower Frio aquifers at Pleasant Bayou may depend on the cooler thermal history of this succession. In more mature areas, extensive albitization would have caused calcite occlusion of porosity at the depths of the lower Frio strata. Thermal maturity data already presented have shown that the upper Frio interval (T2 to T5 marker horizons) has been subjected to an extended period of hot basinal fluid flow which caused the above average maturity. These fluids probably induced albitization, generation of cements, and occlusion of permeability. In the highly geopressed lower Frio (pre-T5 marker horizon) updip basinal fluid flow was probably very slow so that the thermal maturity remained unchanged. Porosity and permeability were preserved in this interval because of a lower influx of Ca^{2+} ions and carbon dioxide. This calcium was released during albitization of feldspars at deeper levels.

SALINITY

High salinities of formation water (>105,000 ppm) occur in the Frio along the upper part of the Gulf Coast including Brazoria County (Morton and others, 1983). A relatively sharp boundary separates this zone from an area of intermediate salinities (35,000 to 70,000 ppm) along the central part of the Gulf Coast (Morton and others, 1983). The high chlorine to bromine ratios and high salinity of the Brazoria and Pleasant Bayou brines and their association with the salt dome province suggest that they contain components formed by salt dissolution (fig. II-25) (Kharaka and others, 1980; Morton and others, 1983).

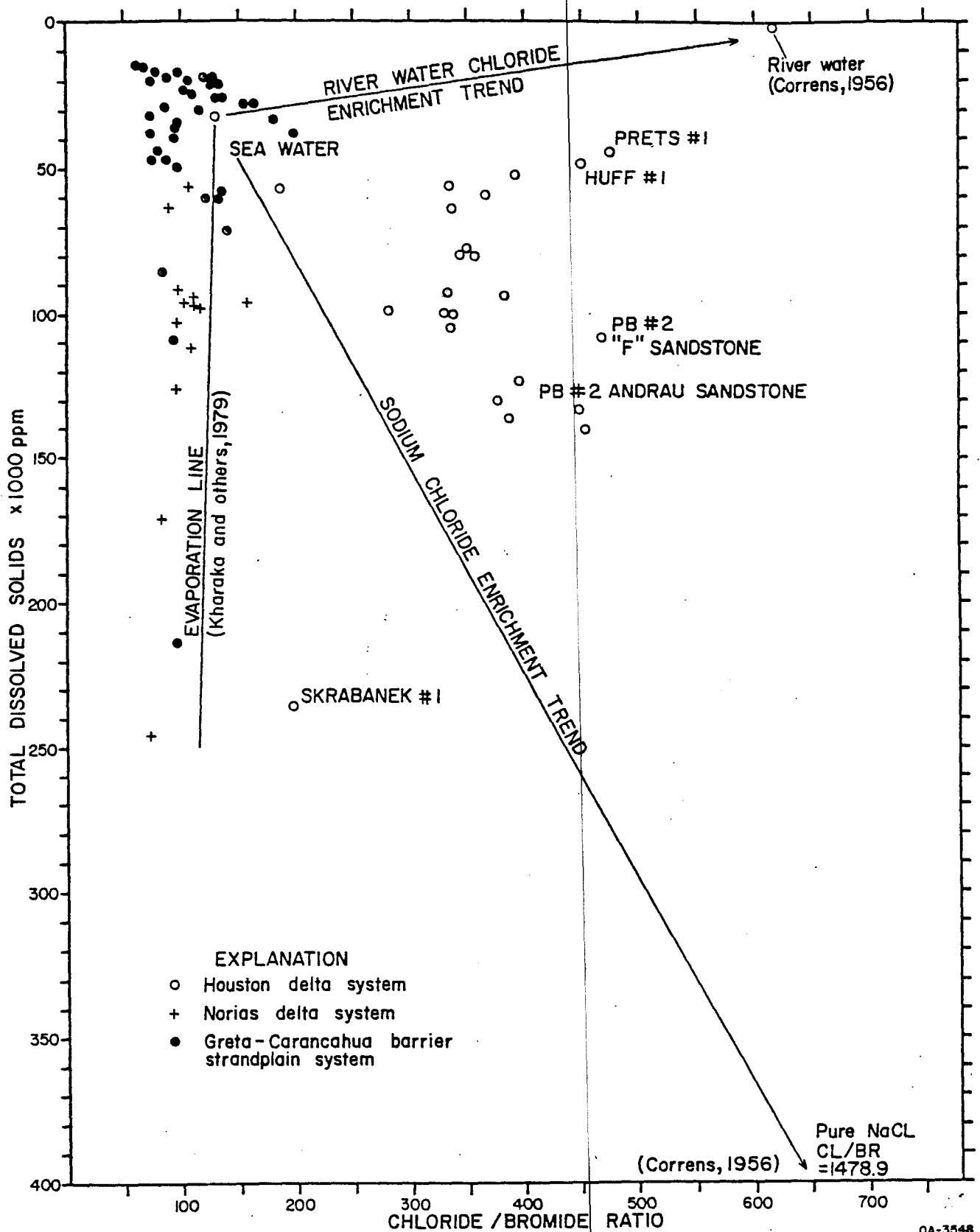


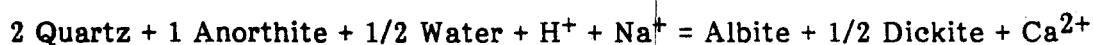
Figure II-25. Chlorine-bromine ratio versus total dissolved solids for wells from the Gulf Coast region of Texas. Data from Morton and others, 1981. Wells within the Houston Delta System (including Pleasant Bayou No. 2) lie near the sodium chloride enrichment line joining sea water to pure salt.

At Pleasant Bayou, major salinity changes cannot be attributed to membrane filtration because there is a marked increase in salinity in the geopressured zone (Morton and others, 1983). Furthermore the produced fluids at Pleasant Bayou are different from the original connate waters formed during deposition and authigenesis of the formation and must have an external source; the chemical changes cannot be attributed to diagenesis (Morton and others, 1983). A deep source for these waters is required if some of the chloride ion is by solution of halite (Morton and others, 1983). However, hydrogen and oxygen isotope data for Pleasant Bayou indicate that the formation waters are modified marine connate waters of the NaCl type (Kharaka and others, 1980). The saline waters within the geopressured zone are not chemically compatible with waters in the overlying normally pressured zone and are more saline than waters in nearby oil and gas fields (Kharaka and others, 1980).

Graphically intergrown diagenetic halite and albite feldspar have been identified in the T3 sandstones at Pleasant Bayou. This paragenesis suggests that migrating solutions were supersaturated with salt and that simultaneous crystallization of halite and albite occurred at temperatures above 212° to 248°F (100° to 120°C) (Loucks and others, 1981; W. R. Kaiser, personal communication, 1984). The alternative interpretation is that the halite crystallized after the core had been dried from supersaturated waters filling a porous feldspar (L. S. Land, personal communication, 1984). The present temperature of the T3 sandstone is around 248°F (120°C) (Gregory and Backus, 1980) consistent with the isotopic data for the crystallization of albite (Loucks and others, 1981). However, pure sodium chloride has a solubility of 39.12 grams per 100 cc water at 212°F (100°C) (Weast, 1976), which means that the T3 fluid phase would have had a salinity in excess of 390,000 mg/L. The sequence of crystallization of this intergrowth will be examined in more detail during the next contract period. The present salinity of the T3 fluids (12,000 mg/L, Morton and others, 1981) is one-thirtieth of that of the fluids that may have been present at the

time the halite crystallized. This low salinity is a result of mixing of deep saline waters with shallow less saline waters (Morton and others, 1983).

The low bromide to chloride ratio in the Frio and Pleasant Bayou brines (fig. II-25) can be explained by halite dissolution without recrystallization (Stoessel and Moore, 1983). The saline brines that migrated through the upper Frio sandstones were probably formed at depth and at high temperatures during a period of continuous halite dissolution and were transported to their present position before any halite recrystallization occurred. These migrating fluids were hot relative to their surrounding rocks and caused a thermal and hydrocarbon maturity peak (fig. II-12). The high salinity of these waters would make calcite extremely soluble, resulting in secondary dissolution of calcite cements (Barnes, 1979). This process would tend to enhance the porosity and permeability migration pathways already developed in the upper Frio sandstones, probably increasing the volume of migrating fluids. Such a process may have continued until the fluid source was exhausted and the temperature began to decrease, at which time crystallization of cements began to impede fluid flow. Stoessel and Moore (1983) suggested that the gradual decrease in the sodium to chloride ratio in the Frio fluids, when chloride concentration is above 1, results from the modifying influence of albitization on halite dissolution represented by the leaching of potassium feldspar, plagioclase, carbonates, and volcanics. This process is approximated by the following reaction:



In the Chocolate Bayou - Pleasant Bayou area, the decrease in sodium and attendant increase in chloride to sodium ratios within the highly geopressed zone may reflect albitization, which depends on the availability of silica and sodium (Milliken and others, 1981; Morton and others, 1981). The high salinity and temperature of the migrating fluids in the upper Frio in Pleasant Bayou would both supply the necessary sodium for albitization and retain the subsequently formed calcium in solution.

Stoessel and Moore (1983) have argued that the low value of the potassium-sodium ratios compared to the sea-water evaporation line indicates the lack of a dilution relationship with salt brine. This is in contrast to the regional and detailed geochemical data presented that suggest a direct link between the highly saline brines and the salt dome province (Morton and others, 1983).

CONCLUSIONS

Hoskins Mound and Stratton Ridge salt domes lie southeast and south of the Pleasant Bayou - Chocolate Bayou fault block and intersect the major growth fault system forming the southeastern margin of the Chocolate Bayou oil and gas field. Deep dissolution of these domes by hot migrating basinal fluids originating in Tertiary-age marine slope shales could produce the high chlorine to bromine ratios of the Pleasant Bayou brines. Shale water and chloride ions are in rough electrostatic equilibrium with saline brines in some geopressed sandstones (Kraemer, 1982). Dewatering of geopressed slope shales (Burst, 1969) assisted by hydrocarbon generation could produce brines; their salinity would be enhanced by dissolution of salt as the fluid migrated past deep salt zones.

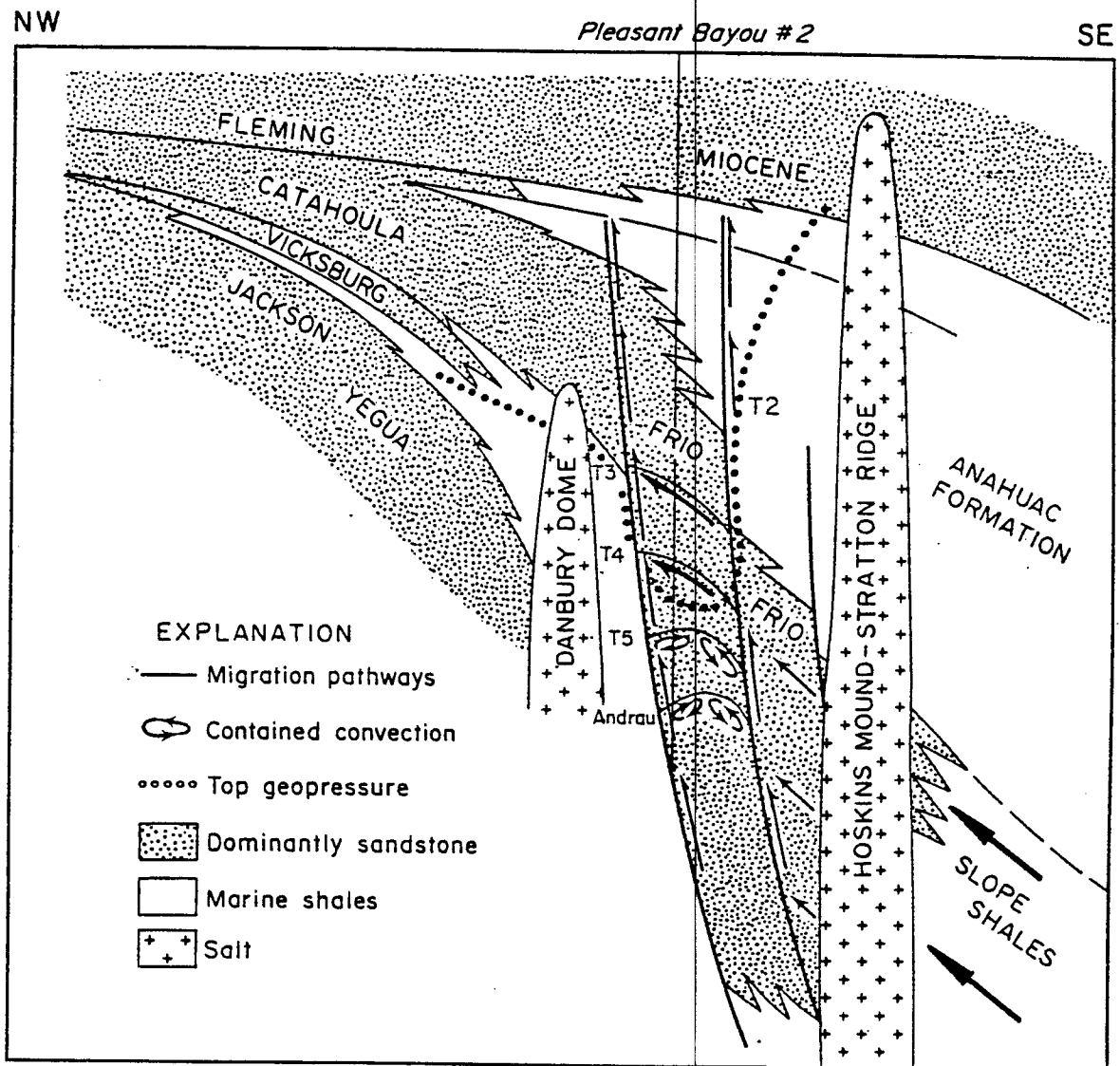
The T3 to T4 sandstones (upper Frio) may form part of a migration pathway up and out of the basin for hydrocarbons that are now trapped in the Chocolate Bayou field (Morton, 1983). Marked changes in salinity and chemical composition over short lateral distances suggest that fluids have migrated out of the basin along faults and discontinuities (Morton, 1983). Shale breaks appear to act as permeability barriers within sandstone bodies (Morton, 1983). Fluid migration would therefore be confined to permeable sandstone conduits and fault lines.

The T3 sandstone (upper Frio) has good lateral continuity throughout the Chocolate Bayou field, and the sandstone corresponds approximately to the boundary between normally pressured and geopressed sandstones (Morton and others, 1983). Landward

migration of fluids through T3 and other upper Frio sandstones may have been assisted by a horizontal pressure gradient that exists between the Pleasant Bayou - Chocolate Bayou fault block and more seaward fault blocks (fig. II-26, Galloway and others, 1982). Evidence indicates that the T3 to T4 section was extensively flushed by hot basinal waters from 14 Ma to the present. The geopressured brines in the Andrau sandstone at Pleasant Bayou, conversely, appear to have formed a contained convecting system and to have gained aromatics from slow updip migration of hydrocarbon-bearing brines. The good permeability of the Andrau sandstone at Pleasant Bayou is a consequence of its isolation from hot water flux, in some areas due to its high geopressure and in others to the presence of a gas cap.

ACKNOWLEDGMENTS

We wish to thank R. A. Morton, W. E. Galloway, W. R. Kaiser, S. P. Dutton, W. G. Dow, and K. W. Schwab for valuable discussions and Z. S. Lin for general engineering concepts. The text was typed by Rosanne M. Wilson under the direction of Lucille C. Harrell. Illustrations were drafted under the direction of R. L. Dillon, Chief Cartographer. Funding for this research was provided by the U.S. Department of Energy, Division of Geothermal Energy, under Contract No. DE-AC08-79ET27111.



QA3414

Figure II-26. Stylized stratigraphic dip section across the Texas Gulf Coast showing the relative position of the GCO/DOE Pleasant Bayou No. 2 geothermal test well (modified from Galloway and others, 1982).

REFERENCES

- Aziz, K., Bories, S. A., and Combarous, M. A., 1973, The influence of natural convection in gas and water reservoirs: *Journal of Canadian Petroleum Technology*, v. 12, p. 41-47.
- Barnes, H. L., 1979, *Geochemistry of hydrothermal ore deposits* (2d ed.): New York, John Wiley, 798 p.
- Bayliss, G. S., and Hart, G. F., 1981, Organic geochemistry of the Sweet Lake geopressed test well: *Proceedings, Fifth Conference on Geopressed Geothermal Energy*, The University of Texas at Austin, p. 303-310.
- Bebout, D. G., Loucks, R. G., and Gregory, A. R., 1978, Frio sandstone reservoirs in the deep subsurface along the Texas Gulf Coast--their potential for production of geopressed geothermal energy: *The University of Texas at Austin, Bureau of Economic Geology Report of Investigations No. 91*, 92 p.
- Bjorlykke, K. O., and Malm, A. O., 1979, Diagenesis in Mesozoic sandstones from Spitsbergen and the North Sea--a comparison: *Geologische Rundschau*, v. 68, p. 1152-1171.
- Blanchard, P., in press, Convection in sedimentary basins?: *Geology*, 11 p.
- Bories, S. A., and Combarous, M. A., 1973, Natural convection in a sloping layer: *Journal of Fluid Mechanics*, v. 57, p. 63-79.
- Bostick, N. H., 1973, Time as a factor in thermal metamorphism of phytoclasts (coaly particles): *Septieme Congres International de Stratigraphie et de Geologie du Carbonifere*, v. 2, p. 183-192.
- _____ 1979, Microscopic measurement of the level of catagenesis of solid organic matter in sedimentary rocks--a review: *Society of Economic Paleontologists and Mineralogists, Special Publication No. 26*, p. 17-43.

- Bottinga, Y., 1969, Calculated fractionation factors for carbon and hydrogen isotope exchange in the system calcite-carbon dioxide-methane-hydrogen-water vapour: *Geochimica et Cosmochimica Acta*, v. 33, p. 49-64.
- Brown, S. W., 1980, Hydrocarbon source facies analysis, Department of Energy and General Crude Oil Company Pleasant Bayou No. 1 and 2 wells, Brazoria County, Texas: Proceedings, Fourth Conference on Geopressured Geothermal Energy, The University of Texas at Austin, p. 132-152.
- Burst, J. F., 1969, Diagenesis of Gulf Coast clayey sediments and its possible relationship to petroleum migration: *American Association of Petroleum Geologists Bulletin*, v. 53, no. 1, p. 73-93.
- Carothers, W. W., and Kharaka, Y. K., 1978, Aliphatic acid anions in oil field waters—implications for origins of natural gas: *American Association of Petroleum Geologists Bulletin*, v. 62, no. 12, p. 2441-2453.
- Chung, H. M., and Sackett, W. M., 1979, Use of stable carbon isotope compositions of pyrolytically derived methane as maturity indices for carbonaceous materials: *Geochimica et Cosmochimica Acta*, v. 43, p. 1979-1988.
- Claypool, G. E., and Kaplan, I. R., 1974, The origin and distribution of methane in marine sediments, in Kaplan, I. R., ed., *Natural gases in marine sediments*: New York, Plenum Press, p. 99-139.
- Cómbarnous, M. A., and Bories, S. A., 1975, Hydrothermal convection in saturated porous media: *Advances in Hydroscience*, v. 10, p. 231-307.
- Correns, C. W., 1956, The geochemistry of the halogens, in Ahrens, L. H., and others, eds., *Physics and chemistry of the earth*, v. 1: London, Pergamon, p. 181-233.
- Costau, H., 1977, Formation waters and hydrodynamics: *Journal of Geochemical Exploration*, v. 7, p. 213-241.
- Craft, B. C., and Hawkins, M. F., 1959, *Applied petroleum reservoir engineering*: Englewood Cliffs, New Jersey, Prentice-Hall, 437 p.

- Craig, H., 1953, The geochemistry of the stable carbon isotopes: *Geochimica et Cosmochimica Acta*, v. 3, p. 53-92.
- Damberger, H. H., 1968, Nachweis der Abhängigkeit der Inkohlung von der Temperatur: *Brennstoff-Chemie*, v. 49, no. 3, p. 73-77.
- Dickey, P. A., and Hunt, J. M., 1972, Geochemical and hydrogeologic methods of prospecting for stratigraphic traps, in King, R. E., ed., *Stratigraphic oil and gas fields--classification, exploration methods, and case histories*: Society of Exploration Geophysicists, Special Publication No. 10, p. 133-167.
- Dow, W. G., 1978, Petroleum source beds on continental slopes and rises: *American Association of Petroleum Geologists Bulletin*, v. 62, p. 1584-1606.
- Ewing, T. E., Light, M. P. R., and Tyler, N., 1984a, Integrated geologic study of the Pleasant Bayou - Chocolate Bayou area, Brazoria County, Texas, in Ewing, T. E., and others, *Consolidation of geologic studies of geopressed geothermal resources in Texas*: The University of Texas at Austin, Bureau of Economic Geology, report prepared for the U.S. Department of Energy under contract no. DE-AC08-79ET27111, p. 90-142.
- _____ 1984b, Thermal and diagenetic history of the Pleasant Bayou - Chocolate Bayou area, Brazoria County, Texas. (abs.): *Gulf Coast Association of Geological Societies Transactions*, p. 90-142.
- Finley, R. J., and Saucier, A. E., 1983, Liquid hydrocarbons in geopressed brines: Memorandum to Dr. R. A. Morton, The University of Texas at Austin, Bureau of Economic Geology, 5 p.
- Flanagan, T. E., 1980, Pore fluid pressure regimes, Brazoria County, Texas: a preliminary study: The University of Texas at Austin, Master's thesis, 118 p.
- Franks, S. G., and Forester, R. W., 1984, Relationships among carbon dioxide, pore fluid chemistry, and secondary porosity, Texas Gulf Coast. (abs.): *American Association of Petroleum Geologists Bulletin*, v. 68, no. 4, p. 478.

- Fuex, A. N., 1980, Experimental evidence against an appreciable isotopic fractionation of methane during migration, *in* Douglas, A. G., and Maxwell, J. R., eds., *Advances in organic geochemistry 1979: Physics and Chemistry of the Earth*, v. 12, p. 725-732.
- Galimov, E. M., 1968, Izotopnyi sostav ugleroda gazov zemnoj kory: *Akademiya Nauk SSSR Izvestiya, Seriya Geologicheskaya*, no. 5, p. 29-44.
- Galloway, W. E., Hobday, D. K., and Magara, K., 1982, Frio Formation of the Texas Gulf Coast Basin--depositional systems, structural framework, and hydrocarbon origin, migration, distribution, and exploration potential: *The University of Texas at Austin, Bureau of Economic Geology Report of Investigations No. 122*, 78 p.
- Gregory, A. R., and Backus, M. M., 1980, Geopressed formation parameters, geothermal well, Brazoria County, Texas: *Proceedings, Fourth Geopressed-Geothermal Energy Conference, The University of Texas at Austin*, p. 235-311.
- Hamilton, J. R., and Stanley, J. G., 1984, eds., Final technical report: *Parcperdue geopressure-geothermal project: Dow Chemical Company, final report prepared for the U.S. Department of Energy under contract no. DE-AC08-79ET27255*, 443 p.
- Hart, J. E., 1971, Stability of flow in a differentially heated inclined box: *Journal of Fluid Mechanics*, v. 47, p. 547-576.
- Hower, J. C., and Davis, A., 1981, Application of vitrinite reflectance anisotropy in the evaluation of coal metamorphism: *Geological Society of America Bulletin, Part 1*, v. 92, p. 350-366.
- Hunt, J. M., 1979, *Petroleum geochemistry and geology*: San Francisco, W. H. Freeman, 617 p.
- James, A. T., 1983, Correlation of natural gas by use of carbon isotopic distribution between hydrocarbon components: *American Association of Petroleum Geologists Bulletin*, v. 67, p. 1176-1191.
- Jogi, P. N., Gray, K. E., Ashman, T. R., and Thompson, T. W., 1981, Compaction measurements on cores from the Pleasant Bayou wells: *Proceedings, Fifth Confer-*

ence on Geopressured Geothermal Energy, The University of Texas at Austin, p. 75-82.

Kaiser, W. R., and Richmann, D. L., 1981, Predicting diagenetic history and reservoir quality in the Frio Formation of Brazoria County, Texas, and Pleasant Bayou test wells: Proceedings, Fifth Conference on Geopressured Geothermal Energy, The University of Texas at Austin, p. 67-74.

Katz, B. J., Pheifer, R. N., and Schunk, D. J., 1984, Interpretation of nonlinear vitrinite reflectance profiles (abs.): American Association of Petroleum Geologists Bulletin, v. 68, no. 4, p. 494.

Keeley, D. F., and Meriwether, J. R., in press, Analysis of fluids from the DOW-DOE L. R. Sweezy No. 1 geopressured energy well: final report prepared for the U.S. Department of Energy under contract no. DE-AC08-70ET27255, 38 p.

Kharaka, Y. K., Carothers, W. W., and Rosenbauer, R. J., 1983, Thermal decarboxylation of acetic acid: implications for origin of natural gas: *Geochimica et Cosmochimica Acta*, v. 47, p. 397-402.

Kharaka, Y. K., Lico, M. S., Wright, V. A., and Carothers, W. W., 1980, Geochemistry of formation waters from Pleasant Bayou No. 2 well and adjacent areas in coastal Texas: Proceedings, Fourth Conference on Geopressured Geothermal Energy, The University of Texas at Austin, p. 11-45.

Knutson, C., 1982, Shale dewatering: Minutes of an Informal Meeting of the Overview Group, prepared for the U.S. Department of Energy, Houston, Texas, p. 28-46.

Kraemer, T. F., 1981, Radium and radon from Gulf Coast geopressured aquifers: Proceedings, Fifth Conference on Geopressured-Geothermal Energy, The University of Texas at Austin, p. 201-204.

_____ 1982, Shale studies: Minutes from DOE/Industry Geopressured Geothermal Resource Development Program Working Group Meeting, prepared for the U.S. Department of Energy, Houston, Texas, p. 20-27.

- Land, L. S., 1984, Evidence for vertical movement of diagenetic fluids, Texas Gulf Coast (abs.): American Association of Petroleum Geologists Bulletin, v. 68, no. 4, p. 498.
- Land, L. S., and Dutton, S. P., 1978, Cementation of a Pennsylvanian deltaic sandstone: isotopic data: Journal of Sedimentary Petrology, v. 48, p. 1167-1176.
- _____ 1979, Reply: cementation of sandstones: Journal of Sedimentary Petrology, v. 49, p. 1359-1361.
- Lapwood, E. R., 1948, Convection of a fluid in a porous medium: Proceedings of the Cambridge Philosophical Society, v. 44, p. 508-521.
- Larese, R. E., and Pittman, E. D., 1984, Effects of diagenesis on porosity development, Tuscaloosa sandstone, Louisiana (abs.): American Association of Petroleum Geologists Bulletin, v. 68, no. 4, p. 498.
- Lewis, C. R., and Rose, S. C., 1970, A theory relating high temperatures and overpressures: Journal of Petroleum Technology, v. 22, p. 11-16.
- Loucks, R. G., Richmann, D. L., and Milliken, K. L., 1980, Factors controlling porosity and permeability in geopressed Frio sandstone reservoirs, General Crude Oil/Department of Energy Pleasant Bayou test wells, Brazoria County, Texas: Proceedings, Fourth Congress on Geopressed Geothermal Energy, The University of Texas at Austin, v. 1, p. 46-82.
- _____ 1981, Factors controlling reservoir quality in Tertiary sandstones and their significance to geopressed geothermal production: The University of Texas at Austin, Bureau of Economic Geology Report of Investigations No. 111, 41 p.
- Lundegard, P. D., Land, L. S., and Galloway, W. E., 1984, The problem of secondary porosity: Frio Formation (Oligocene), Texas Gulf Coast: Geology, v. 12, no. 7, p. 399-402.
- McKibbin, R., and O'Sullivan, M. J., 1980, Onset of convection in a layered porous medium heated from below: Journal of Fluid Mechanics, v. 96, p. 375-393.

- McKibbin, R., and Tyvand, P. A., 1983, Thermal convection in a porous medium composed of alternating thick and thin layers: *International Journal of Heat and Mass Transfer*, v. 26, p. 761-780.
- Milliken, K. L., Land, L. S., and Loucks, R. G., 1981, History of burial diagenesis determined from isotopic geochemistry, Frio Formation, Brazoria County, Texas: *American Association of Petroleum Geologists Bulletin*, v. 65, p. 1397-1413.
- Morris, R. L., and Biggs, W. P., 1967, Using log-derived values of water saturation and porosity: *Transactions of the Society of Professional Well-Log Analysts*, Paper X, p. X1-X26.
- Morton, R. A., 1981, Pleasant Bayou No. 2--a review of rationale, ongoing research and preliminary test results: *Proceedings, Fifth Conference on Geopressured Geothermal Energy*, The University of Texas at Austin, p. 55-57.
- _____ 1983, Site reviews: Minutes from DOE/Industry Geopressured Geothermal Resource Development Program Working Group Meeting, prepared for the U.S. Department of Energy, Houston, Texas, p. 71-82.
- Morton, R. A., Garrett, C. M., Jr., Posey, J. S., Han, J. H., and Jirik, L. A., 1981, Salinity variations and chemical compositions of waters in the Frio Formation, Texas Gulf Coast: The University of Texas at Austin, Bureau of Economic Geology, report prepared for the U.S. Department of Energy under contract no. DE-AC08-79ET27111, 96 p.
- Morton, R. A., Garrett, C. M., Jr., and Posey, J. S., 1983, Variations in chemical compositions of Tertiary formation waters, Texas Gulf Coast, in Morton, R. A., Ewing, T. E., Kaiser, W. R., and Finley, R. J., *Consolidation of geologic studies of geopressured geothermal resources in Texas*: The University of Texas at Austin, Bureau of Economic Geology, report prepared for the U.S. Department of Energy under contract no. DE-AC08-79ET27111, p. 63-136.

- Nield, D. A., 1968, Onset of thermohaline convection in a porous medium: *Water Resources Research*, v. 4, no. 3, p. 553-560.
- O'Connor, D., 1984, Internal report on the vitrinite reflectance analyses of 1 sample (14,078') from the GCO/DOE Pleasant Bayou No. 1 well: Robertson Research Inc., prepared for The University of Texas at Austin, Bureau of Economic Geology, 8 p.
- Price, L. C., 1976, Aqueous solubility of petroleum as applied to its origin and primary migration: *American Association of Petroleum Geologists Bulletin*, v. 60, no. 2, p. 213-244.
- Price, L. C., Wenger, L. M., Girg, T., and Blount, C. W., 1983, Solubility of crude oil in methane as a function of pressure and temperature; *Organic Geochemistry*, v. 4, no. 3/4, p. 201-221.
- Pryor, W. A., 1971, Reservoir inhomogeneities of some recent sand bodies: *Society of Petroleum Engineering Transactions*, v. 253, p. 1229-1245.
- Reznikov, A. N., 1967, The geochemical conversion of oil condensates in the zone of katagenesis: *Geologiya Nefti i Gaza*, no. 5, p. 24-28.
- Schaefer, R. G., Leythaeuser, D., and Von der Dick, H., 1983, Generation and migration of low-molecular weight hydrocarbons in sediments from site 511 of DSDP/IPOD Leg 71, Falkland Plateau, South Atlantic in Bjoroy, M., ed., *Advances in organic geochemistry*: Chichester, England, John Wiley, p. 164-174.
- Schoell, M., 1983, Genetic characterization of natural gases: *American Association of Petroleum Geologists Bulletin*, v. 67, p. 2225-2238.
- Schwab, K. W., 1980, Visual kerogen and vitrinite reflectance analyses of the Pleasant Bayou No. 1 well, Brazoria County, Texas: *Proceedings, Fourth Conference on Geopressured Geothermal Energy*, The University of Texas at Austin, p. 85-131.
- _____ 1984, Report on vitrinite reflectance analyses of 7 core chip samples from Chocolate Bayou - Danbury dome area: Geo-Strat Inc., report prepared for The University of Texas at Austin, Bureau of Economic Geology, 27 p.

- Selley, R. C., 1979, Concepts and methods of subsurface facies analysis, sessions 7, 8, 9, Diagenetic controls of porosity: Short course, Johannesburg, Republic of South Africa, 10 p.
- Slider, H. C., 1976, Practical petroleum engineering methods: an energy conservation science: Tulsa, Petroleum Publishing Co., 559 p.
- Stahl, W. J., 1977, Carbon and nitrogen isotopes in hydrocarbon research and exploration: Chemical Geology, v. 20, p. 121-149.
- _____ 1978, Reifeabhängigkeit der kohlenstoff-isotopenverhältnisse des methans von erdöl-gasen aus Norddeutschland: Erdöl und Kohle, v. 31, 11 p.
- Stahl, W. J., Faber, E., Carey, B. D., and Kirksey, D. L., 1981, Near-surface evidence of migration of natural gas from deep reservoirs and source rocks. American Association of Petroleum Geologists Bulletin, v. 65, p. 1543-1550.
- Stahl, W. J., and Tang, C. H., 1971, Carbon isotope measurements of methane, higher hydrocarbons, and carbon dioxide in natural gases from northwestern Taiwan: Petroleum Geology of Taiwan, v. 8, p. 77-91.
- Stahl, W. J., and Carey, B. D., Jr., 1975, Source-rock identification by isotope analyses of natural gases from fields in the Val Verde and Delaware basins, west Texas: Chemical Geology, v. 16, p. 257-267.
- Stoessel, R. K., and Moore, C. H., 1983, Chemical constraints and origins of four groups of Gulf Coast reservoir fluids: American Association of Petroleum Geologists Bulletin, v. 67, p. 896-906.
- Surdam, R. C., Crossey, L. J., and Lahamn, R., 1984, Mineral oxidants and porosity enhancement (abs.): American Association of Petroleum Geologists Bulletin, v. 68, no. 4, p. 532.
- Teichmuller, M., and Teichmuller, R., 1954, Die stoffliche und strukturelle Metamorphose der Kohle: Geologie Rundschau, v. 42, p. 265-296.

- Thomson, M., 1983, Rice University Future Plans: Minutes from DOE/Industry Geopressure Geothermal Resource Development Program Working Group Meeting, prepared for the U.S. Department of Energy, Houston, Texas, p. 132-145.
- _____ 1984, Pleasant Bayou No. 2/Brazoria Well: Rice University, Minutes of an informal meeting of the Drilling and Testing Working Subgroup, Houston, Texas, Prepared for the DOE/Holmes and Narver, Inc., Las Vegas, Nevada, p. 173-184.
- Timur, A., 1968, An investigation of permeability, porosity and residual water saturation relationships for sandstone reservoirs: Transactions of the Society of Professional Well-log Analysts, Paper J, p. J1-J18.
- Tissot, B. P., and Welte, D. H., 1978, Petroleum formation and occurrence: New York, Springer Verlag, 538 p.
- Tyler, N., 1982, Unpublished well log description: The University of Texas at Austin, Bureau of Economic Geology.
- Weast, R. C., 1976, Handbook of chemistry and physics: Cleveland, CRC Press, p. A1-A157.
- Weber, J. E., 1973, On thermal convection between non-uniformly heated planes: International Journal of Heat and Mass Transfer, v. 16, p. 961-970.
- Wege, E., 1954, Chemisch-physikalische und petrographische Untersuchungen an Kohlen, Koksen und Graphiten; VI. Untersuchungen über das Reflexionsvermögen und die Reflexionsanisotropie von Vitriniten: Brennstoff-Chemie, v. 35, p. 1-6, 33-41.
- Weres, O., Maynard, I. M., Harnden, W., and Newton, A., 1984, Downhole sampling of geopressured gas wells: The University of California, Lawrence Berkeley Laboratory, final report prepared for the Gas Research Institute, contract no. 5081-212-0552, 53 p.
- Wood, J. R., and Hewett, T. A., 1982, Fluid convection and mass transfer in porous sandstones—a theoretical model: Geochimica et Cosmochimica Acta, v. 46, p. 1707-1713.

- Wright, N. J. R., 1980, Time, temperature and organic maturation--the evolution of rank within a sedimentary pile: *Journal of Petroleum Geology*, v. 2, p. 411-425.
- Young, A., Monaghan, P. H., and Schweisberger, R. T., 1977, Calculation of ages of hydrocarbons in oils--physical chemistry applied to petroleum geochemistry: *American Association of Petroleum Geologists Bulletin*, v. 61, p. 573-600.
- Zarella, W. M., Mousseau, R. J., Coggeshall, N. D., Norris, M. S., and Schrayner, G. J., 1967, Analysis and significance of hydrocarbons in surface brines: *Geochimica et Cosmochimica Acta*, v. 31, p. 1155-1166.
- Zhuze, T. P., Ushakova, G. S., and Yushkevich, G. N., 1962, The influence of high pressures and temperatures on the content and properties of condensate in the gas phase of gas-oil deposits: *[Soviet] Geochemistry* 8, p. 797-806.